Department of Structural Engineering
Faculty of Engineering
NTNU- Norwegian University of Science and Technology

ACCESSIBILITY

Open

MASTER THESIS 2018

SUBJECT AREA:	DATE:	NO. OF PAGES:
Structural Reliability and Uncertainty Modelling	11.06.18	130 + 8 Appendix

TITLE:

Probabilistic Methods in Management and Inspection of Buried Steel Pipe Bridges

Sannsynlighetsmodeller i forvaltning og inspeksjon av nedgravde stålrørsbruer

BY:

Henrik Solheim

SUMMARY:

This thesis studies how probabilistic methods and analyses can support management and inspection of bridges. The methods are displayed through a case study of buried steel pipe bridges. Bayesian networks, influence diagrams, reliability analyses, Markovian processes, regression analyses and cost, risk and benefit analyses are studied. The topics of consideration are decision making for inspectors, condition of buried steel pipe bridges, deterioration predictions, failure predictions and replacement strategies.

Management and inspection of bridges can benefit from the use of probabilistic analyses. The expert's experience and knowledge, physical theory and probability theory are all important elements in optimal management. Bayesian networks and influence diagrams can be applied to several topics related to inspection and management of structures, and these methods may contribute to optimal decisions.

RESPONSIBLE TEACHER: Professor Jochen Köhler

EXTERNAL SUPERVISOR: Knut Ove Dahle, Norwegian Public Roads Administration

CARRIED OUT AT: Department of Structural Engineering, NTNU

Abstract

Management and inspection of existing bridges involve decision making. Loading, resistance and deterioration of bridges are uncertain. Inspection reduces uncertainty, but the uncertainty is usually not considered on a theoretical basis. There is, however, well-established probabilistic theory to handle uncertainties. Using a structured probabilistic approach might optimise decisions by weighing cost towards benefit.

Norwegian Public Roads Administration manages more than 17,500 national and county bridges in Norway. They have their own practise and guidelines for inspection of bridges. The focus in this study is directed towards buried corrugated steel pipe bridges. A corrugated steel pipe bridge is regarded a flexible pipe, as the surrounding soil is stiffer than the wall of the pipe. Both the steel pipe and the surrounding soil contribute to the bearing capacity.

Bayesian decision analyses are used to guide a consistent decision-making process. The benefit from risk reduction is considered in these analyses. Different measurements and actions are analysed. Bayesian theory is also used to get a better understanding of the condition of the pipe bridges. Bayesian networks illustrate the variables of the structural system graphically, and this is quite useful for complex structural systems as the buried steel pipe bridges.

Structural reliability analyses can also assess the condition of the pipe bridges. First order reliability analysis is used to calculate the probability of yield of the pipe bridge steel wall. With a simple example, it is shown that a Bayesian network might connect the probability of yield with the probability of complete structural failure.

Estimation of deterioration is important for management of bridges, and strategies and budgeting can be made upon deterioration predictions. A statistical approach considers observations of damage development for 157 buried pipe bridges. The damage observations are divided into four degrees. A continuous-time Markov process is used to predict the deterioration. The model is fitted to observations with a maximum likelihood estimation. A prediction of deterioration is also made for a selection of bridges based on the climate at their location. The deterioration dependent on climate is modelled in a dynamic Bayesian network.

Failure prediction is also relevant for decision making. Five of the 157 bridges have failed. A sequential Markov process is used to predict failures for this bridge stock. Five new failures are estimated to occur within the next six years if nothing is done and all the bridges continue to deteriorate. A dynamic Bayesian network can consider a higher complexity prediction which is also dependent on variables. This makes it suitable for predicting failure of an individual bridge and predicting failures in the whole bridge stock.

Replacement strategies are studied for the bridge stock and individual bridges. Since several of the bridges are in a very bad condition, replacement has been a preferred action. Replacement strategies are assessed by modifying the deterioration prediction. Improving the bridge stock condition seems to be beneficial as it reduces risk. The risk is high with the current condition of the bridge stock. Replacement analysis of individual bridges can indicate when the bridges should be replaced and which bridges to prioritise.

Abstrakt

Forvaltning og inspeksjon av eksisterende bruer involverer beslutningstaking. Det er usikkerhet knyttet til last, kapasitet og forverring av tilstand. Inspeksjon reduserer usikkerhet, men usikkerhet er vanligvis ikke behandlet på et teoretisk grunnlag. Det finnes veletablerte sannsynlighetsmodeller som kan behandle usikkerhet. En strukturert tilnærming basert på sannsynlighet kan optimalisere beslutninger ved å veie kostnad mot nytte.

Statens vegvesen forvalter mer enn 17.500 fylkesveg- og riksvegbruer i Norge. De har deres egen praksis og retningslinjer for inspeksjon av bruer. Fokuset i dette studiet er rettet mot korrugerte stålrørsbruer. En korrugert stålrørsbru består av et fleksibelt rør med omliggende masser som har høyere stivhet enn det tynnveggede røret. Både stålrøret og omliggende masser bidrar til bæreevne.

Bayesianske beslutningsanalyser kan brukes til å veilede en konsistent beslutningsprosess. Slike analyser betrakter nytte fra risikoreduksjon. Ulike målemetoder og tiltak kan analyseres. Bayesianske metoder kan også brukes til å danne bedre forståelse for tilstandene til bruene. Variabler som beskriver konstruksjoner kan illustreres grafisk med bayesianske nettverk. Slike nettverk er svært nyttige for komplekse konstruksjoner som stålrørsbruer, og et bedre bilde av konstruksjonene dannes.

Pålitelighetsanalyser kan også brukes til å vurdere tilstanden til bruene. Et eksempel ved bruk av førsteordens pålitelighetsmetode er gitt. Metoden brukes til å beregne sannsynlighet for flyt av stålrørsveggen til en bru. Det er også vist at pålitelighetsanalysene kan koples opp mot bayesianske nettverk, og sannsynligheten for flyt av rørveggen er koplet opp mot sannsynlighet for total konstruksjonsvikt.

En estimering av forverring av brutilstander kan støtte forvaltning av bruer. Tiltaksstrategier og budsjetter kan planlegges ut i fra forverringsmodeller. En statistisk tilnærming som tar for seg skadeobservasjoner av 157 stålrørsbruer er gitt. Skadeobservasjonene er delt inn i fire skadegrader. Skadeutvikling er predikert ved bruk av en Markov-prosess i kontinuerlig tid. Modellen er tilpasset observasjoner ved bruk av en maksimal sannsynlighetsestimering. En prediksjon av forverring er også gjennomført for et utvalg av stålrørsbruer basert på klimaet ved bruenes beliggenhet. Et dynamisk bayesiansk nettverk illustrer forverring basert på klima.

Sviktanalyser er også viktig for beslutningstaking. Fem av de 157 stålrørsbruene har sviktet. En sekvensiell Markov-prosess har blitt brukt til å estimere fremtidige konstruksjonsvikt. Om ingenting gjøres for å forbedre tilstandene til de verste bruene, forventes det å forkomme fem nye svikt innen de seks neste årene. Et dynamisk bayesiansk nettverk kan modellere sviktpredikasjon med avhengighet til flere variabler. Slike nettverk kan derfor brukes til å analysere svikt av individuelle bruer samt svikt for en samling av bruer.

Strategier for utskifting av stålrørsbruer er tatt i betraktning for individuelle bruer og forvaltning av alle bruene. Utskifting har vært et foretrukket tiltak siden flere av bruene er i svært dårlig tilstand. For å studere utskiftningsstrategier, har det blitt gjort endringer i modellen for skadeutvikling. Forbedring av tilstanden til bruene synes å være gunstig da det reduserer risiko. Risikoen er høy for den nåværende tilstanden til bruene. Utskiftningsanalyse av individuelle bruer kan indikere når bruene skal utskiftes og hvilke bruer som bør prioriteres.

Acknowledgement

I would like to thank my supervisor Professor Jochen Köhler for providing me an interesting topic to study and for continuously guiding me through my work. His expertise is truly inspiring. It has been a great honour to work under his supervision. I would also like to thank PhD candidate Jorge Mendoza Espinosa for all the help he has given me through my progress.

I would like to express my deep appreciation to Knut Ove Dahle. He has connected my studies with practical aspects of management and inspection of bridges. His supervision has been important for my studies, and he has shown a great interest in research to support bridge management. Furthermore, I am grateful to everyone from Norwegian Public Roads Administration who have devoted their time in order to help me with my studies.

Contents

Executive summary 1

Chapter 1 · Introduction 7
1.1 Background 7
1.2 Management and inspection of structures - uncertainties 7
1.3 Methods to support bridge management and inspection 8
1.4 Problem formulation 9
1.5 Structure of study 9

Chapter 2 · Inspection of bridges by Norwegian Public Roads Administration 11
2.1 General 11
2.2 Damage assessment 11
2.3 Material testing, measurement, instrumentation and special inspection 15
2.4 Conclusion 16

Chapter 3 · Buried steel pipe bridges - management, consequences and costs 17
3.1 General 17
3.2 Management and inspection 17
3.3 Consequences and costs 19
3.4 Replacement cost 23
3.5 Failure cost 25
3.6 Conclusion 26

Chapter 4 · Buried steel pipe bridges - structural system and deterioration 27
4.1 General 27
4.2 Structural system 27
4.3 Deterioration 35
4.4 Conclusion 39

Chapter 5 · Bayesian decision analysis 41
5.1 General 41
5.2 Decisions and uncertainty 41
5.3 Priori analysis 42
5.4 Posterior analysis 44
5.5 Preposterior analysis 46
5.6 Conclusion 48

Chapter 6 · Bayesian network 49
6.1 General 49
6.2 Introduction to Bayesian network and influence diagram 49
6.3 Dynamic Bayesian network and influence diagram 54
6.4 Bayesian networks for buried steel pipes 56
6.5 Conclusion 62

Chapter 7 · Structural reliability analysis 63
7.1 General 63
7.2 Limit state 63
7.3 Structural reliability methods 63
7.4 Probability of yield of pipe wall 66
7.5 Conclusion 76

Chapter 8 · Deterioration prediction 77
8.1 General 77
8.2 Deterioration observation 77
8.3 Markov chain for bridge deterioration 82
8.4 Predicting deterioration model 86
8.5 Buried pipe deterioration 89
8.6 Deterioration dependent on variables 96
8.7 Conclusion 102

Chapter 9 · Failure prediction 103
9.1 General 103
9.2 Time dependent probability of failure 103
9.3 Failure and reliability function 104
9.4 Failure prediction for bridge stock 105
9.5 Dynamic Bayesian network for failure prediction 108
9.6 Conclusion 111

Chapter 10 · Replacement strategies 113
10.1 General 113
10.2 Risk and cost-benefit analysis 113
10.3 Individual bridge replacement analysis 116
10.4 Bridge stock replacement strategies 120
10.5 Conclusion 123

Chapter 11 · Conclusions and recommendations 125
11.1 Probabilistic methods in inspection and management of bridges 125
11.2 Buried steel pipe bridges 126
11.3 Recommendations and outlook 128

References 129

Appendix 131
Appendix A: Yield of pipe wall - FORM analysis with MATLAB 131
Appendix B: Bridge stock deterioration observations 133
Appendix C: Bridge stock deterioration prediction with MATLAB 137

Executive summary

The main results from the studies of buried steel pipe bridges are given in this executive summary. A corrugated steel pipe bridge is a quite complex structure. The condition of the structure is both dependent on the condition of the corrugated steel pipe and the condition of the surrounding soil. Geotechnical engineering includes many uncertainties, and it might be difficult to predict the behaviour of the soil. A Bayesian network is made to illustrate the variables and dependencies that affect the structural performance of a buried steel pipe bridge. This network is shown in figure 1. The network shows that there are many dependencies between loading variables and structural condition variables. The surrounding soil contributes to an earth load on the pipe, but the soil is also supporting the pipe.

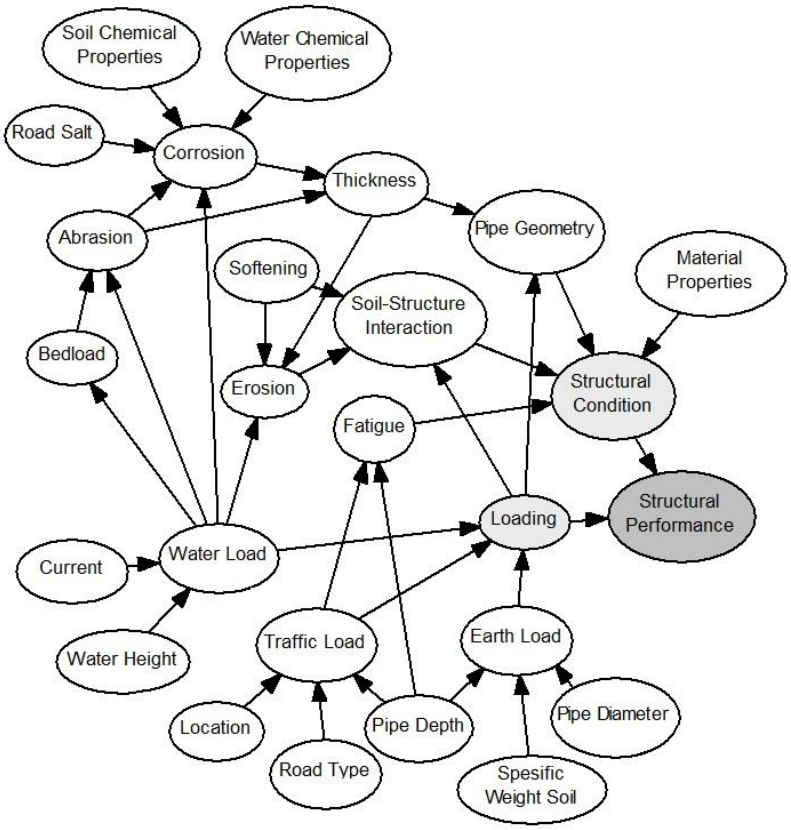

Figure 1: Bayesian network for a buried steel pipe bridge

There exist simplified formulas to calculate the performance of corrugated steel pipe bridges. Corrugated steel pipes have a flexible bending stiffness relative to the soil, but the stiffness in ring compression is very large for the pipes, Moser (2001). The earth load might be considered to act as a prism load, Moore (2001). All the soil above the pipe is carried by the walls of the pipe, and this is assumed to create a ring compression in the pipe.

Deterioration affects the structural capacity. Corrosion reduces the wall thickness. El-Taher's study (2009) shows that the relation between the yield capacity of the pipe wall and the smallest continuous wall thickness of the pipe is almost proportional. This is the case if the pipe has proper support from the soil. Erosion might strongly reduce the buckling capacity of the pipe, El-Taher (2009).

First order reliability analysis is used to assess the probability of yield of the pipe wall. A set of assumed variables are given. The prism load simplification is used to model the earth load. A BK10 traffic load from manual R412, NPRA (2003), is also considered in the loading. The mean diameter of the pipe is 3.5 m. It is assumed that there is proper support from soil and that yield is the failure mechanism for the pipe wall. The yield capacity is assumed to be proportional with the smallest continuous wall thickness, El-Taher (2009). Figure 2 shows a plot of the probability of yield for some common pipe depths and continuous wall thicknesses of less than 1 mm.

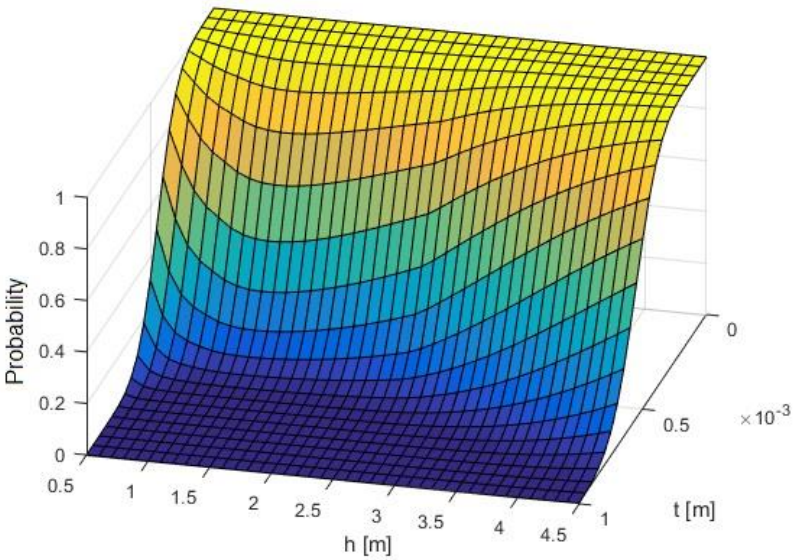

Figure 2: Probability of yield for different combinations of pipe depth and wall thickness

It is seen that the probability of yield might become significant for combinations of depths and thicknesses in this range. The traffic load is most critical at shallow depths since the pipe carries a larger portion of the traffic load at shallow depths. At deeper depths, the earth load becomes larger. These properties explain the curvature of the probability of yield plot. The pipe bridge might be standing even though there is yield of the pipe wall. This is because the loads might be transferred through the soil rather than the pipe. The effect of loads being transferred through the soil is called the arching effect, Moser (2001).

Norwegian Public Roads Administration has a bridge stock of corrugated steel pipe bridges in Trøndelag. These bridges are assessed through inspection and the observations are stored in a database. Damage observations for 157 corrugated steel pipe bridges are studied further. NPRA assigns four damage degrees through inspection, from damage degree 1, small damage, to damage degree 4, critical damage. The damage observations of consideration are damages that affect the structural system's bearing capacity at the time of observation or as the damage continues to deteriorate. Corrosion of the steel pipe and erosion of surrounding soil are typical examples of such damages, but other damages as major damage to the wingwall are also considered. Damage degree 1 to 4 are assigned state 1 to 4. In addition, five failures of pipe bridges have occurred, and failure is assigned state 5. There are in total 284 state observations, and these are sorted by the age of the bridge at observation. This is plotted, and the result is shown in figure 3. The smallest dot equals one observation and the largest dot equals eight observations.

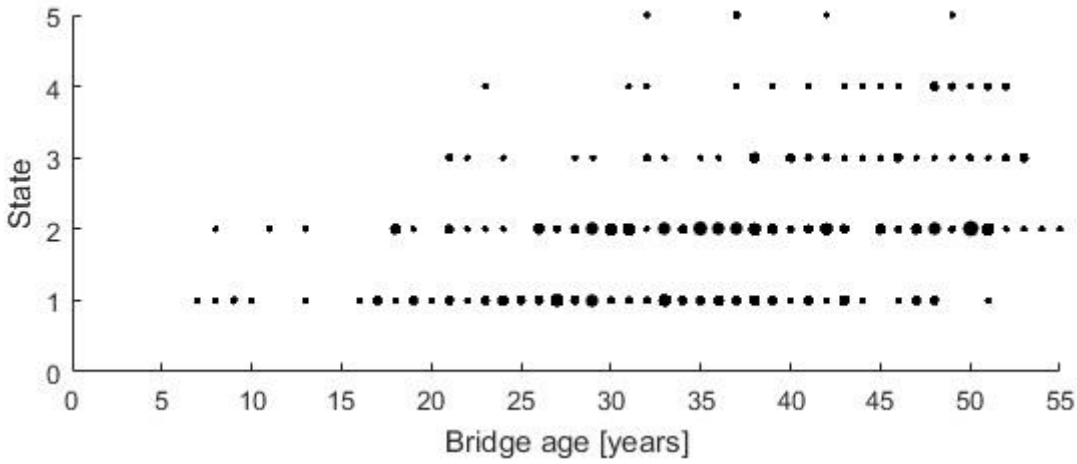

Figure 3: State observations sorted by bridge age at observation

First, all damage observations excluding failures are considered. A prediction of deterioration is made. All bridges are assumed to be in state 0, no damage, right after construction. A continuous-time Markov process is fitted to the observations with a maximum likelihood estimation. This procedure is based on a proposed framework by Kallen (2007). Based on the current condition of the bridge stock, a future prediction is made, figure 4. This prediction assumes that there are no actions nor failures, and damage degree 4 is the absorbing state.

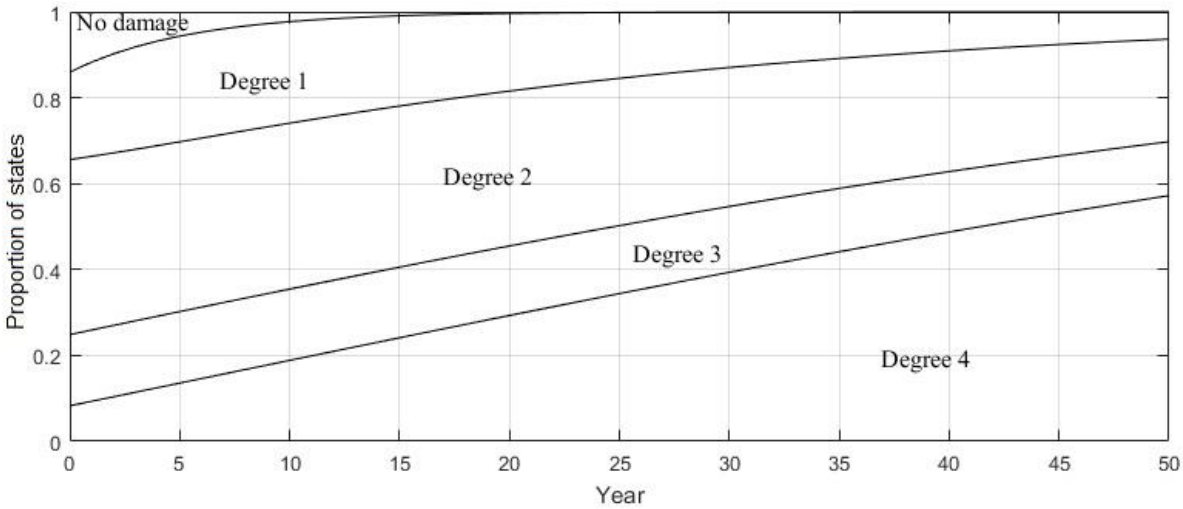

Figure 4: Worsening bridge stock condition

A failure prediction is also made for the bridge stock. This is modelled with a sequential deterioration failure model, which assumes that a bridge goes through all states before failure occur. The model is a continuous-time Markov process. A damage degree 4 bridge is predicted to have an annual probability of failure of 0.05. Figure 5 shows a failure prediction for the bridge stock. This prediction assumes that no improving actions are made and the bridge stock continues to deteriorate. It is predicted that there will occur five failures within the bridge stock for the next six years. Five failures have occurred during the past five years, and this prediction seems realistic.

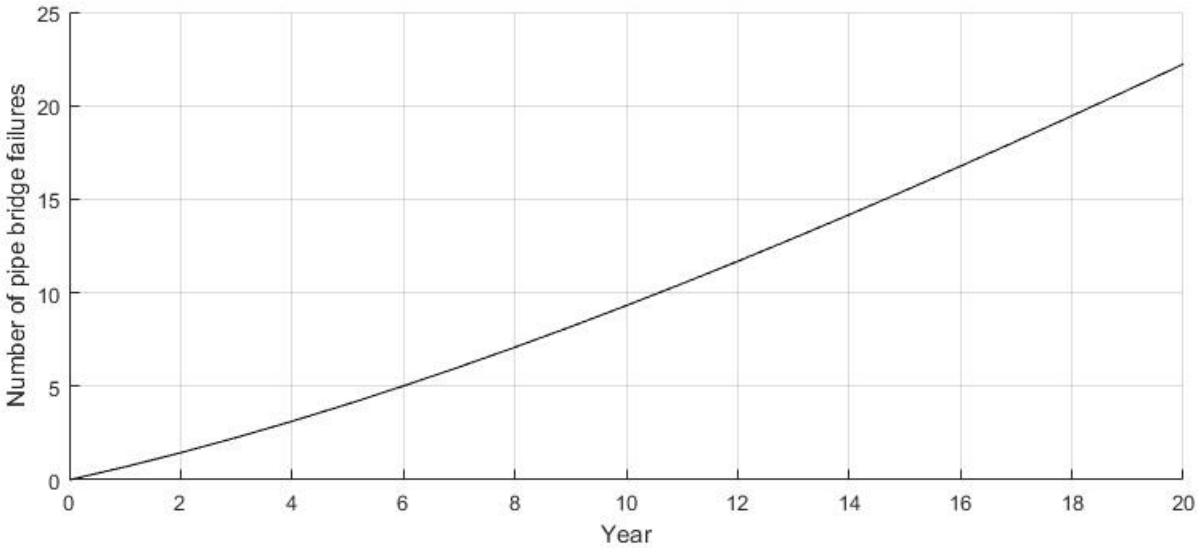

Figure 5: Bridge stock failure prediction

The costs for a planned replacement and a failure including reconstruction is studied. To quantify the benefit of reducing risk, these costs should be known. The costs are divided into costs to the owner of the bridge and to the users of the bridge. Owner costs mainly include design cost and construction cost, while user costs mainly include traffic disruption cost and accidental cost. The user cost may be seen from the society's point of view.

The difference in planned replacement cost and failure cost for the owner is studied by assessing the experience of inspectors at NPRA. The design cost may be 20% larger for a failure compared to a planned replacement. When it comes to the construction cost, the costs can be fairly similar for a planned replacement and a failure. It is more likely that a temporary bridge will be necessary if failure occur, and this will increase the failure cost.

User costs are studied by considering detour costs given by Samstad (2017) and accidental costs that are considered for road investments, manual V712, NPRA (2018). The detour costs are dependent on alternative roads and the additional driving time and length associated with the alternative roads. A planned replacement might close the road for 3 days, while a failure might close the road for 3-10 days. For a planned replacement, a side track can be planned, and this can minimise traffic disruption. Accidental risk can be very large for a failure. It is dependent on the probability of accidents. For some assumed probabilities, it is shown that the accidental risk might be more than 10 million NOK.

Since the risk associated with failures are high, the benefit from risk reduction can be great. Some replacement strategies are studied for the bridge stock. These strategies are studied by modifying the Markovian deterioration model. It is seen that today's bridge stock condition can be maintained by replacing 13% of damage degree 4 bridges every year. With this strategy, there will be a significant amount of damage degree 4 bridges in the bridge stock. On average, one bridge must be replaced every 7.3 months.

A strategy that improves the bridge stock condition is also studied. It is assumed that all bridges deteriorating to damage degree 4 are replaced within a year. 10% of damage degree 3 bridges are replaced every year, and ideally, these should be the most critical damage degree 3 bridges.

The bridge stock condition with this strategy is shown in figure 6. This strategy maintains a bridge stock condition with far less damage degree 3 and 4 bridges. The average time between replacements is 6.1 months when the bridge stock condition has reached a steady state. This is not very different from the replacement frequency that maintains today's condition. An improvement of the bridge stock condition seems to be beneficial. Increased investment in improving bridge stock condition can strongly reduce failures.

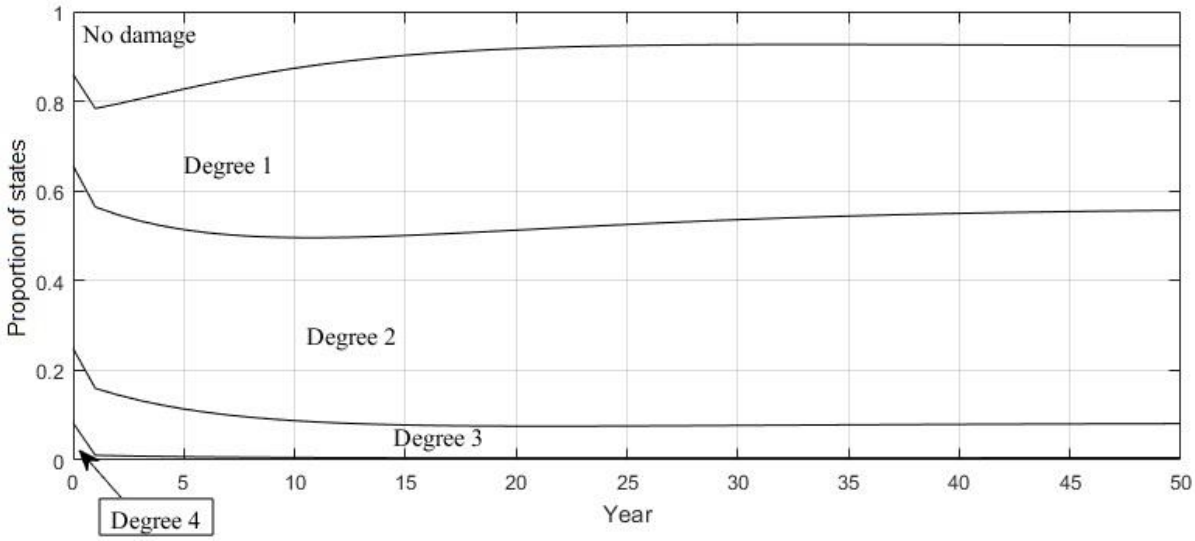

Figure 6: Improving bridge stock condition

Chapter 1

Introduction

1.1 Background

The government agency Norwegian Public Roads Administration (Statens vegvesen) is responsible for management of more than 17,500 national and county bridges. To encourage good decision making, the agency has developed guidelines for inspection and maintenance of bridges. Guidelines from manual V441 by NPRA (2010) give practical and simple guidance for inspection. They describe how visual inspection and measurements can be done, and how to classify the damage and the need for action.

The monetary value is large for the bridge stock managed by NPRA. The potential benefit of optimizing the decision making is therefore great. For this thesis, focus is directed towards buried corrugated steel pipe bridges. NPRA has 157 corrugated steel pipe bridges in Trøndelag. Most of these structures are built between 1960 and 1990. The conditions of the pipes vary from non-visible damage to highly damaged with corrosion and erosion of the supportive soil. In recent years, several failures have occurred.

1.2 Management and inspection of structures - uncertainties

Management and inspection of structures include uncertainties. The resistance and the loading of structures are uncertain, and so is deterioration. Inspections reduces these uncertainties by giving more information about the condition of the structure. Actions as whether to do further measurements, maintenance, rehabilitation, replacement or nothing is made upon the information provided by inspection.

The deterioration of a structure is illustrated in figure 1.2.1. R is the structure's resistance and S is the loading on the structure. Failure occur if the loading is larger than the resistance. The resistance of the structure decreases over time due to deterioration. At a given time, one may ask whether it is beneficial to invest in measurements to reduce uncertainties connected to the resistance and loading. Different measurements might also be compared. The figure illustrates possible outcomes from renewal and life-extending action.

The goal is to maximise the expected benefit by optimising a set of decisions and the point in time in which they are applied. The cost for maintenance becomes larger as damage develops. At an early stage, the cost for maintenance will be smaller, but there is limitation in the potential improvement of the structure. For a given cost, the balance between cost and benefit will have its optimum.

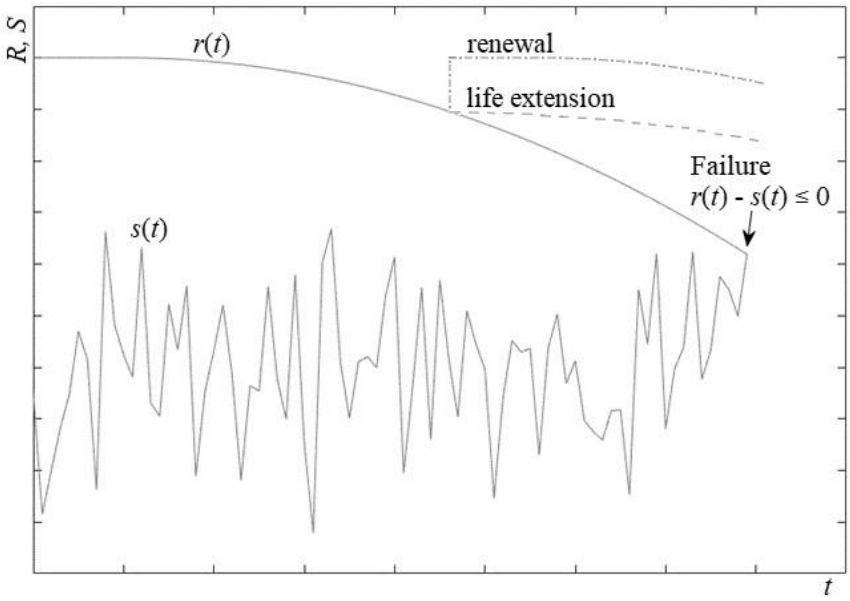

Figure 1.2.1: Resistance and loading over time

1.3 Methods to support bridge management and inspection

The inspector has a very important role in management of structures. In addition to the expert's experience and knowledge, physical theory and probability theory can accompany the assessment of existing structures. The management and inspection of bridges can be optimised by combing these methods.

It is of interest to put focus on uncertainties as there are large uncertainties connected to the inspection process. The main focus in this study is probabilistic approaches, but it is also connected with physical theory and the inspector's practise.

Bayesian networks can be used to combine such analysis in a consistent manner and in an illustrative way. These networks consider uncertain variables and their dependencies. Utilities and decisions can be included in the network of uncertain variables in an influence diagram. By doing this, the costs of different actions can be quantified towards the benefit of reducing risk. From such analysis, different actions can be compared, which makes it possible to find the most beneficial options in the inspection process.

Another aspect of this document is the difference in analysis of a bridge stock and an individual bridge. Some methods are well suited to describe the bridge stock. A Markov process may be used to describe the deterioration of a bridge stock. Understanding the bridge stock is important for right budgeting and optimal strategies. Other approaches might be applied for individual bridge assessment. Assessing an individual bridge is important for good understanding of the condition of the bridge, right prioritisation and good decision making.

1.4 Problem formulation

This thesis studies how probabilistic methods and analyses can support management and inspection of bridges. The methods are displayed through a case study of buried steel pipe bridges. Bayesian networks, influence diagrams, reliability analyses, Markovian processes, regression analyses and cost, risk and benefit analyses are studied. The topics of consideration are decision making for inspectors, condition of buried steel pipe bridges, deterioration predictions, failure predictions and replacement strategies.

1.5 Structure of study

The inspection practise is first considered by looking at guidelines developed by Norwegian Public Roads Administration, chapter 2. In chapter 3, management, consequences and costs related to buried steel pipe bridges are studied. The structural system and deterioration of buried steel pipe bridges are given attention in chapter 4. All these topics are covered in order to give an understanding of the management and inspection process as well as physical theory. In later chapters, probabilistic methods are used to assess these topics further.

Bayesian decision trees illustrate how uncertainties related to inspection and decision making can be handled in a consistent manner. This method is shown in chapter 5. The theory is extended by looking at Bayesian networks and influence diagrams which can treat higher complexity problems and guide inspection of bridges in an illustrative way, chapter 6. Bayesian networks are also used to illustrate the variables and dependencies related to the structural system and loading of buried steel pipe bridges.

Next, reliability analysis is used to evaluate the probability of yield of the steel pipe wall, chapter 7. First order reliability analysis is used for the reliability analysis. This method is fast, and it allows for studying the sensitivity of variables. The probability of yield is connected with the probability of failure in a very simple Bayesian network.

Bridge deterioration is considered in chapter 8. A Markovian process is used to describe the deterioration of the pipe bridge stock managed by NPRA. This is done by fitting a continuous-time Markov process to observation of damage development of the bridge stock. Maximum likelihood estimation is used for the regression analysis. The damage development for a selection of bridges within the bridge stock is also studied.

In chapter 9, failure predictions are carried out. The failure prediction for the bridge stock is based on a Markovian deterioration model. For failure assessment of an individual bridge, a dynamic Bayesian network is used to illustrate how such analysis might be performed.

Replacement strategies are studied in chapter 10. Risk, cost and benefit analysis are used to support replacement assessment of individual bridges. Different bridge stock replacement strategies are studied by modifying a deterioration model.

Chapter 2

Inspection of bridges by Norwegian Public Roads Administration

2.1 General

Today's common practice for bridge inspections in Norway is presented in this chapter by looking at some of the main elements from the guideline manual for inspection of bridges V441 by NPRA (2000).

Manual R411 gives the following definition of bridge inspection: *Inspeksjon er visuell kontroll kombinert med oppmålinger og materialundersøkelser som utføres for å bedømme bruenes tilstand og sikkerhetsnivå. Inspeksjonen skal avdekke behovet for driftstiltak og/eller vedlikehold samt eventuelt behov for forsterkning eller ombygning.*

The definition states that inspection of bridges involves visual inspection combined with measurements and material testing in order to grade the state and safety level of the bridge. The inspection shall reveal the need for operational measures and/or maintenance as well as possible need for upgrade or replacement.

2.2 Damage assessment

2.2.1 General

Chapter 5 in the manual V441, NPRA (2000), treats assessment of damages. The manual states that assessment of bridge damage includes assessing which type of damage the damage belongs to, the severity of the damage for the bridge and the cause of the damage.

Usually damages are considered and assessed on basis of visual inspection, measurements and testing material. In some cases, structural calculations, economic considerations or structural monitoring over time shall be performed to give the right evaluation of damages.

To keep consistency in the evaluation of damages, Norwegian Public Roads Administration has introduced classification of damage type, damage degree, damage consequence and the cause of damage.

2.2.2 Damage type

The main categories of damage types are:

- damage not related to material
- damage of ground
- damage of concrete
- damage of steel
- damage of stone
- damage of timber
- damage of road surface/moisture insulation
- deficiency
- other damages/deficiencies

2.2.3 Damage degree and consequence

Damage degree is introduced to give an indication of the seriousness of the damage as well as how soon an action towards the damage should be performed. Norwegian Public Roads Administration has set four levels of damage degrees:

1 Small damage/deficiency: no action required
2 Medium damage/deficiency: action required within 4-10 years
3 Large damage/deficiency: action required within 1-3 years
4 Critical damage/deficiency: immediate action required or at latest within ½ years

Damage consequence indicates which consequence a damage brings for the bridge and the environment. The following consequences are used:

B Damage/deficiency that threatens the bearing capacity
T Damage/deficiency that threatens road safety
V Damage/deficiency that can increase maintenance cost
M Damage/deficiency that can affect the environment/aesthetic

In addition to these categories, traffic costs should also be considered when relevant.

Damage degree and consequence is combined to give simple information about a damage. A 3T-damage is a large damage that reduces road safety, and which should be repaired within 1-3 years.

A damage can have a damage degree associated with each damage consequence. For example, corrosion of a buried pipe bridge can be a small damage in light of bearing capacity, large in light of maintenance cost and small in light of aesthetics/environment. This damage is then a 1B, 3V and 1M damage.

2.2.4 Assessment of damages

The relation between damages shall be considered. Primary damage can lead to secondary damage. A primary damage shall in general be treated before it leads to secondary damage.

The damage development is important in consideration of damage and consequence. Manual V441, NPRA (2000), illustrates some different types of deterioration, figure 2.2.1. The four general damage development characteristics are:

- no further damage development
- reducing damage development
- linear damage development
- exponential damage development

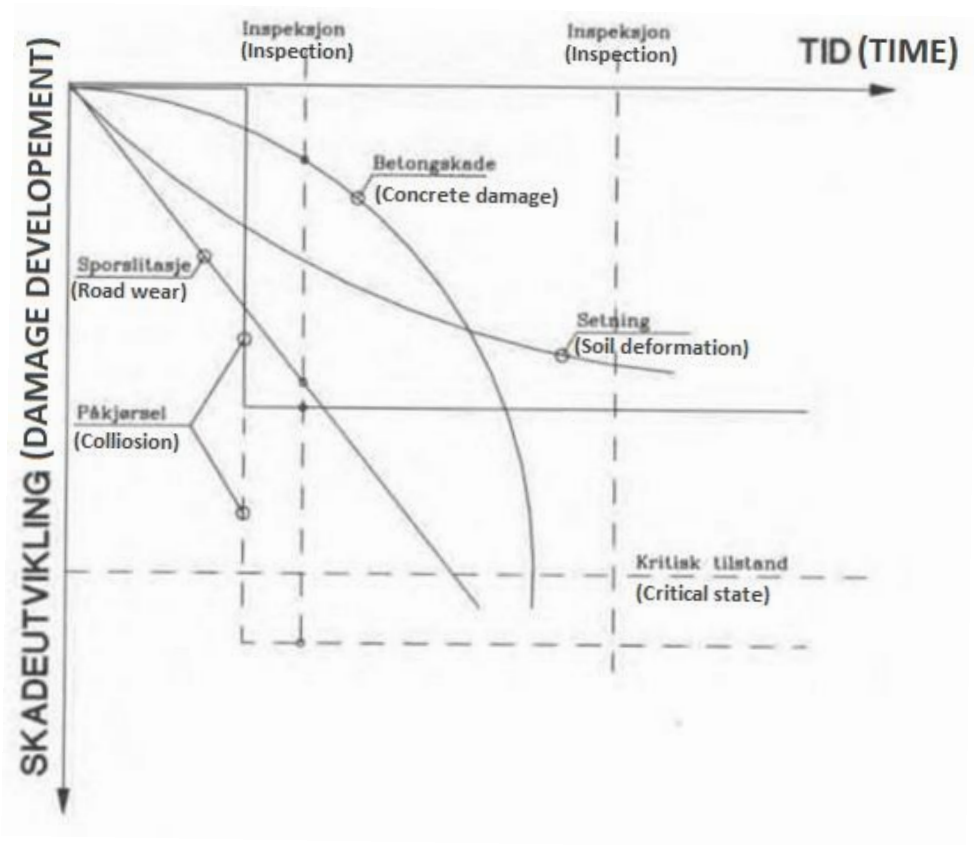

Figure 2.2.1: Damage development (V441, NPRA 2000)

Collision damage might belong to no further damage development category. The damage will not develop further, but it is important to know if the damage might lead to secondary damages. Soil deformation is a damage where the damage development is often reduced over time. Road wear of the road surface will often have a linear damage development. Many concrete damages belong to the exponential damage development category. Thin concrete cover makes the concrete vulnerable to chloride penetration and carbonate-induced corrosion.

2.2.5 Maintenance priority

A prioritisation of maintenance can be made on basis of the damage assessment. From the damage degree and consequence classification, the consequence of delayed maintenance can be estimated. Extra care for damages that affects the bearing capacity and road safety should be considered, as these damages can lead to necessity of road traffic reduction or special road safety measures in case the damage is not treated in recommended time.

2.2.6 Cause of damage

It is important to understand the cause of the damage to do corrective repair. It is especially important to understand the cause of a primary damage which can lead to further damages. The manual divides cause of damages for bridges into nine main categories:

10 Faulty design
20 Faulty material
30 Faulty execution
40 Lack of operation/maintenance
50 Environmental attack
60 Loading
70 Damage from accident
80 Damage from usage
90 Other/unknown

Category 60 indicates that the damage is caused by loading. Subcategory 62 indicates that the damage is caused by earth load.

Norwegian Public Roads Administration states that the cause of damage is mainly determined by visual inspection. Measurements and material testing may be included in the determination of cause of damage.

2.2.7 Degree of damage consequence

A new approach in the evaluation of damages by NPRA includes the degree of a damage consequence. The degree of damage consequence ranges from 1 to 4.

To illustrate this concept: two bridges with a similar damage with the same damage degree is considered. The damage causes consequence for the road safety. One of the bridges has a high speed limit, while the other bridge has a low speed limit. For the bridge with high speed limit, the degree of road safety consequence is higher as the probability of accident will be higher when the driver approaches the damaged road in a high speed. The damage consequence degree for the low speed limit is lower as the driver has more control in low speed.

The priority of action for the damage is suggested to be the product between damage degree and damage consequence degree. From this, a priority chart can be developed. Green indicates lower priority, yellow indicates medium priority and red indicates high priority in the damage assessment. The priority table is shown below, table 2.2.1.

Table 2.2.1: Priority scheme

Damage consequence degree				
4	4	8	12	16
3	3	6	9	12
2	2	4	6	8
1	1	2	3	4
	1	2	3	4
	Damage degree			

2.2.8 Brutus

Brutus is Norwegian Public Roads Administration's tool in management, operation and inspection of bridges. It consists of a database where information of each bridge is stored. The most important modules of the program are the buildings, inspection, maintenance and cost module.

2.3 Material testing, measurement, instrumentation and special inspection

2.3.1 Material testing, measurement and instrumentation

Chapter 7.1 in manual V441, NPRA (2000), states that it might be necessary to perform material testing, measurement, and instrumentation as supplement to visual control to reveal hidden damages or to get a better understanding about a damage: extent of damage, cause of damage, damage degree and damage consequence. The manual further gives guidelines on how to perform testing. In many cases, testing will require special routines, knowledge and tools. Some measurements might be included in the main inspection and simple inspections, but if the measurements are more specific, the measurements are done through special inspection.

2.3.2 Special inspection

If the main inspection reveals large need for repair or the damage classification is not sufficient, special inspection should be performed. Special inspection is an inspection with higher requirements than the main inspection. Special inspection shall be accurate enough to classify damage type, damage consequence, extent of damage and the cause of damage. Static calculations might also be necessary.

2.3.3 Utility

The utility and necessity of performing measurements and special routines shall be realistic. In the question of utility of measurement comes also the comparison of utility between different measurements. For measuring chloride content in concrete, different methods are available. In-field measuring methods are simple and relatively cheap compared to laboratory measurements, but the accuracy for in-field methods are lower than for laboratory methods. It

may be difficult to justify the choice of one method over the other if the utility of the method is not quantified.

2.4 Conclusion

The manual gives a practical and simple guidance in the inspection of bridges. Decisions and classifications may however differ between different inspectors. There are no clear threshold criterions for the different classifications. Decisions as whether to do measurements, special inspections and which actions to make is not always obvious. Chapter 5 in this document, introducing Bayesian decision analysis, shows how these decisions may be performed in a more consistent manner.

Chapter 3

Buried steel pipe bridges - management, consequences and costs

3.1 General

The condition of the corrugated steel pipe bridges manged by NPRA varies from no damage to critical damage with corrosion, thickness reduction of pipe wall and erosion of supportive soil. There have been incidents of collapses while traffic has been running over the pipes. These failures can lead to loss of life. High risk for collapse can occur in flooding events. This will possibly lead to closing of the road with necessary emergency repair. Without doubt, the consequences from damages of these pipes can be very large. It is also an uncertain situation, and the evaluation of pipe conditions and necessary actions has been weak according to Norwegian Public Roads Administration. The extent and risk of bad structural conditions has not been sufficiently known.

This chapter introduces topics related to management and inspection of buried steel pipe bridges. It is important to understand costs and consequences from buried steel pipe bridges for the decision making, and this therefore presented in this chapter.

3.2 Management and inspection

3.2.1 General

Topics related to management and inspection of steel pipe bridges include typical failure modes, consequences, actions and inspection measurements. A manual by the Department of Transport of Main Roads (2015), Queensland, Australia, considers inspection of corrugated metal culverts. This manual is of inspiration for several parts of this section.

3.2.2 Failure modes

Metal pipes may fail by web crushing or buckling. Some of the main reasons for failure of the metal pipes are large traffic load, loss of cross-sectional area, erosion of soil and softening of soil. Even though there is buckling or yield of the metal pipe, the structural system might still be standing due to the arching effect. In this case, loads are transferred through the surrounding soil, rather than the pipe.

Since both the condition of the soil and the pipe is important for the condition of the structure, loss of soil could also lead to consequence for the function of the structure. Flooding can wash away soil and create chasm over the road. Soil can also be washed away from the inside of the pipe if there are holes in the pipe wall from corrosion and water is running through it. A

damaged wingwall can lead to loss of soil. Earthquake and frost heave can create ground movement.

Complete failure of the structural system will often be a combination of damage to the pipe and surrounding soil.

3.2.3 Actions

According to Queensland Department of Transport of Main Roads some of the actions to treat a deteriorated pipe are:

- Do nothing
- Restrict heavy vehicles
- Restrict heavy vehicles after periods of flood
- Close road and monitor the structure after observed changes
- Temporary install supportive bars inside the pipe at emergency
- Construct temporary side-track at emergency
- Eliminate pipe
- Extend lifetime with maintenance
- Rehabilitate pipe with aim of new design life
- Replace pipe

Methods to extend the life of the pipe includes: supportive bars, application of thin concrete layer to protect inside wall towards corrosion, other corrosion protections and joint repairs. Rehabilitation may be done with relining by sliding in a new pipe into the existing pipe. A new pipe may be made from high-density polyethylene, PVC, reinforced concrete or steel. Relining may be performed while traffic is running. Velocity of water running through pipe might increase from relining. Replacing the pipe may be done with removal of soil and full or partly road closure. It may also be done with the soil in place and traffic running by using some tunnelling methods, jacking or boring.

Norwegian Public Roads Administration has applied a thin concrete layer to protect towards internal corrosion for some pipes. There are uncertainties related to this method. It may hide corrosion of the external surface of the pipe. For highly deteriorated pipes, the preferred action is replacement.

3.2.4 Inspection

In inspection of metal pipes, the manual by Queensland DTMR suggest collecting the following information:

- Pipe type
- Pipe geometry
- Corrugation geometry
- Depth of pipe crown
- Wall thickness
- Maximum outside diameter
- Voids in surrounding soil
- Defects

There are several measurement methods to get more information about the steel pipes, depending on which information is of interest. A few of these methods are mentioned here.

An ultrasonic thickness gauge can be an effective tool in measuring the effective thickness of the pipe wall. The gauge uses ultrasonic waves to measure the thickness in a non-destructive way. The ultrasonic sensor is pressed into the metal at a point from one side of the pipe. By the time the wave takes from being sent and received by the sensor, the instrument measures the effective thickness at that point. It is especially useful when only one side of the pipe is accessible, which is usually the case. The measurement may indicate deterioration of wall thickness.

Geotechnical measurements may be relevant to get a better understanding of the geotechnical conditions. The modulus of elasticity of soil surrounding culvert affects the structural strength of the pipe system, as the soil is part of the system. A dynamic penetration test may be used in order to get an estimation of the properties of the soil. Dynamic cone penetrometer uses a weight that drops over a cone and makes it penetrate through the soil. This gives estimation of soil type and layers, soil elasticity and deformation properties. Queensland DTMR illustrates a suggestion of where to take measurements with dynamic cone penetrometer. This is shown in figure 3.2.1. The left measurement is done 1.5 meters from the culvert wall, the middle measurement is done as close as possible to the culvert, and the right measurement is done between two culverts.

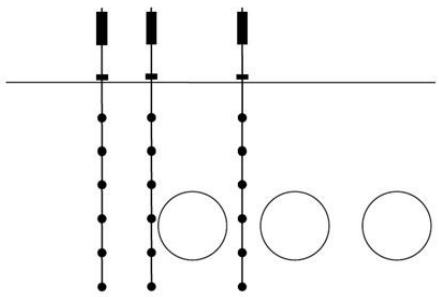

Figure 3.2.1: Dynamic cone penetrometer measurements (QDTMR 2015)

Norwegian Public Roads Administration does in general not perform testing and measurement with instruments for normal inspections. The condition is usually assessed by visual inspection.

3.3 Consequences and costs

3.3.1 General

Consequences related to buried pipe bridges is presented in this chapter. The life-cycle cost is also presented, and it is important to create a picture of costs over time. Cost might be divided into cost to the owner of the bridge and cost to the user of the bridge.

3.3.2 Consequences related to pipe bridges

There are many aspects of consequences related to the deterioration of corrugated steel pipe bridges. As previously stated, Norwegian Public Roads Administration divide consequences of

existing bridges into four types of consequences: bearing capacity, road safety, maintenance cost and aesthetics and environment.

Irregularities in the road causes danger to the road safety. These irregularities may arise from road chasm from flood and deformation of the pipe which leads to deformation of the road. Consequences in relation to road safety ranges from damage of vehicles, injuries to people and in the most severe case, death.

A pipe with high corrosion and erosion might not be very aesthetical. These corrugated pipe bridges are, however, often very discrete bridges. There is a top layer of soil, and in many cases, one might not even notice the bridge is there. No further focus will be directed towards the environmental and aesthetical aspects in this paper.

The maintenance cost includes costs for maintaining the pipe bridge. This may for example be the cost for removing stones in the pipe, cleaning vegetational growth or maintaining good soil conditions after a period with flood and erosion.

Emergency actions may lead to high costs and consequences. These costs are sometimes not considered in the budget. It includes possible emergency repair, replacement, and construction of side-track.

3.3.3 Bridge life-cycle cost

Costs and consequences can be expressed in a life-cycle perspective. These are costs for both the owner and the user. Life-cycle cost include an initial design and construction cost, C_0, inspection, maintenance and operation cost, C_I, rehabilitation and replacement cost, C_R and failure cost, C_F. In addition, a general user cost, C_U, includes costs or loss due to conditions of the bridge that might affect the user, as reduced road safety. Several of these costs are uncertain, and probabilistic. A formula for the expected life-cycle cost may be expressed as:

$$E[C] = E[C_0 + C_I + C_R + C_F + C_U] \tag{3.3.1}$$

3.3.4 User cost

User cost includes cost or loss related to accidents and traffic disruptions leading to detours and delays. The cost may be divided into cost to the society and cost to the private users. The social cost is connected to consequences to the society. Private user cost affects the users' private economy. Focus is directed towards social cost. The user cost term will imply cost to the users in the perspective of the society.

The amount of traffic on the road is important for the user cost. The culverts are both on Norwegian national roads and county roads. The national roads have larger amount of traffic, connects the regions of the country together and are important for long-distance travel. County roads have a smaller amount of traffic and are important for the accessibility and infrastructure within the county.

Norwegian Public Roads Administration has a database for the annual average daily traffic, AADT, for all roads. The database gives information about the amount of light vehicle traffic and heavy vehicle traffic.

3.3.5 Cost of accidents

Accidents can lead to injuries to people. This may lead to high medical costs. The injured might experience daily challenges and a reduced life quality. An accident may affect the people that care about the injured. This is especially the case when an accident involves death. The Norwegian Institute of Transport Economics has quantified the costs from different accidents. These costs include both monetary costs related to the injuries and costs related to consequences as reduced life quality and reduced life expectancy. Based on this research, Norwegian Public Roads Administration gives the costs for different accidents in their manual V712, NPRA (2018):

Table 3.3.1: Social cost for different accidents (V712, NPRA 2018)

Accident	Cost NOK/ accident (2016)
Death	30,200,000
Critical injury	27,100,000
Serious injury	9,600,000
Minor injury	730,000
Material damage	38,000

The accidental cost, C_A, is the sum of cost for each accident, C_{Ai}, times the probability of the accident, P_{Ai}.

$$C_A = \sum_{i=1}^{N} P_{A_i} \cdot C_{A_i} \tag{3.3.2}$$

3.3.6 Cost of traffic disruption

The bridge condition and activities related to the bridge might lead to traffic disruptions as delays and detours. The social cost indicates the society's willingness to pay for avoiding delays and detours. This is related to consequences for environment, health, safety, infrastructure and reduced wealth for industry and people in the society's perspective. Special consideration towards traffic disruption should be taken into account if there are special circumstances. This may be roads with highly valuable freight transport. Vulnerable circumstances will also need special consideration. This may be the case if emergency vehicles highly depend on the road.

When the road is closed due to circumstances related to the bridge, users may prefer alternative roads. The user cost for longer distance detours are given by NPRA (2018), manual V712, based on studies by Samstad (2017). The cost includes costs for fuel, oil and tire, repairs and maintenance and capital costs as shown in table 3.3.2. The costs are differentiated between light vehicles and heavy vehicles. The capital cost for light vehicles are assumed to be distance dependent. For heavy vehicles the capital cost is assumed to be time dependent, and it is

included in an operational cost which also include salary cost to driver, administration, garage and fees. This user operational cost is given in table 3.3.3.

Table 3.3.2: Detour cost by detour distance (Samstad 2017)

	Cost NOK/km (2016)	
Detour cost	**Light vehicles (< 3.5 tonnes)**	**Heavy vehicles (> 3.5 tonnes)**
Fuel	0.32	1.72
Oil/tire	0.23	1.09
Repair	0.89	1.29
Capital cost	0.5	-
Sum	1.74	4.10

Table 3.3.3: Operation cost for heavy vehicles (Samstad 2017)

Operation cost	**Cost NOK/ vehicle-hour (2016)**
Heavy vehicles	676
Bus	487

The cost from detour due to traffic disruption, C_T, may be expressed as in equation 3.3.3. $AADT_l$ and $AADT_h$ are the annual average daily traffic of light and heavy vehicles, respectively. The detour cost by distance is c_{dl} for light vehicles and c_{dh} for heavy vehicles. c_{oh} is the operational cost for heavy vehicles. l_d is the distance of the detour, and t_d is the time it takes to drive the detour. The number of days the traffic is disrupted is t_D. The operation cost might be divided to include bus operation cost if the portion of heavy vehicles being busses is known.

$$C_T = \left(AADT_l \cdot c_{dl} \cdot l_d + AADT_h(c_{dh} \cdot l_d + c_{oh} \cdot t_d)\right) \cdot t_D \tag{3.3.3}$$

Delays also bring consequences to users. It is difficult to estimate the circumstances around an unforeseen event, and the cost for delays are difficult to estimate. The Norwegian Institute of Transport Economics has analysed the value of travel time per person for different distances, report 1389 (2015). The time value for travellers based on this study is given by manual V712, NPRA (2018), and it is shown in table 3.3.4 here. The validity of this data for unforeseen events is questionable, as the value of travel time is based on foreseen travel time reduction.

Table 3.3.4: Time value for travellers (manual V712, NPRA 2018)

	Value in NOK/person-hour (2016)					
	Light car			**Bus**		
Type of travel	<70 km	70 -200 km	>200 km	<70 km	70 -200 km	>200 km
Business travel	449	449	449	449	449	449
Commute	100	217	217	70	94	94
Leisure travel	85	169	169	64	79	97

3.4 Replacement cost

3.4.1 General

The replacement cost is an important cost in the decision making of existing culverts. It is one of the major parameters in the assessment of benefit-cost. The total cost for renewal of the pipe can be divided into different costs. Owner costs include design cost, $C_{R,D}$, and construction cost, $C_{R,C}$. The user costs include an accidental cost, $C_{R,A}$, and a traffic disruption cost, $C_{R,T}$.

$$C_R = C_{R,D} + C_{R,C} + C_{R,A} + C_{R,T} \tag{3.4.1}$$

3.4.2 Design cost

The design cost at planned replacement, $C_{R,D}$, is the cost for design of a new culvert or bridge. This includes a cost for a hydrology report, $C_{R,hydro}$, that predicts the drainage basin and water flow for design of the pipe. It also includes a design cost with calculations and drawings of a new pipe or bridge, $C_{R,design}$.

$$C_{R,D} = C_{R,hydro} + C_{R,design} \tag{3.4.2}$$

3.4.3 Construction cost

Construction cost at planned replacement, $C_{R,C}$, consist of all costs related to the construction of a new culvert. This includes cost for in-field preparations, $C_{R,prep}$, alerting construction cost, $C_{R,alert}$, cost for a new pipe, $C_{R,pipe}$, executing construction cost, $C_{R,exe}$, and, when necessary, the cost for a temporary bridge, $C_{R,temp}$. The temporary bridge cost, $C_{R,temp}$, has an initial cost and a rental cost.

$$C_{R,C} = C_{R,prep} + C_{R,alert} + C_{R,pipe} + C_{R,exe} + C_{R,temp} \tag{3.4.3}$$

Some important variables for the construction cost are the size and the type of the pipe bridge. Figure 3.4.1 shows examples of different number of pipes. Norwegian Public Roads Administration will usually replace system I with a new small to normal size pipe culvert, system II will usually be replaced with a new pipe culvert or a smaller bridge, and system III will usually be replaced with a bridge.

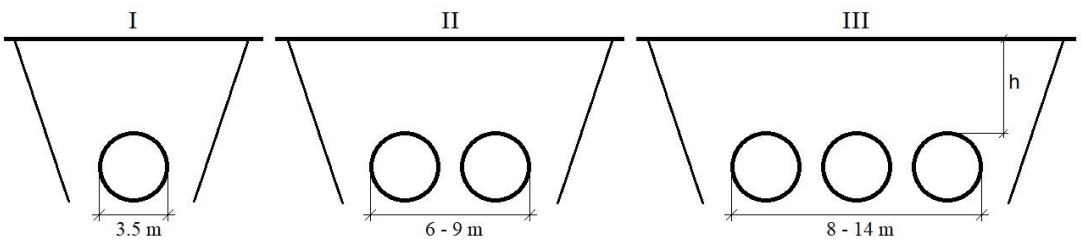

Figure 3.4.1: Common corrugated pipe systems

The amount of soil is an important parameter for the cost of replacing the pipe as this decides the amount of soil to be dug. The height of covering soil, *h*, is less than four meters for most of

NPRA's pipe bridges. The length of the pipe is another important parameter for the amount of covering soil, as shown in figure 3.4.2. This length is usually around 20-30 meters, but ranges from 4-300 meters. Very long structures are rare.

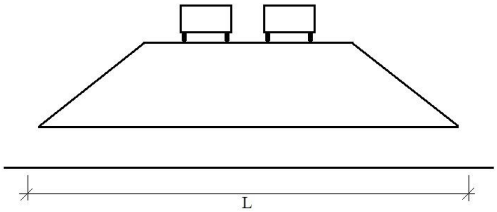

Figure 3.4.2: Length of pipe

3.4.4 Accidental cost

Accidental cost may include accidental cost for workers and conditions associated with the replacement and construction work itself as well as accidents related to traffic. In general, with good planning, the probability for traffic accident should be low when the replacement is planned. Equation 3.3.2 may be used for accidental replacement cost, $C_{R,A}$.

3.4.5 Traffic disruption cost

The traffic disruption cost is dependent on the conditions. This includes conditions as alternative roads and alternative transportation options. The cost of traffic disruption with detours, $C_{R,T}$, is expressed as in equation 3.3.3. The time with detour might be the time with construction, $t_D = t_{const}$. A constructed side track might reduce or eliminate this cost, but there will be a cost associated with the side track.

3.4.6 Example cost

An example of cost related to planned replacement of a buried pipe is shown. A single normal size buried pipe is considered. The total design cost is assumed to be $C_{R,D}$ = 1,000,000 NOK. This includes the hydrology report which is about 100,000 NOK. The total construction cost is set to $C_{R,C}$ = 4,000,000 NOK. This cost is highly dependent on the size of the project. It is assumed that a temporary bridge is not necessary. Accidental cost for planned replacement of the bridge is neglected, $C_{R,A} = 0$.

The road is assumed to have an annual average daily traffic of *AADT* = 3,450 vehicles/day, which consists of 3,000 light vehicles/day and the rest is heavy traffic. The detour is assumed to be 10 km and it takes 0.2 hours to drive this route. Construction time is three days and it is necessary to take the detour for these three days, $t_D = t_{\mathrm{const}} = 3$ days. From equation 3.3.3, the expected detour cost is:

$$C_{R,T} = \left(3{,}000 \cdot 1.74 \cdot 10 + 450 \cdot (4.10 \cdot 10 + 676 \cdot 0.2)\right) \cdot 3 = 395{,}000 \text{ NOK (2016)}$$

The total planned replacement cost is:

$$C_R = 1{,}000{,}000 + 4{,}000{,}000 + 395{,}000 = 5{,}395{,}000 \text{ NOK (2016)}$$

3.5 Failure cost

3.5.1 General

When a culvert fails, there are risk associated with the failure. A new culvert or bridge must be constructed to replace the failed culvert. The expected cost from failure has many of the same costs as a planned replacement, but the cost for each element will often be different. The failure cost, C_F, include design cost, $C_{F,D}$, construction cost, $C_{F,C}$, accidental cost, $C_{F,A}$ and traffic disruption cost, $C_{F,T}$.

$$C_F = C_{F,D} + C_{F,C} + C_{F,A} + C_{F,T} \tag{3.5.1}$$

3.5.2 Design cost

From experience by inspectors at Norwegian Public Roads Administration, the cost for a hydrology report may be 20% larger after a sudden failure compared to a planned replacement. The design of a new bridge may be 10% - 30% larger at failure compared to planned replacement. A rough estimate for the design cost at failure, $C_{F,D,}$ is:

$$C_{F,D} = 1.2 \cdot C_{R,hydro} + 1.2 \cdot C_{R,design} \tag{3.5.2}$$

3.5.3 Construction cost

It is more likely that a temporary bridge will be necessary at failure, and the time for a temporary bridge will often be longer for failure compared planned replacement. Other construction costs are often quite similar between a failure and a planned replacement from the experience of inspectors at NPRA. An estimate for the construction cost at failure, $C_{F,C,}$ may therefore have many of the same elements as a planned replacement, equation 3.4.3. The temporary bridge cost at planned replacement, $C_{R,temp}$, is replaced with a temporary bridge cost at failure, $C_{F,temp}$.

$$C_{F,C} = C_{R,prep} + C_{R,alert} + C_{R,pipe} + C_{R,exe} + C_{F,temp} \tag{3.5.3}$$

3.5.4 Accidental cost

The probability for accidents from a failure is quite significant, and this leads to high risk. Equation 3.3.2 should be used to calculate the expected failure cost, $C_{F,A}$. The risk is high from the failure itself. In addition, a temporary bridge and the replacement of a bridge itself might contribute to risk.

3.5.5 Traffic disruption cost

The cost from traffic disruption due to failure, $C_{F,T,}$ could become very high. A failure is not planned, and alternative roads and solutions might be limited. A temporary bridge might be used for longer time, and this will possibly also disrupt traffic. There will be a response time, t_{resp}, before work can begin after failure. In addition, the road will be closed during construction

of a new bridge, t_{const}. Equation 3.3.3 with $t_D = t_{resp} + t_{const}$ may be used for detour cost. The response time could typically be 2-7 days from NPRA's experience.

3.5.6 Example cost

The example failure cost is based on assumptions similar to the planned replacement example. Design cost may be 20% larger for failure, $C_{F,D}$ = 1,200,000 NOK. It is assumed that a temporary bridge is not necessary. The total construction cost is then similar to a planned replacement, $C_{F,C}$ = 4,000,000 NOK.

Some predictions or assumptions in regards of accident probabilities must be made in order to calculate an expected accidental cost. It is assumed that the probability for one death is 0.1. That is one death per tenth failure. The probability for one person being critical injured is assumed to be 0.15. Two deaths or two people being injured are also considered, and the probability for these are assumed to be 0.02 and 0.05, respectively. With these assumptions, the expected accidental cost is:

$$\begin{aligned} C_{F,A} &= 30{,}200{,}000 \cdot (0.10 + 2 \cdot 0.02) + 27{,}100{,}000 \cdot (0.15 + 2 \cdot 0.05) \\ &= 11{,}003{,}000 \text{ NOK (2016)} \end{aligned}$$

It is assumed that it takes five days to respond and start construction if there is failure. There will therefore be five additional days where detour is necessary:

$$\begin{aligned} C_{F,T} &= \big(3{,}000 \cdot 1.74 \cdot 10 + 450 \cdot (4.10 \cdot 10 + 676 \cdot 0.2)\big) \cdot (3 + 5) \\ &= 1{,}052{,}000 \text{ NOK (2016)} \end{aligned}$$

The total expected failure cost is:

$$C_F = 1{,}200{,}000 + 4{,}000{,}000 + 11{,}003{,}000 + 1{,}052{,}000 = 17{,}255{,}000 \text{ NOK (2016)}$$

3.6 Conclusion

Management, costs and consequences related to buried steel pipe bridges have been discussed in this chapter. Analysis of costs and consequences are important for decision making related to bridges. A failure might have especially large consequences for the user of the bridge. It might also have a large monetary impact which is not taken account for in the budget.

Chapter 4

Buried steel pipe bridges - structural system and deterioration

4.1 General

The structural system and deterioration of steel pipe bridges are studied and presented in this chapter. It is important to have an understanding of the structural system and the deterioration processes in order to make the right decisions.

4.2 Structural system

4.2.1 General

In order to get an understanding of the capacity and loading of corrugated steel pipes, the structural system is considered. In the following chapter, theory describing loading and structural behaviour of corrugated steel pipes will be introduced. Manual V220 (2010) by NPRA consider design of buried pipes. Some of the methods will be discussed, together with additional theory.

4.2.2 Structural behaviour under loading

4.2.2.1 Flexible and stiff pipe classification

The distribution of loading on the pipe is highly dependent on the stiffness of the pipe and the properties of the surrounding soil. A pipe which is considered stiff has a stiffness larger than the surrounding soil. A flexible pipe has less stiffness than the surrounding soil.

I. D. Moore (2001) suggest to either consider the loading to act on the pipe-soil system, which is appropriate for flexible pipes, or to consider the loading to act directly on the pipe itself, appropriate for stiff pipes.

Typical flexible pipes are corrugated steel pipes, thin walled concrete culverts and plastic pipes. Concrete culverts, prefabricated concrete element culverts and in-situ casted concrete culverts are often considered stiff pipes according to V220, NPRA (2010). Since the pipes of consideration are corrugated steel pipes, attention will be paid toward flexible pipe behaviour.

4.2.2.2 Flexible pipe behaviour

A flexible pipe gets vertical deflection from vertical loading. This reduces its vertical diameter. The vertical reduction leads to a horizontal deflection, increasing horizontal diameter. This type of deflection-behaviour is called ovaling (Moore 2001). Due to surrounding soil, horizontal deflection is restraint, which leads to horizontal forces acting on the flexible pipe.

Another characteristic from the pipe-soil system is seen from the soil's tendency of transferring compression forces around the pipe, supporting the load by acting like a masonry arch (Moser 2001). This effect is called the arching affect.

Due to a flexible pipe's high axial stiffness and low bending stiffness, the moments in flexible pipe are in general neglectable (Moore 2001). It is common to see a ring compression in the flexible pipe.

4.2.2.3 Sprangler's model

Several models have been created to describe the stress distribution from earth load on a flexible pipe. One of the most well-known models is created by Sprangler. A vertical earth load is applied to the top of the pipe. The horizontal load is dependent on the horizontal displacement, and the supporting load in the bedding acts on a certain part of the lower section of the pipe. Figure 4.2.1 shows the basis of Sprangler's model from 1956, given by Moser (2001).

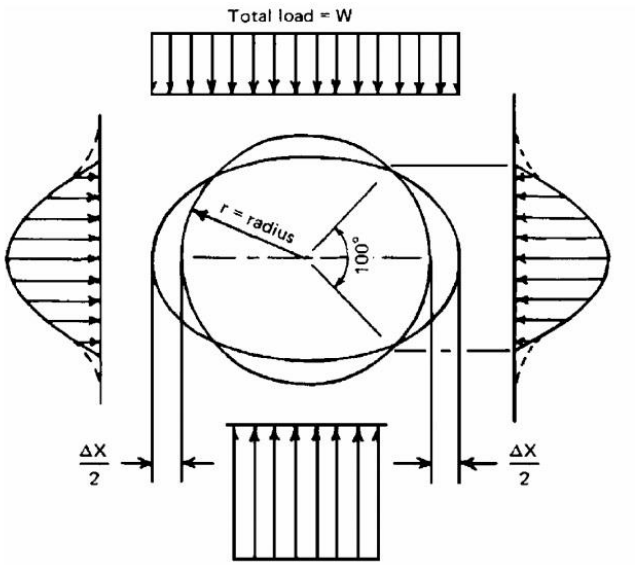

Figure 4.2.1: Sprangler's pressure distribution (Moser 2001)

Spangler derived the following formula, Iowa formula, for calculating the deflection of a flexible pipe:

$$\Delta X = \frac{D_L K W_c r^3}{EI + 0.061 e r^4} \tag{4.2.1}$$

where D_L = deflection lag factor, K = bedding constant, W_c = Marston's load per unit length pipe, r = mean radius of pipe, E = Young's modulus of pipe, I = moment of inertia of pipe wall, e = modulus of passive resistance of sidefill and ΔX = horizontal deflection (Moser 2001).

4.2.2.4 Earth load by Manual V220, NPRA 2010

The vertical earth load is presented in V220, NPRA 2010, as given in equation 4.2.2.

$$\sigma_v = N_A \cdot \gamma \cdot h \tag{4.2.2}$$

σ_v is the vertical pressure on the system, N_A is a factor dependent on the stiffness of the pipe, γ is the specific weight of the soil and h is the depth to the crown of the pipe.

The horizontal earth load acting on the pipe is:

$$\sigma_h = K \cdot \sigma_v \tag{4.2.3}$$

where σ_h is the horizontal load on the pipe. K is a factor giving the relationship between horizontal and vertical load. In many cases K is close to 1, but may for flexible pipes be even larger than 1.

Figure 4.2.2 illustrates possible earth pressure distribution for a stiff pipe (a) and a flexible pipe (b), according to V220, NPRA (2010). For the stiff pipe, the earth load acts on the pipe itself, and since it is stiffer than the surrounding soil, the pipe attracts larger portion of the earth load. Canadian Highway Bridge Design Code (2006, Ref 4) recommends values from 1.2 to 1.4 for a stiff pipe. For a flexible pipe, V220, NPRA (2010), states that the value N_A will take values of less than 1. This is generally explained by the arching effect where surrounding soil is transferring vertical compression.

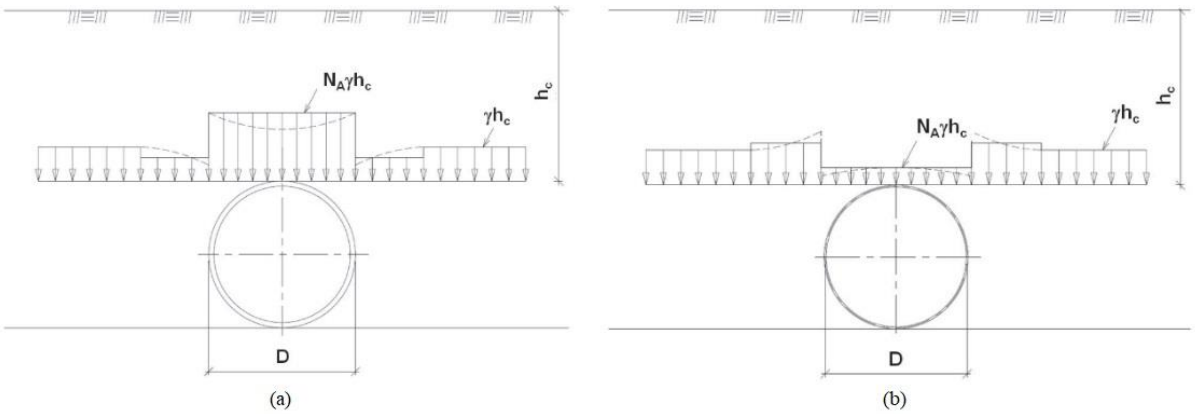

Figure 4.2.2: Vertical earth load distribution for a stiff pipe (a) and a flexible pipe (b) (V220, NPRA 2010)

4.2.2.5 Prism load

Prism loading gives a simpler approach to the loading calculations of a flexible pipe. Figure 4.2.3 shows an illustration of the prism load. The flexible pipe is assumed to carry the load from the prism above it. The weight of the prism above the pipe, W, then leads to a ring compression force, N. Introducing a constant depending on the properties of the pipe and the soil, k, the relation might be expressed as in equation 4.2.4. This equation is given by QDTMR (2015).

$$N = \frac{1}{2} W k \tag{4.2.4}$$

The weight of the soil above the pipe might be simplified to equal the soil in a prism above the crown, $W \approx h\gamma$. h is the depth to the crown of the pipe and γ is the specific weight of the soil.

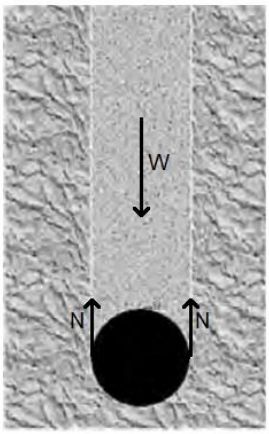

Figure 4.2.3: Ring compression force N from applied prism load W (Moser 2001, modified)

A *k*-value of 1, with no shear forces between prism and surrounding soil, leads to the expression of $N = W/2$. Moser explained this relationship to be realistic, but also somewhat conservative for calculating the forces in the pipe. Even though most other researchers agree with the method being slightly conservative due to the arching effect, Haggag (1989) found examples of the opposite, where the *k*-value might exceed 1. This illustrate the large uncertainties related to loads on buried pipes and simplified models.

If there are several pipes next to each other, then there is less possibility for arching effect. $k = 1$ might be a good estimate for several pipes, and it should in most cases be less conservative then it will be for a single pipe.

4.2.2.6 Traffic load

According to V220, NPRA (2010), the traffic load from a point load can be estimated to work as a pressure at the height of the crown on the pipe-soil system from Boussinesq equation:

$$\sigma_v = \frac{3Fh^3}{2\pi s^5} \tag{4.2.5}$$

where F is a point load, h is the height to the crown and s is the distance from the point load F to the crown. V220, NPRA (2010), calculates the pressure to an equivalent line load, $p_{traffic}$, by:

$$p_{traffic} = \frac{\sigma_v \pi h}{2} \tag{4.2.6}$$

The manual V220, NPRA (2010), assumes the maximal compression in the pipe wall to be equal to the line load, $p_{traffic}$, for smaller depth to diameter ratios, $h/D < 0.25$. For larger depth to diameter ratios, $h/D > 0.75$, the compression is set to $p_{traffic}/2$. A linear interpolation is used for values in-between. It is less likely that the live load creates a perfect ring compression by being evenly transformed to each side of the pipe for more shallow depths. It is therefore considered that one wall of the pipe must hold the whole force for concentrated force at shallow depth. A concentrated force might also create bending moment in the pipe for shallow depths, and shallow depths must therefore be carefully assessed.

An evenly distributed live load, q, may be contribute in accordance with the prism load method. Then the distributed load contributes to a compressive force, N_q, in the pipe as given in equation 4.2.7.

$$N_q = \frac{1}{2} q D k \tag{4.2.7}$$

D is the diameter of the pipe, and k is the prism load constant.

Design traffic loads for different road classifications are given by Norwegian Public Roads Administration manual R412 (2003). These are shown in table 4.2.1. The metal pipes of consideration are mostly parts of roads with classification Bk10. A dynamic amplification factor of 1.4 is included in the loads.

Table 4.2.1: Traffic loads for different road classifications from manual R412, NPRA (2003)

Load type	Load illustration		Bk10	BkT8	Bk8	Bk6
Wheel load	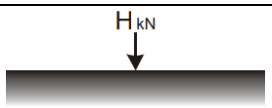	H [kN]	80	56	56	42
Single axle load	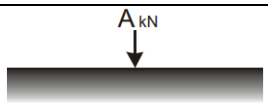	A [kN]	160	112	112	84
Tandem axle load	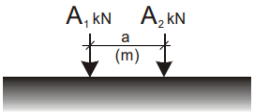	A_1 [kN]	65	40	40	30
		A_2 [kN]	160	112	112	84
		a [m]	1.3	1.2	1.2	1.2
Tridem axle load	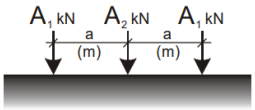	A_1 [kN]	70	60	50	40
		A_2 [kN]	140	84	84	56
		a [m]	1.3	1.2	1.2	1.2
Vehicle load	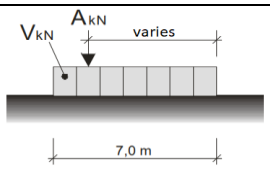	A [kN]	40	32	32	24
		V [kN]	300	280	220	180
Truck load	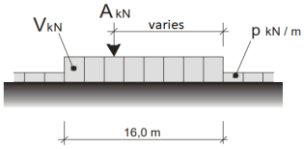	A [kN]	40	32	32	24
		V [kN]	500	400	320	280
		p [m]	6	6	6	6

Figure 4.2.4 shows the distance between loads and the minimal distance between vehicles in two loaded lanes.

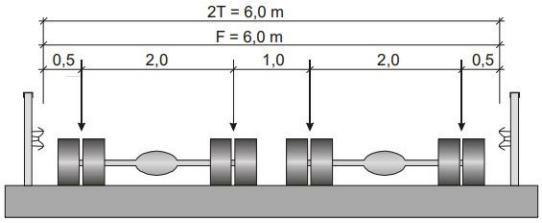

Figure 4.2.4: Two loaded lanes (R412, NPRA 2003)

The line load, $p_{traffic}$, is calculated at the crown of the pipe. Calculations are based on equations from V220, NPRA (2010), and traffic load properties from R412, NPRA (2003). The wheel load and all axle loads are considered. For several point loads, F_i, the equation becomes:

$$p_{traffic} = \frac{\sigma_v \pi h}{2} = \frac{\pi h}{2} \sum_{i=1}^{N} \frac{3F_i h^3}{2\pi s_i^5} \tag{4.2.8}$$

As an example, a single axle contributes to a line load of:

$$p_{traffic} = \frac{3h^4}{4} \left(\frac{F}{h^5} + \frac{F}{(a^2 + h^2)^{\frac{5}{2}}} \right) \tag{4.2.9}$$

where F is the load from each wheel, and a is the distance between the wheels. The point of consideration for the line load is a point vertically under one of the wheels. This gives the critical consideration for shallow depths.

Figure 4.2.5 shows the calculated line load for different crown depths for one lane loaded after Bk10 road classification.

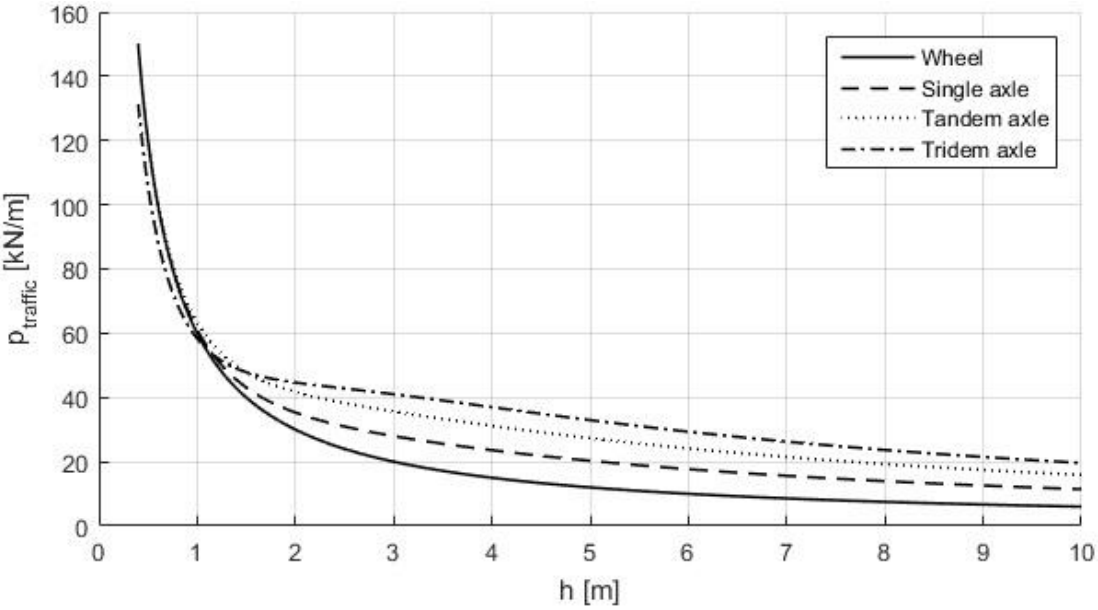

Figure 4.2.5: $p_{traffic}$ from one lane loaded after Bk10 classification

For shallow depths, the line load is largest for concentrated loads. The pipe has to carry a large portion of concentrated loads at shallow depths, as the effect of the load being distributed over the soil is less. The line load from axle loadings are therefore relatively similar to the line load from a wheel load for shallow depths. For larger depths, the total loading becomes more important than the concentration of loading.

The calculated line load for two lanes loaded after Bk10 road classification is shown in figure 4.2.6.

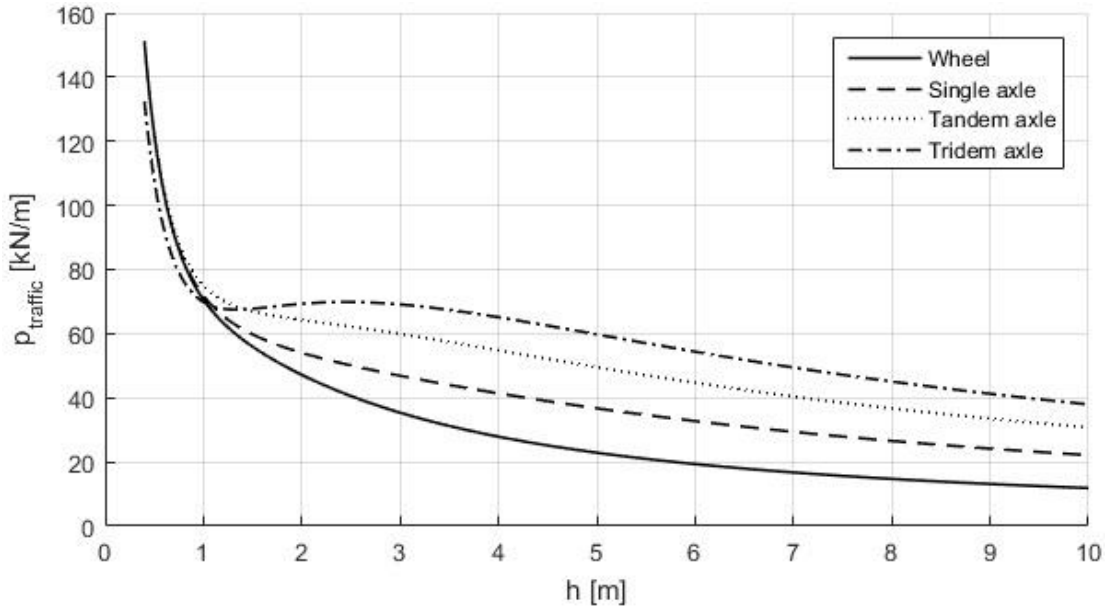

Figure 4.2.6: $p_{traffic}$ from two lanes loaded after Bk10 classification

The vehicle load and truck load from table 4.2.1 could also be considered. These loads will create a relatively low force at shallow depths, as the representation of the loads have low concentration of forces. Since the distributed component of the loads are distributed over a larger area, one might consider equation 4.2.7 for including this component in the ring compression calculation. This will, however, not create a critical load for a normal sized pipe at normal depths, $h < 10$. The vehicle load and truck load are therefore not further considered.

4.2.2.7 Ring compression from earth load and traffic load

The ring compression from a combination of earth load and traffic load is calculated to display a total ring compression. Ring compression from earth load is calculated with a prism load simplification and the prism load constant, k, is assumed to be 1. For traffic loads, the ring compression is set equal to $p_{traffic}$ for depth to diameter ratios of $h/D < 0.25$ and to $p_{traffic}/2$ for depth to diameter ratios of $h/D > 0.75$.

A pipe with a diameter of $D = 3.5$ m is considered. This is a common diameter for the pipes of consideration by NPRA. Figure 4.2.7 shows the total ring compression for two lanes loaded by a tandem and tridem axle loading as well as one lane loaded by a tandem axle. The specific weight of the soil is assumed to be $\gamma = 20$ kN/m^3.

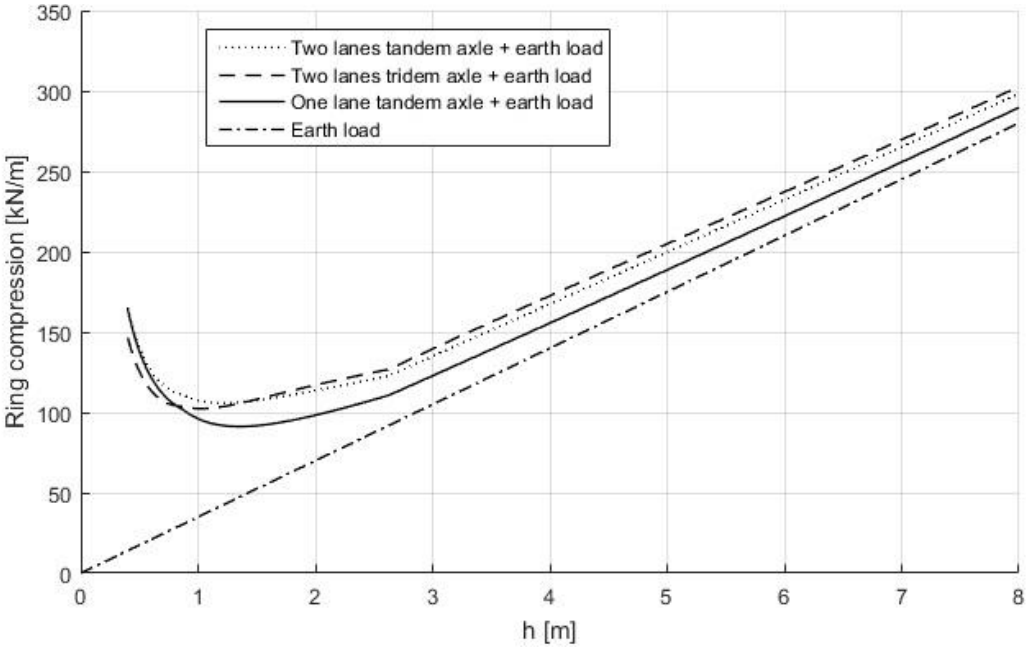

Figure 4.2.7: Ring compression for different depths, D = 3.5 m and γ = 20 kN/m^3

For shallow depths, the traffic load is the dominating load. As the depth increase, the effect of the traffic load becomes less. The earth load dominates at deeper depths, based on the assumed prism load formula.

4.2.2.8 Other conditions of consideration

Other considerations should be included in case of relevance. Some of these include non-circular cross sections, hydrostatic pressure, water in pipe, non-uniform bedding support, differential settlement and ground movement.

Non-circular culverts will have some stress concentrations. Non-uniform bedding support and differential settlement can cause bending moment and shear in the pipe. Ground movement can be caused by earthquake and frost heave.

4.2.3 Structural capacity

4.2.3.1 General

Moore (2001) lists the most common failure modes for a flexible pipe without consideration of deterioration. Typical material failure is seen by yielding or crushing. The deflection shape is characterized by ovaling. A global buckling mode is possible.

4.2.3.2 Wall crushing

The maximum and minimum circumferential stress is calculated from

$$\sigma = \frac{N}{A} \pm \frac{M}{W} \tag{4.2.10}$$

Wall crushing and yielding will occur if the stress is larger than the yield stress capacity f_y.

An alternative method to calculate the stress in the pipe is given by Moore (2001):

$$\varepsilon_\theta = \frac{-\sigma}{E_p}\ (profiled\ pipe)$$
$$\varepsilon_\theta = \frac{-\sigma\left(1-\nu_p^2\right)}{E_p}(plain\ pipe) \tag{4.2.11}$$

where ε_θ is the circumferential strain (positive in tension), σ is the circumferential stress, E_p and ν_p is the pipe's Young's modulus and Poisson's ratio, respectively.

The maximum strain ε_{max} is then calculated from the semi-empirical expression:

$$\varepsilon_{max} = D_f\left(\frac{t}{D}\right)\left(\frac{\Delta D_v}{D}\right) \tag{4.2.12}$$

Where D_f is a shape factor ranging from 4.5 to 8, t is the thickness ($2y$ for corrugated pipes), D is the diameter, and ΔD_v is the vertical deflection of the pipe.

4.2.3.3 Buckling

Moore (2001) suggest the following equation for the critical buckling load:

$$N_b = 2\sqrt{\frac{E_p I_p E'}{r}} \tag{4.2.13}$$

Where E_pI_p is the stiffness of the pipe wall, r the pipe radius and E' an empirical value of the soil stiffness.

4.3 Deterioration

4.3.1 General

There are many studies on the mechanics of buried pipes. The change in buried pipe properties over time, however, have just now gotten attention to be studied (Chen et al. 2008). Mohamed El-Taher considers the effect of corrosion and soil erosion for corrugated metal culverts in his PhD thesis (2009), supervised by I.D. Moore. El-Taher's studies includes mainly finite element analysis of the deterioration. Some of the main findings from his thesis will be presented in this chapter.

Another topic of interest within deterioration include fatigue, but for steel pipes with a depth of more than one meter, one may neglect fatigue according to V220, NPRA (2010).

4.3.2 Corrosion

4.3.2.1 General

Corrosion is a major problem for steel pipes. The corrosion often takes place at the invert of the culvert where water is present. Flowing water containing sand and gravel might accelerate the corrosion by mechanically breaking down the protective galvanized layer or oxide layer

created by corrosion. This process is called abrasion. Chlorides in the water might also accelerate the corrosion of the pipe, and it can cause pitting corrosion. If chlorides and sulphate is present in the surrounding soil, the pipe might experience pitting corrosion at the external surface.

4.3.2.2 Capacity studies

In the studies of effect of corrosion, El-Taher considered five cases of culverts with variable diameter and depth, as shown figure 4.3.1.

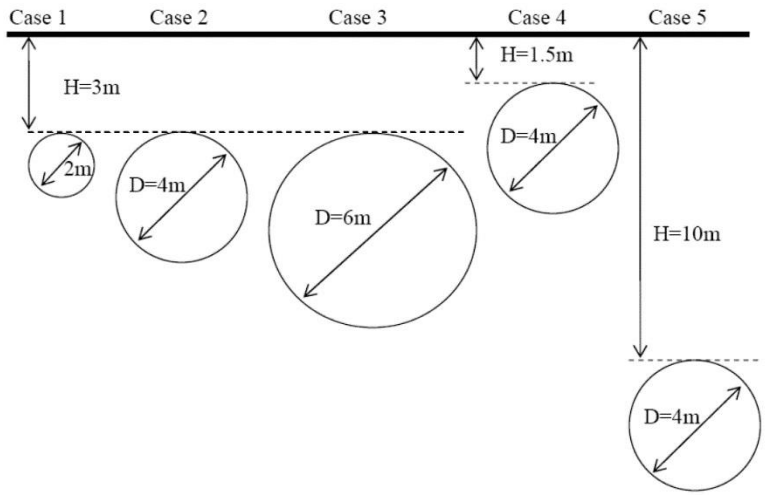

Figure 4.3.1: Cases of study (El-Taher 2009)

Three corrosion patterns were considered, 90°, 135° and 180° internal corrosion of the pipe, as illustrated in figure 4.3.2. The corrosion was modelled as reduction in thickness.

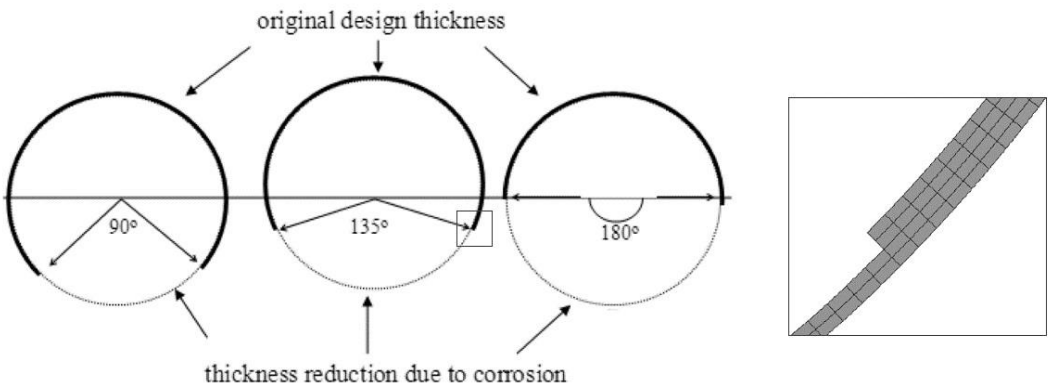

Figure 4.3.2: Reduced cross-sectional thickness from corrosion (El-Taher 2009)

4.3.2.3 Yield capacity

El-Taher's studies found that there was a tendency of proportional reduction in yield capacity and reduction in thickness. The thrust and moment in the buried pipe was barely affected by the cross-sectional reduction. Since the pipe is flexible and the surrounding soil is stiffer, the reduced pipe stiffness has little effect on the arching effect and the main compressive thrust. Figure 4.3.3 shows the relation between yield capacity at the edge of corroded zone and cross-sectional thickness for the 15 combinations of cases and reduced cross-sectional zone.

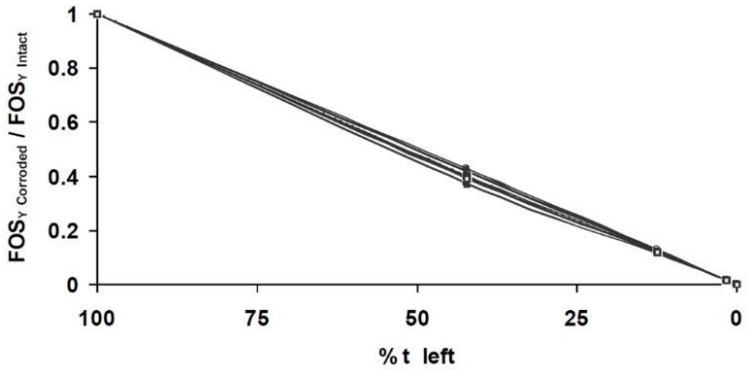

Figure 4.3.3: Relation between yielding and cross-sectional thickness (El-Taher 2009)

4.3.2.4 Buckling capacity

The effect of corrosion on buckling was also studied by El-Taher. The figures below illustrate the buckling capacity in relation to the thickness reduction. All 15 combinational cases were considered. The buckling capacity is barely affected by smaller cross-sectional reduction. Large reduction gives a sudden large capacity reduction. The effect is largest for the 180° invert corrosion, which seems to linearly reduce its buckling capacity to about 20% for a cross sectional reduction to 50%. However, Chen et al. (2008) states that for buried pipes with proper support from the soil, the yield capacity is generally the limit state.

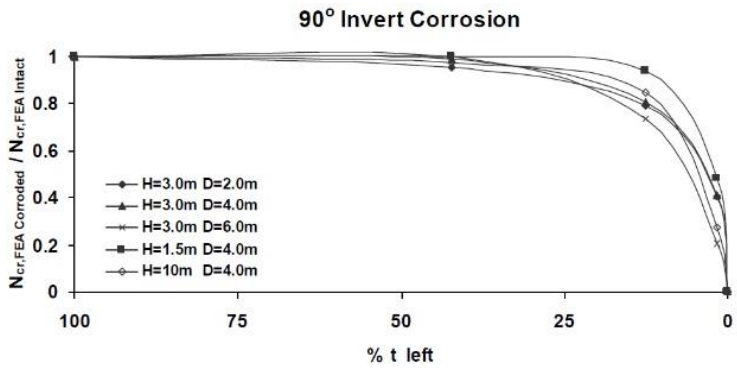

Figure 4.3.4: Buckling capacity for 90° invert corrosion (El-Taher 2009)

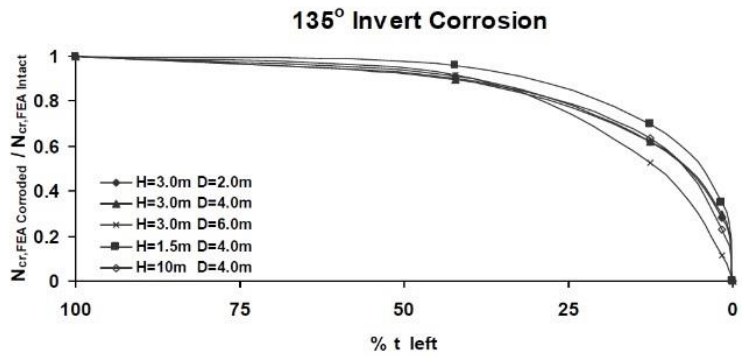

Figure 4.3.5: Buckling capacity for 135° invert corrosion (El-Taher 2009)

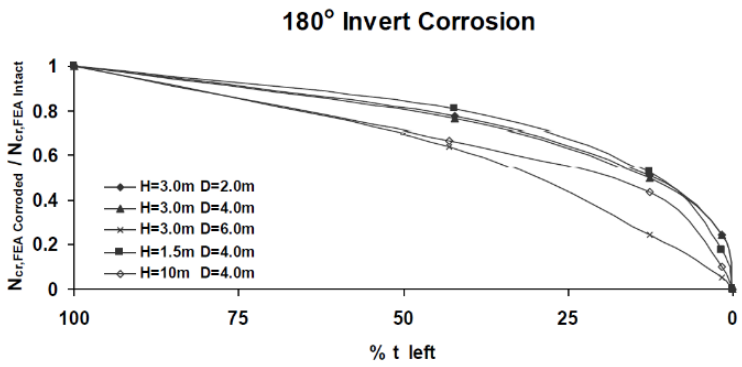

Figure 4.3.6: Buckling capacity for 180° invert corrosion (El-Taher 2009)

4.3.3 Erosion

4.3.3.1 General

Erosion of surrounding soil usually takes place when soil is being washed away with water. Granular material is often used for bedding, and this might migrate with the flowing water. If there are parts with total wall section loss due to corrosion, the soil might migrate through these holes with the flowing water in pipe. Water flow behind the culvert might cause loss of backfill. High caution should be paid towards erosion during flooding events.

4.3.3.2 Capacity studies

The effect of erosion was also studied by El-Taher. Figure 4.3.7 shows examples of finite element models used to study this effect.

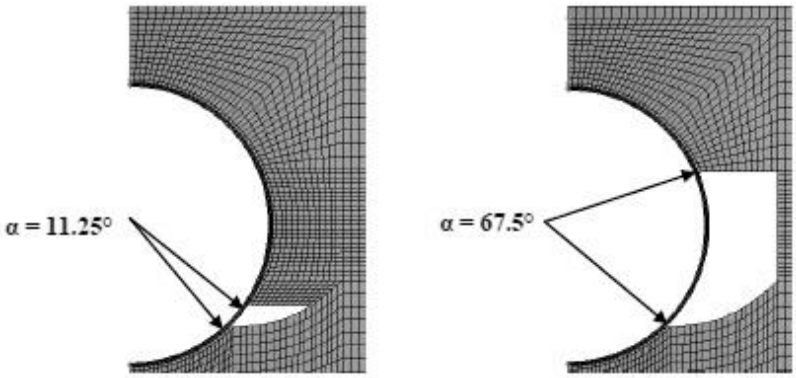

Figure 4.3.7: Pipe with soil erosion (El-Taher 2009)

4.3.3.3 Yield capacity

El-Taher found that erosion of supporting soil may lead to a decrease in compressive thrust of the pipe. This is because erosion leads to the load being transferred to the soil more so than the pipe around the eroded area. Erosion will often occur between the haunch and springline where the effect of corrosion is large. If the thrust load of the pipe at this weak part is reduced due to erosion, the load capacity leading to yield could increase.

4.3.3.4 Buckling capacity

While not necessarily giving an adverse effect for yield capacity, erosion will decrease the buckling capacity. This might lead to buckling being the critical limit state. For a combination of erosion, with and without symmetry, and corrosion, the model in figure 4.3.8 was developed. A combination of symmetrical erosion and large area of corrosion will give a very low buckling capacity. The effect of reduced buckling capacity also seems to reach its critical state even at smaller erosion angles.

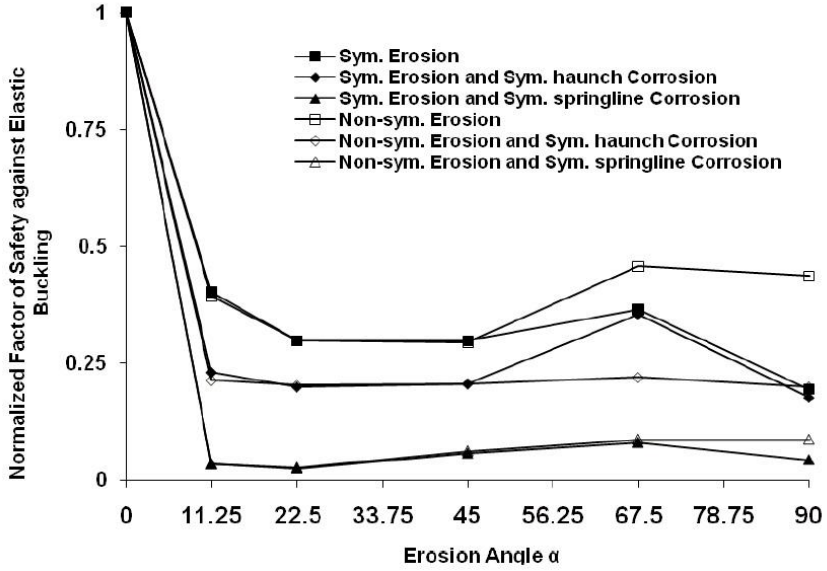

Figure 4.3.8: Reduced buckling capacity due to erosion and corrosion (El-Taher 2009)

4.4 Conclusion

A steel pipe bridge is a quite complex structure, and both the pipe and the surrounding soil is important for the structural system. Geotechnical engineering includes many uncertainties. It is difficult to exactly describe the behaviour of the soil. However, there exist simplified formulas, as the prism load to describe the loading of the pipe, and the ring compression assumption, assuming there is only compression in the pipe.

There are several types of deterioration and the change in structural capacity is presented. El-Taher's study (2009) indicates that the yield capacity might be proportional to the smallest thickness of the wall. Erosion mainly affects the buckling capacity. In the case of larger parts with erosion, buckling capacity might need to be studied. If the pipe has good support from surrounding soil, then yielding will generally occur before buckling.

Chapter 5

Bayesian decision analysis

5.1 General

An introduction to probabilistic Bayesian decision analysis is given in this chapter. The theory is mainly inspired by literature by Benjamin and Cornell (1970). The major focus is how one could make an optimal decision when there are uncertainties involved in the decision process. In a priori decision analysis, the decision analysis is based on current available information and prior probabilities. Terminal analysis is analysis when there is new information available. New information is combined with previous information and priori probabilities are reassessed to posterior probabilities by following Bayes' rule. This reduces uncertainties and can be done with for example measurements of the state of a structure. In preposterior analysis the posterior probabilities are included, and the decision problem is considered in light of new information. The decision analysis can give information whether it is economical to do obtain more information, and which way of obtaining new information would be preferred. The theory is illustrated with an imaginary example related to inspection of a corrugated steel pipe.

5.2 Decisions and uncertainty

5.2.1 Uncertainty in civil engineering

There is uncertainty in loading, the properties of materials, the state of the structure, in fact, there is uncertainty involved in all fields of civil engineering. Inspection of bridges and culverts are no exception. The state of the structure is uncertain, and aging processes make these uncertainties even larger. Loading of the structure is also often quite uncertain, it might be different from the design load the structure was once designed for. To get an understanding about the possible states of the structure and their probabilities, the uncertainties must be studied.

5.2.2 Decision under uncertainty

Engineering analyses include making decisions, and as there is uncertainty involved in elements of the decision procedure, one must make a decision under uncertainty. A decision can be made on basis of given information about the state. Another option is to achieve more information about the state of nature, and in this way reducing the epistemic uncertainty. Reduction of uncertainty includes costs. It is therefore not always economical to obtain new information.

5.3 Priori analysis

5.3.1 The decision problem

A pipe bridge has internal corrosion and thickness reduction is visible from the inside of the pipe. If there is external corrosion, the pipe's condition is worse. The wall thickness may then be less than expected and it might deteriorate faster. If there is external corrosion, the preferred action is to replace the pipe due to a high probability of failure. The problem lays in the uncertainty whether there is external corrosion or not.

5.3.2 True state, action and utility

There are uncertainties about the state, but there is one state which is the true state. The space of true states will be presented as Θ, where the possible true states are $\theta_0, \theta_1, \ldots, \theta_n$.

In the illustrative example, the true state of the corrugated pipe's external surface is broken down to a simplification of two possible discrete states:

$$\begin{aligned} &\theta_0\text{: no corrosion of external surface} \\ &\theta_1\text{: corrosion of external surface} \end{aligned} \tag{5.3.1}$$

From the current state of information, the inspector assigns a priori probabilities for the different states from the inspector's experience and belief. In this example, the priori probabilities are $P'[\theta_0] = 0.75$ and $P'[\theta_1] = 0.25$.

In the decision problem, there are several available actions. The actions of consideration for this example are whether one should do nothing until next inspection or whether one should replace the pipe. Other actions as applying a concrete layer to stop internal corrosion could also be considered. The action space of possible actions is defined as A, where $a_0, a_1, \ldots, a_n$ are possible actions. In this example:

$$\begin{aligned} &a_0\text{: do nothing} \\ &a_1\text{: replace the pipe} \end{aligned} \tag{5.3.2}$$

Either if the engineer chooses to do action a_0 or action a_1, the true state will either be θ_0 or θ_1.

The utility of each state-action pair, u, must be quantified. Costs are based on example costs from chapter 3. The cost is -5,395,000 NOK for replacement. No additional risk is assigned a replaced pipe for the time of consideration. The cost for failure is -17,255,000 NOK, and this also includes reconstruction. If there is no external corrosion, then the probability of failure for the existing bridge is assumed to be 0.05 until next inspection. If there is external corrosion, then the probability of failure is assumed to be much larger, and it is assumed to be 0.50 until next inspection. The expected utility for each outcome of no replacement is calculated:

$$\begin{aligned} E[u|a_0,\theta_0] &= 0.05 \cdot (-17{,}255{,}000) = -863{,}000 \text{ NOK} \\ E[u|a_0,\theta_1] &= 0.50 \cdot (-17{,}255{,}000) = -8{,}628{,}000 \text{ NOK} \end{aligned} \tag{5.3.3}$$

The utilities for the action-state pairs are given in table 5.3.1.

Table 5.3.1: Utilities of state-action pairs

	Action, *A*	
True state, *Θ*	a_0: do nothing	a_1: replace pipe
θ_0: no external corrosion	-863,000 NOK	-5,395,000 NOK
θ_1: external corrosion	-8,628,000 NOK	-5,395,000 NOK

5.3.3 A priori decision tree

The decision tree is shown in figure 5.3.1. An action is made, and one state is the true state.

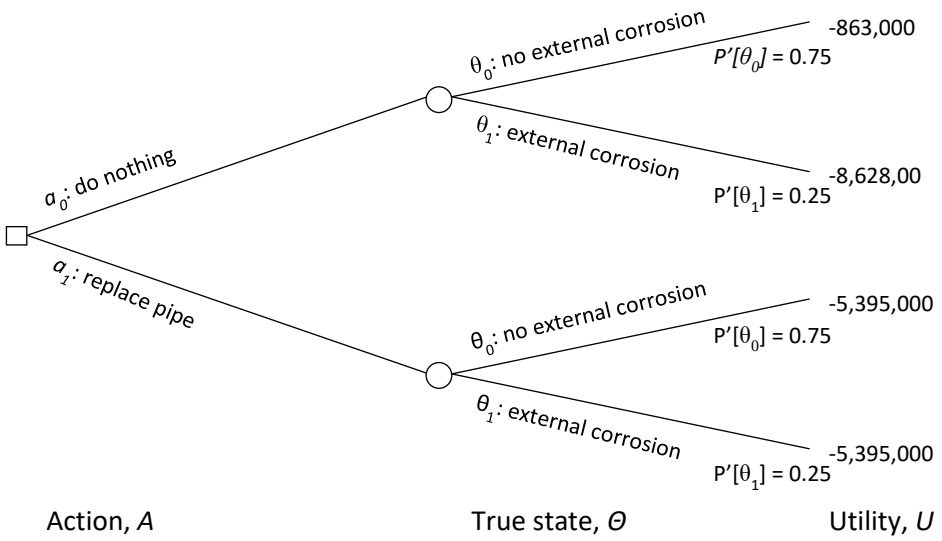

Figure 5.3.1: A priori decision tree

The expected value of each action is calculated as:

$$\begin{aligned} E'[u|a_0] &= P'[\theta_0]\cdot u[\theta_0|a_0] + P'[\theta_1]\cdot u[\theta_1|a_0] \\ &= 0.75\cdot(-863{,}000) + 0.25\cdot(-8{,}628{,}000) = -2{,}804{,}000 \\ E'[u|a_1] &= P'[\theta_0]\cdot u[\theta_0|a_1] + P'[\theta_1]\cdot u[\theta_1|a_1] \\ &= 0.75\cdot(-5{,}395{,}000) + 0.25\cdot(-5{,}395{,}000) = -5{,}395{,}000 \end{aligned} \tag{5.3.4}$$

The expected value from priori analysis is:

$$\begin{aligned} E'[u] &= -\min(|E'[u|a_0]|, |E'[u|a_1]|) \\ &= -\min(2804000\,, 5395000) = -2{,}804{,}000 \text{ NOK} \end{aligned} \tag{5.3.5}$$

From a priori analysis, decision a_0, do nothing, is the most economical decision, with an expected cost of -2,804,000 NOK. The decision tree with calculated expected values for the different actions and the choice of action is shown in figure 5.3.2.

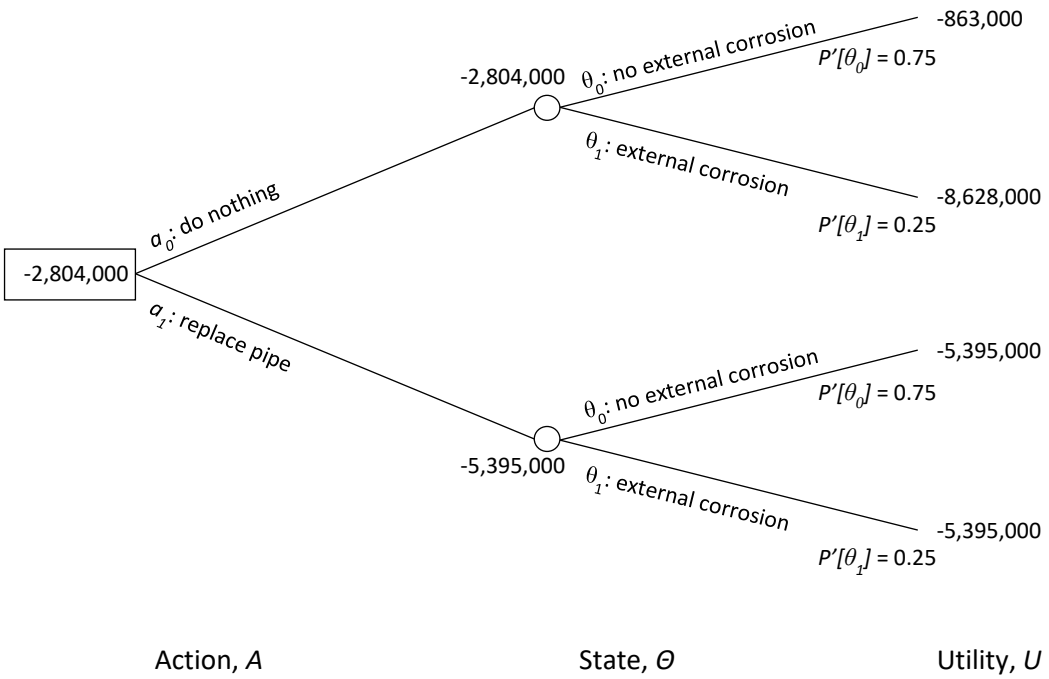

Figure 5.3.2: A priori decision tree with expected utilities

5.4 Posterior analysis

5.4.1 New information

New information about the state is found through experiment, *E*. An experiment e_1 is considered. The experiment involves measuring the thickness of the corrugated pipe with an ultrasonic thickness gauge. If the thickness is measured to be less than expected from the pipe's initial geometry and with the internal corrosion taken into account, it might indicate external corrosion of the pipe. Two possible indications belong to the space of experiment outcomes *Z*. They are:

$$\begin{aligned} &z_0\text{: measurement indicates no external corrosion} \\ &z_1\text{: measurement indicates external corrosion} \end{aligned} \tag{5.4.1}$$

The probabilities $P[z_k|\theta_i]$ are given by the accuracy of the measurement. The measurement can indicate the true state correctly, but there is still some probability for wrong indication. The accuracy of the measurement from experiment e_1 is given in the table 5.4.1.

Table 5.4.1: Experiment e_1 accuracy

	True state, Θ	
Indication, *Z*	θ_0: no external corrosion	θ_1: external corrosion
z_0: no external corrosion	$P[z_0\|\theta_0] = 0.85$	$P[z_0\|\theta_1] = 0.15$
z_1: external corrosion	$P[z_1\|\theta_0] = 0.15$	$P[z_1\|\theta_1] = 0.85$

5.4.2 Reassessment of probabilities

From Bayes' rule, posterior probabilities are calculated based on new information and priori probabilities.

$$P''[\theta_i] = P[\theta_i|z_k] = \frac{P[z_k|\theta_i]P'[\theta_i]}{\sum_j P[z_k|\theta_j]P'[\theta_j]} \tag{5.4.2}$$

Given no external corrosion indication, the posterior probabilities are calculated in the following way:

$$\begin{aligned} &P[z_0|\theta_0]P'[\theta_0] = 0.85 \cdot 0.75 = 0.6375 \\ &P[z_0|\theta_1]P'[\theta_1] = 0.15 \cdot 0.25 = 0.0375 \\ &P[z_0] = 0.6375 + 0.0375 = 0.675 \\ &P''[\theta_0] = \frac{0.6375}{0.6375 + 0.0375} = 0.9444 \\ &P''[\theta_1] = \frac{0.0375}{0.6375 + 0.0375} = 0.0555 \end{aligned} \tag{5.4.3}$$

Given external corrosion indication:

$$\begin{aligned} &P[z_1|\theta_0]P'[\theta_0] = 0.15 \cdot 0.75 = 0.1125 \\ &P[z_1|\theta_1]P'[\theta_1] = 0.85 \cdot 0.25 = 0.2125 \\ &P[z_1] = 0.1125 + 0.2125 = 0.3250 \\ &P''[\theta_0] = \frac{0.1125}{0.1125 + 0.2125} = 0.3462 \\ &P''[\theta_1] = \frac{0.2125}{0.1125 + 0.2125} = 0.6528 \end{aligned} \tag{5.4.4}$$

Given external corrosion indication, the probability for the true state actually being external corrosion is 0.65, while without any experiment the probability of external corrosion is 0.25.

From expected value calculations, given external corrosion indication, it is now seen that action a_1, replace the pipe, is the preferred action. This is shown from the decision tree in figure 5.4.1.

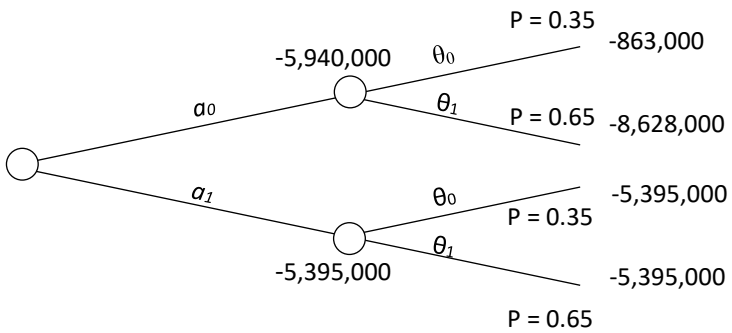

Figure 5.4.1: Decision tree for experiment e_1 given external corrosion indication

5.5 Preposterior analysis

5.5.1 Optimal decisions

The complete decision model in preposterior analysis is considering which experiment is the optimal one, and which action should be taken dependent on the outcome of the experiment.

5.5.2 Cost of experiment

Doing an experiment includes cost. This has to be included in the decision model. If the value of reducing uncertainties are larger than the cost of the experiment, then the experiment is economical. The cost of experiment 1, measuring the pipe thickness with a gauge, is assumed to be -100,000 NOK. This cost will now be added to all the action-state pairs for the experiment, as it is a cost that adds up no matter the outcome, if the experiment is chosen.

5.5.3 Additional experiment

For comparison, another experiment e_2 is considered. The experiment involves measuring thickness of the metal pipe wall, as well as measuring the corrosive aggressiveness of surrounding soil.

Table 5.5.1: Experiment e_2 accuracy

	True state, Θ	
Indication, Z	θ_0: no external corrosion	θ_1: external corrosion
z_0: no external corrosion	$P[z_0\|\theta_0] = 0.90$	$P[z_0\|\theta_1] = 0.05$
z_1: external corrosion	$P[z_1\|\theta_0] = 0.10$	$P[z_1\|\theta_1] = 0.95$

The cost for doing the experiment is higher and it is assumed to be -500,000 NOK.

5.5.4 Preposterior decision tree

In the preposterior decision tree, all experiments are considered. The prior analysis with no measurements is presented as experiment e_0. For experiments which include measurements, posterior analysis gives probabilities for the different outcomes, $P[z_k]$, as well as reassessed probabilities for the different states given an outcome $P''[\theta_i]$.

The posterior expected utilities are:

$$E[u|e,z,a] = \sum_i u(\theta_i|a,e,z)P[\theta_i|e,z] \tag{5.5.1}$$

The expected utility for each experiment-outcome pair is calculated from:

$$u\,(e,z) = \max_a[E(u(e,z,a)|e,z] \tag{5.5.2}$$

Expected utility for each experiment is:

$$E[u(e)] = \sum_k u(e, z_k) \cdot P[z_k|e] \tag{5.5.3}$$

Figure 5.5.1 shows the complete decision tree.

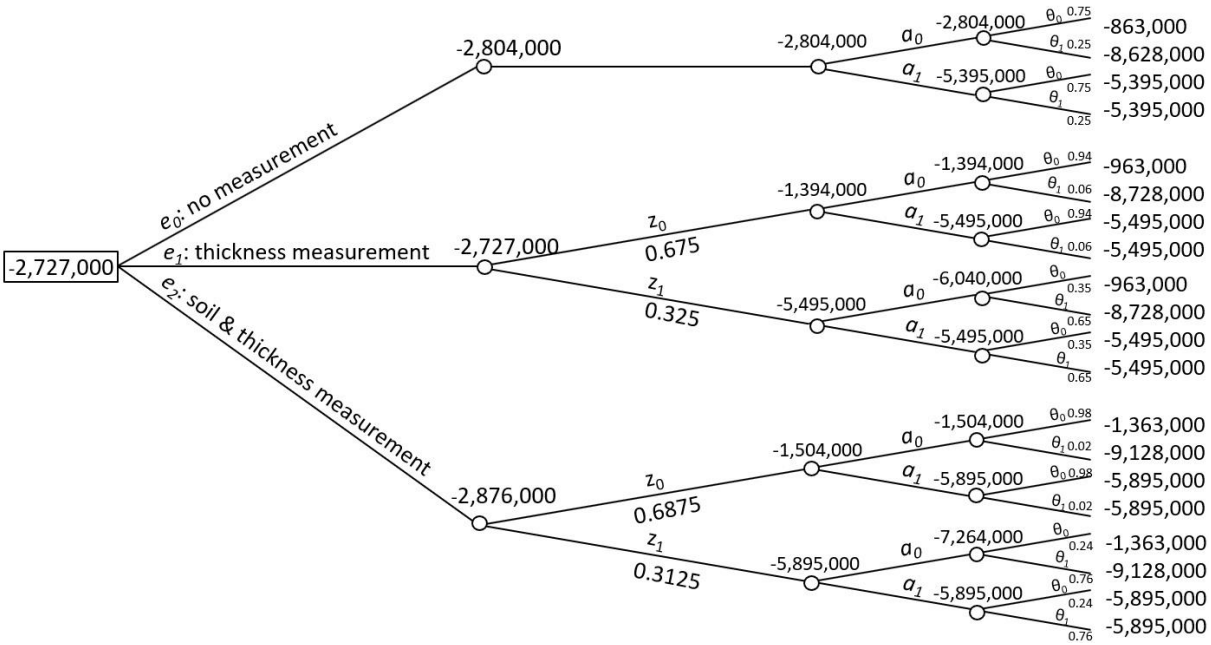

Figure 5.5.1: The complete decision tree

From the result of the complete decision tree, experiment e_1 is the preferred experiment as it has the lowest expected cost: -2,727,000 NOK. Performing this experiment is therefore recommended. Given an indication of external corrosion, replacing the pipe gives lowest expected cost, while given an indication of no external corrosion, doing nothing gives lowest expected cost.

Experiment e_2 gives a higher expected cost, -2,876,000 NOK, than not doing any measurements, -2,804,000 NOK. Due to the high experiment cost, this experiment is not recommended over doing no measurements.

5.5.5 Value of information

Doing an experiment is economical if it cost less than the value from the reduction of risk the experiment brings. Experiment e_1 is economical in case it cost less than:

$$\begin{aligned}&2{,}804{,}000\ (\text{expected utility from no experiment})\\&-\ (2{,}727{,}000 - 100{,}000)(\text{expected utility from experiment, without experiment cost})\\&=\ 177{,}000\ \text{NOK}\end{aligned}$$

Since the reduction of risk from experiment 1 has a value of 177,000 NOK and the cost of the experiment is less than this, 100,000 NOK, it is economical.

For experiment e_2 the value of risk reduction is:

$$2{,}804{,}000 - (2{,}876{,}000 - 500{,}000) = 428{,}000 \text{ NOK}$$

The experiment cost more than this, and that is why it is not economical.

5.6 Conclusion

Decision analysis breaks down the problem and the elements are studied in detail. It uses the engineer's information in a consistent manner. The analysis considers the connection between probabilities and consequences. In engineering practise, decisions are often made upon the most likely state, but through decision analysis the consequence of less likely states are also considered. A less likely state with large consequence might affect the decision in decision analysis in a way which an engineer would elsewise have hard time quantifying.

The complexity of engineering problems is often quite large. The probabilities of the state will often follow a continuous distribution. Many variables are involved in engineering problems. Computational power can be very useful in handling larger models with more sophisticated state distributions. Bayesian networks represents random variables and their dependencies. The problem is presented graphically. The next chapter considers Bayesian networks.

Chapter 6

Bayesian network

6.1 General

This chapter introduces how Bayesian networks can be used for inspection of corrugated steel pipes. The theory presented is mainly based on literature by Jensen & Nielsen (2007) and Straub (2015). The software used for building Bayesian networks is GeNIe 2.2.4.

6.2 Introduction to Bayesian network and influence diagram

6.2.1 Nodes and connections

Bayesian network is a graphical probabilistic model. The model consists of random variables which are presented by nodes. Variables may be deterministic or continuous. The variables are connected to each other with directional links. If a link goes from variable *A* to a variable *B*, *B* is the child of *A*, and *A* the parent of *B*. The child depends on its parent. A conditional probability table is assigned to each variable, and for a *A*, which depends on its parent *B*, the probability is presented as $P[A|B]$. With an additional parent *C* the probability is $P[A|B,C]$.

Figure 6.2.1 shows a serial connection of *A*, *B* and *C*. In this network, *B* depends on *A*, and *C* depends on *B*. In case the state of *B* is certain, then *A* and *C* are independent, and *A* and *C* are said to be d-separated.

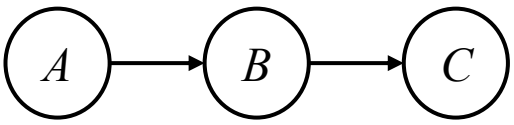

Figure 6.2.1: Serial connection of A, B and C

A diverging network is shown in figure 6.2.2. Here *A* is parent of *B* and *C*. If the parent *A* is not known, then information about one child will give some information about the other child of *A*. If the state of *A* is known, then the children becomes independent.

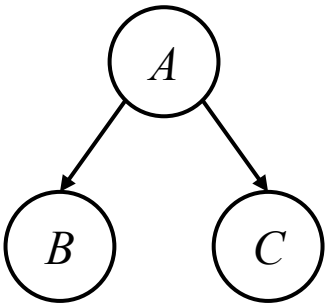

Figure 6.2.2: Diverging connection where B and C are children of A

When a variable has several parents, as *A* has in figure 6.2.3, it is a converging connection. If the state of *A* is unknown, then its parents, here *B* and *C*, are independent. If the state of *A* is known, however, then its parents are dependent.

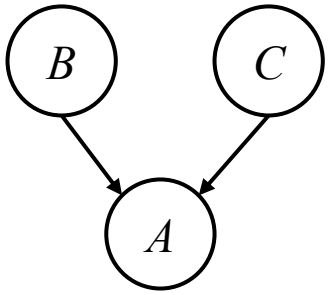

Figure 6.2.3: Converging connection where B and C are parents of A

6.2.2 Simple example

A simple example is used to illustrate some of these properties of Bayesian networks. The performance of the steel pipe, *P*, is dependent on the condition of the steel pipe, *C*, and the loading of the pipe, *L*. *C* and *L* are parents of *P*. The condition of the pipe and the loading are assumed not to be linked for this example. The network is shown in figure 6.2.4.

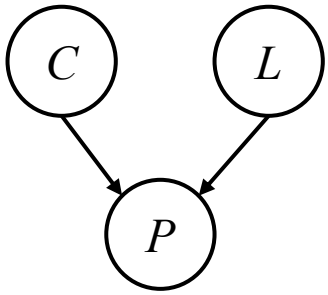

Figure 6.2.4: Steel pipe condition network

The variables are simplified to be discrete, while they will be of continuous nature for the real case. The state of the pipe performance is either no failure or failure, the pipe condition is either good or bad, and the loading is either normal or large. The probabilities to assess are *P[C]*, *P[L]* and *P[P|C,L]*. Assuming a probability for the condition to be good of 0.85 and bad of 0.15, the probability table for *C* becomes:

Table 6.2.1: Condition state probability table

Condition state	**Probability**
C = Good	0.85
C = Bad	0.15

The table for the loading *L* is set to be:

Table 6.2.2: Loading state probability table

Loading state	**Probability**
L = Normal	0.90
L = Large	0.10

The conditional probabilities for the pipe performance is assumed to be:

Table 6.2.3: Performance state probability table

	C = Good		*C* = Bad	
Performance state	*L* = Normal	*L* = Large	*L* = Normal	*L* = Large
P = No failure	0.999	0.95	0.93	0.85
P = Failure	0.001	0.05	0.07	0.15

The probability for failure is:

$$\begin{aligned} P[P = Failure] &= \sum_{C,L} P[P = Failure|C, L] \cdot P[C] \cdot P[L] \\ &= 0.001 \cdot 0.85 \cdot 0.9 + 0.05 \cdot 0.85 \cdot 0.1 + 0.07 \cdot 0.15 \cdot 0.9 + 0.15 \cdot 0.15 \cdot 0.1 \\ &= 0.0167 \end{aligned} \tag{6.2.1}$$

The simple Bayesian network is represented with the software GeNIe, figure 6.2.5. Each node has its possible states and probabilities assigned to it.

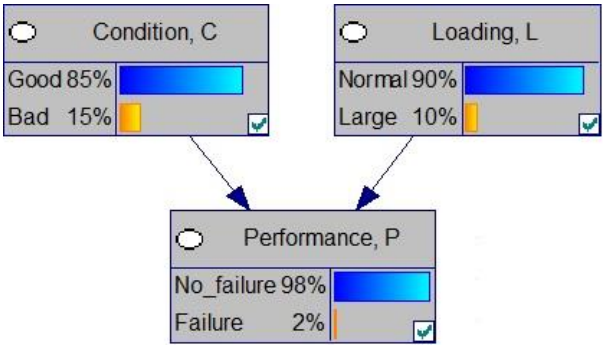

Figure 6.2.5: Nodes in GeNIe

New information is an important aspect of Bayesian networks. Given there was a structural failure, the probabilities about the condition and loading is reassessed by using Bayes' rule, similar to of chapter 5.4. With the state of performance known, there is evidence of performance.

$$\begin{aligned} P[C = Bad|P = Failure] &= \sum_{L} \frac{P[P = Failure|C = Bad, L] \cdot P[C = Bad] \cdot P[L]}{P[P = Failure]} \\ &= \frac{0.07 \cdot 0.15 \cdot 0.9 + 0.15 \cdot 0.15 \cdot 0.1}{0.0167} = 0.700 \end{aligned} \tag{6.2.2}$$

Figure 6.2.6 illustrates how the probabilities are reassessed in GeNIe with evidence of failure for performance. The probability for the pipe condition to be bad is 70%, as calculated. Also, the probability for the loading to be large is higher with evidence of failure.

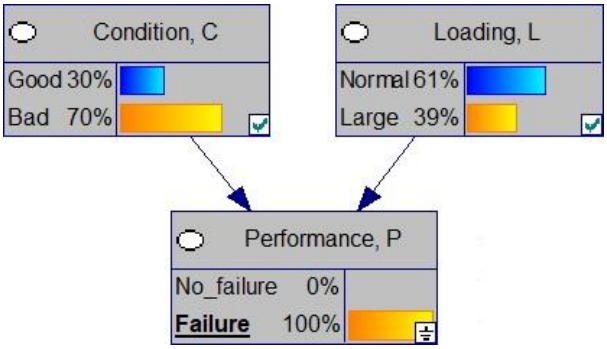

Figure 6.2.6: Reassessed probabilities given structural failure

6.2.3 Influence diagram

Decisions and utilities might be included into a Bayesian network. This is called an influence diagram. For a buried pipe, a decision whether to perform testing and measurements to obtain new information about the pipe state could be introduced. The decision may also include different measurement options. Another decision node may include different actions as whether to replace the pipe, extend its life or do nothing.

Utilities relate to the consequences from decisions and the state of the variables. Consequences relates to, as discussed, monetary values, aesthetic, environment, safety and more. The connection of uncertain variables, utilities and the decision options make basis for finding the optimal decision which leads to lowest negative utilities for an inspection case.

6.2.4 Bayesian network for decision tree

The combination of nodes with uncertainties, decisions and utilities are illustrated with the same example as for the Bayesian decision tree in chapter 5. Figure 6.2.7 illustrates this decision problem as a Bayesian network.

The experiment node is a decision node with three possible experiments. It is connected to its utility node, which gives cost for the different experiments. The indication node is connected with the true state node and the experiment decision. The true state of the corrosion is uncertain with 0.75 probability of no external corrosion and 0.25 probability of external corrosion. The indication node includes the accuracy of indicating the true state through measurements, and this accuracy depends on the experiment chosen. Another decision node, the action node, has the two actions of either doing nothing or replacing the pipe. This is connected with the utility node, which gives different utilities for combinations of true state-action pairs.

All calculations run through the nodes, and the expected cost for each possible experiment is displayed. These are exactly the same as for the decision tree in chapter 5.

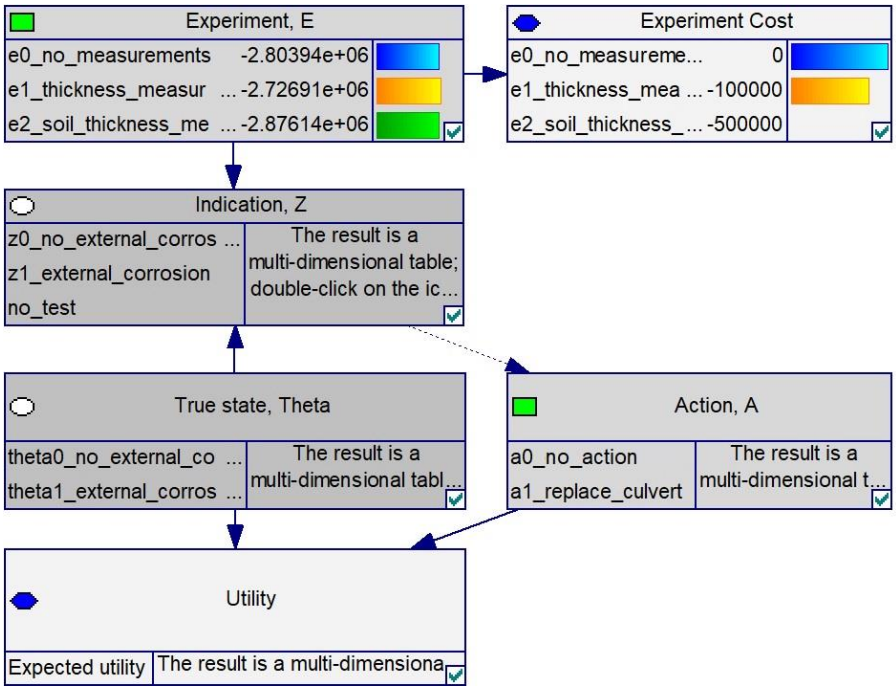

Figure 6.2.7: Expected cost for different experiments

Experiment e_1 gives the lowest expected cost and it is chosen. The indication node gives the accuracy for e_1, and with the dependencies from the true state node, the probability of different indications is calculated. This is shown in figure 6.2.8.

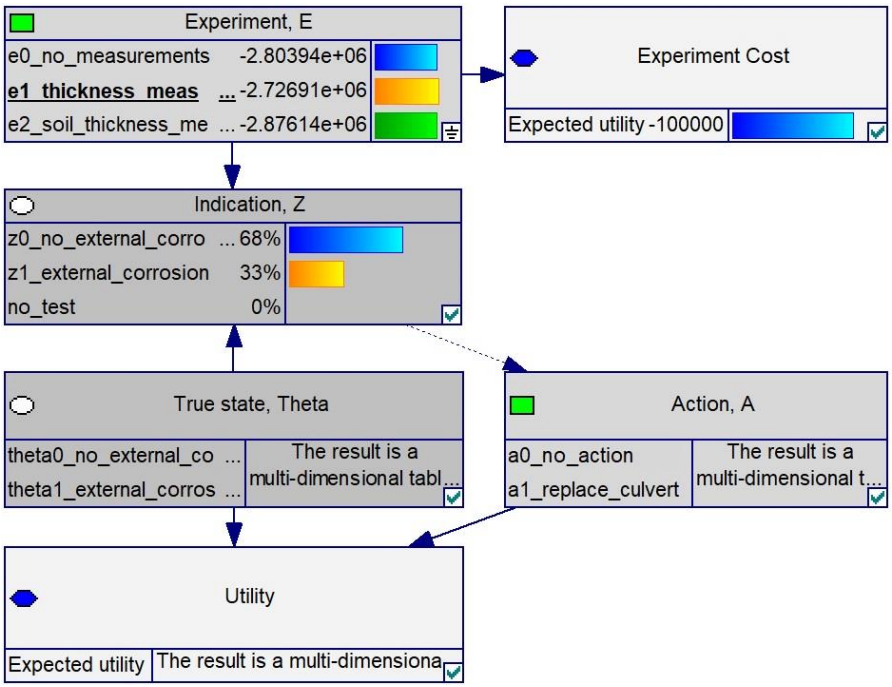

Figure 6.2.8: Thickness measurements and probabilities of indications

Figure 6.2.9 shows a situation given an indication of external corrosion. The probability of true states with evidence of this indication is then calculated. By this, the most economical action is to replace the pipe. The expected cost is -5,495,000 NOK.

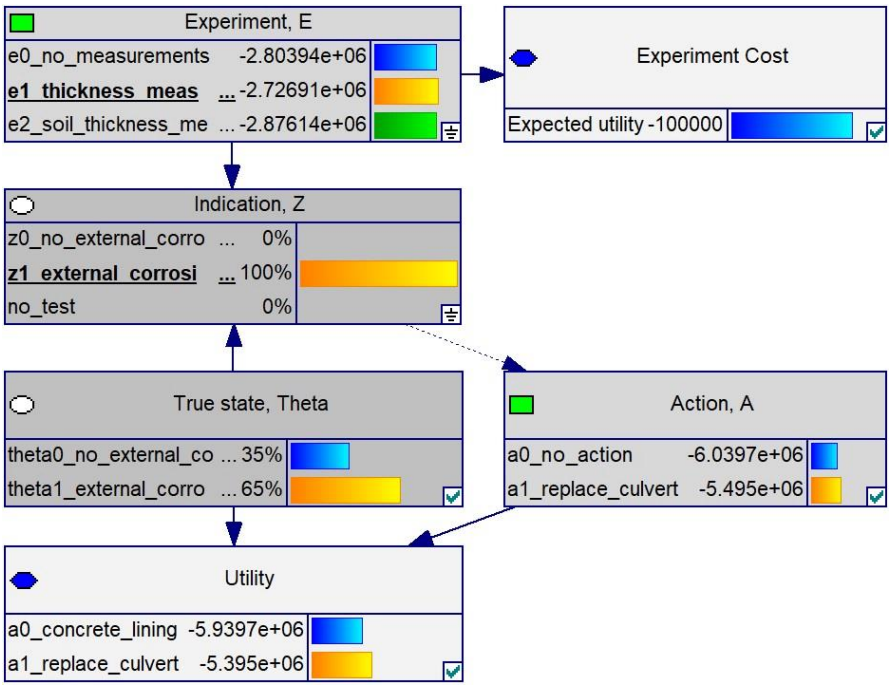

Figure 6.2.9: Indication of external corrosion, true state probabilities and expected cost of different actions

6.3 Dynamic Bayesian network and influence diagram

6.3.1 Simplest dynamic Bayesian network

A dynamic Bayesian network is a Bayesian network that considers relation between variables in time steps. The simplest dynamic Bayesian network is created by only considering one variable (Straub 2015). Figure 6.3.1 shows an example of this for the variable X from time step 1 until T. Another name for this model is a Markov model. This model has the Markovian property of being memoryless. That is, the state in the next step is only dependent on the current state and not any states before that. The random variable X may for example be the state of a bridge, and the network might represent bridge deterioration. Chapter 7 studies this case for the buried steel pipes by NPRA.

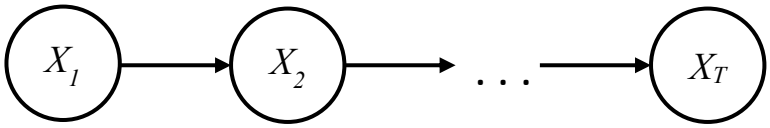

Figure 6.3.1: Simple dynamic Bayesian network

Another representation of this network is shown in figure 6.3.2. This compact representation shows one time step for variable X. The number 1 indicates that connection goes from X at t to X at $t + 1$.

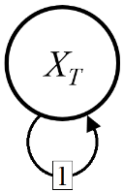

Figure 6.3.2: Alternative representation of network from figure 6.3.1

6.3.2 Uncertainty in observation

A slightly more complex dynamic Bayesian network is shown in figure 6.3.3. Let I be the observed state of X. This model is a hidden Markov model. It is a Markov process because the state of the variable X at time $t + 1$ is only dependent on the state at the previous time t. The word hidden emphasizes the uncertainty in the observation of the state X. The model assumes that there is some information about the process of the state X that is hidden from the observer. The observed state I is only dependent on the hidden state X at the same time step. If the observation is perfect without uncertainty, then the observed state is a direct observation of the true state X and no information is hidden.

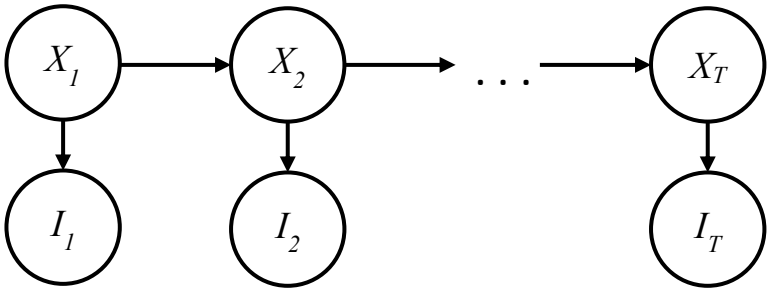

Figure 6.3.3: Dynamic Bayesian network with inspection uncertainty

6.3.3 Dynamic influence diagram

A dynamic Bayesian network might be extended to include decisions and utilities, and this is then a dynamic influence diagram. Figure 6.3.4 shows a dynamic influence diagram as an extension to the dynamic Bayesian network in figure 6.3.3. This dynamic influence diagram is given by Straub (2015), but it is modified here.

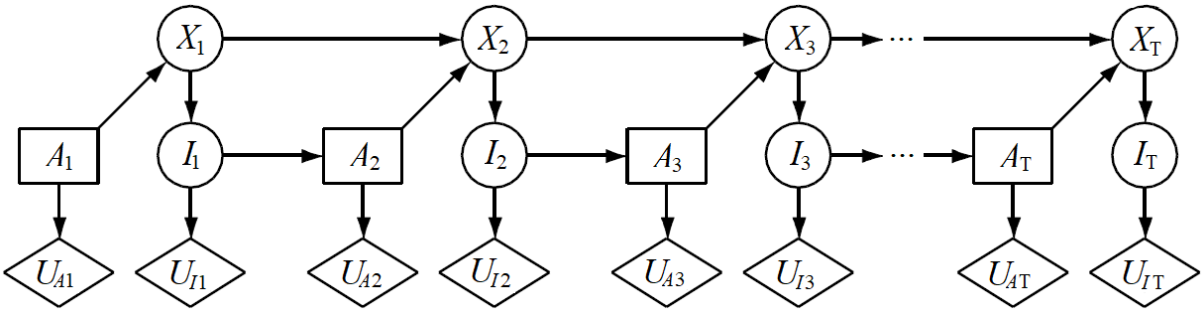

Figure 6.3.4: Dynamic influence diagram for bridge inspection

X_t is the condition of the bridge at time step t and I_t is the condition of the bridge assessed by inspection at the same time step. For each time step, an action A_t for the bridge is made based on the condition assessed by inspection. This action might be whether to replace the bridge, rehabilitate the bridge, do maintenance, do nothing or any other preferred actions. A cost U_{At} is associated with the action. There is also a utility U_{It} that includes the benefit and risk associated with the condition of the pipe. This utility is dependent on the condition assessed by inspection.

6.3.4 More complex dynamic Bayesian networks

A dynamic Bayesian network can be more complex and does not need to be memoryless. For example, the state X at time step $t + 2$ might be dependent on both its state at time step t +1 and time step t. A variable can also be dependent on several variables in previous time steps. In this thesis, relative simple dynamic networks will be considered in order to keep practical applications manageable.

6.4 Bayesian networks for buried steel pipes

6.4.1 Variables and dependencies

A buried steel pipe is somehow a simple structure, but in other ways it is quite complex. The interaction of soil and structure for a flexural pipe make a challenge in fully understanding the system. Some variables might affect both the loading of the structure and the capacity of the structure. One of these being the soil surrounding the pipe. The soil gives an earth load on the pipe, but in the same time, surrounding soil is supporting the pipe. Creating a Bayesian network for a flexible pipe can be very useful as it gives an understanding about the entire system and the dependencies between variables.

Figure 6.4.1 shows a suggestion to a Bayesian network representing some major variables for the system. The structural performance is of interest, which depends on the structural condition, its resistance, and the loading of the structure. The proposed model has a practical application in mind. It may be expanded with more detailed variables.

The loading is dependent on the traffic, earth and water load. Structural condition depends on material properties, pipe geometry, soil-structure interaction. Material properties could be divided into elasticity modulus, yield stress, Poisson's ratio and more. Pipe geometry gives shape of the wall, thickness and cracks, which is important for yield and buckling resistance.

Soil-structure interaction includes how the soil is supporting the pipe, its density around the pipe and its stiffness. Both the geometry and the soil-structure interaction depend on the loading. High loading might give more support from soil to the structure, it may also give deflection of the pipe, which changes its geometry. Cycles of traffic load may lead to fatigue of the pipe, yet this effect decrease with soil depth, as the stress range at the pipe become less with the loading distributed over larger soil depth.

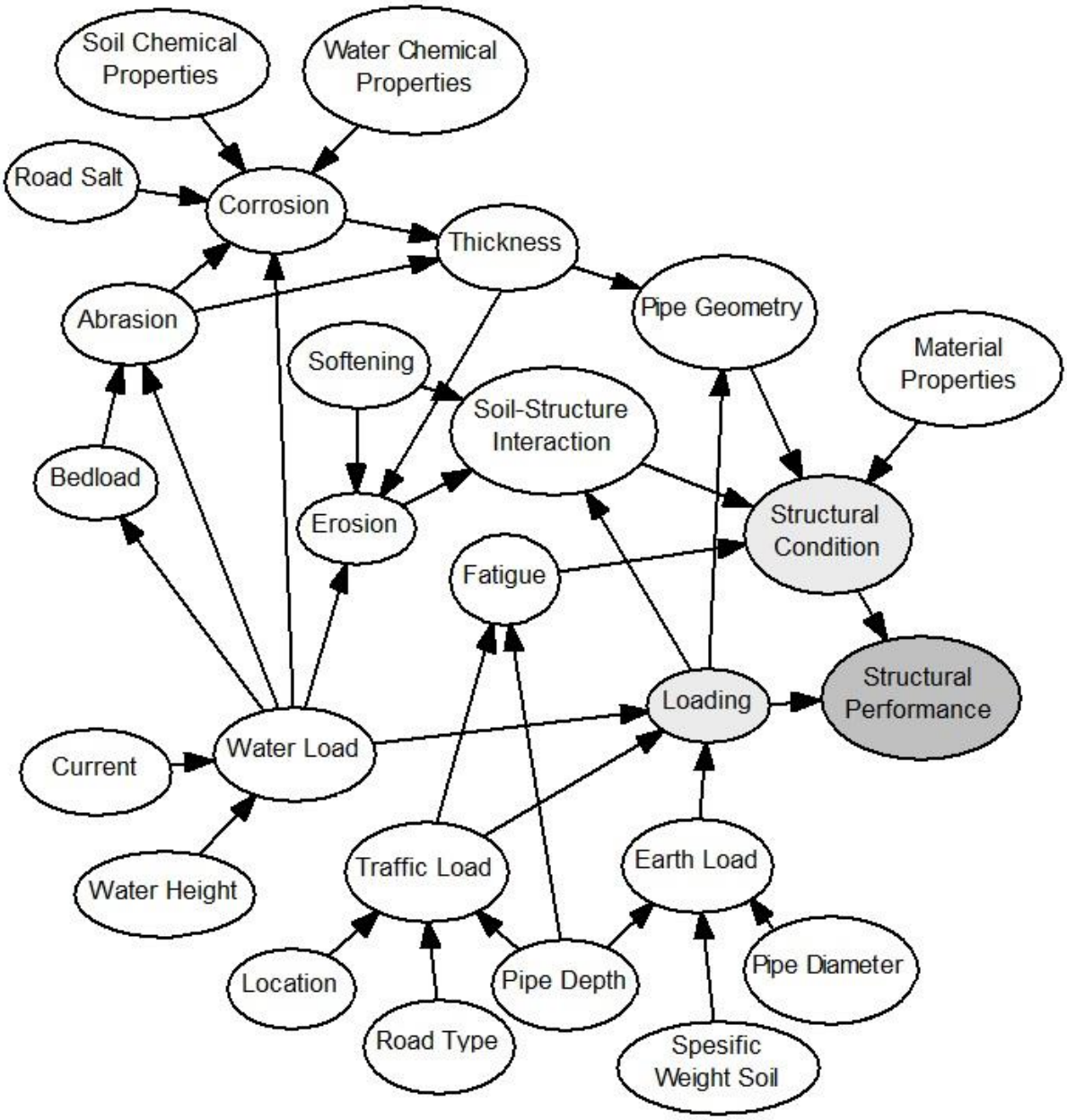

Figure 6.4.1: Bayesian network for a buried steel pipe

The water load is a load on the structure, and also one of the main variables causing erosion of soil, abrasion of the pipe and corrosion. A flood may lead to large sudden erosion. Water flow together with bedload (sand and gravel in the water) cause abrasion of the steel pipe. Abrasion will damage galvanised layer and remove rust. This can initiate corrosion and increase corrosion speed. The water load, together with properties of surrounding substances and environmental impact as road salt influence corrosion. Corrosion and abrasion will reduce the thickness of the pipe.

6.4.2 Decision making

6.4.2.1 General

A demonstrational example is given. The decision problem is extended by looking at structural performance from loading and structural conditions, several actions: no action, life extension, rehabilitation and replacement, and a possible thickness measurement experiment. In this example, the different actions improve the structural condition to different degrees. It should be mentioned that different options have different lifetime, which should be considered in the decision making. The action influences the structural condition in the second time period. This is therefore a dynamic influence diagram with one time step.

The structural performance is connected to four consequences from no consequence to very large consequence. A medium consequence is a consequence with need for reconstruction but only minor consequence for traffic. This consequence is assigned a cost of -6,000,000 NOK. Large consequence is assigned a cost of -30,000,000 NOK, and this might be a critical injury as well as need for reconstruction. A very large consequence might be death or several critical injuries, and it is assigned a utility of -60,000,000 NOK.

The experiment cost is -100,000 NOK, replacement cost is -5,395,000 NOK, rehabilitation cost is -3,500,000 NOK and life extension cost -1,000,000 NOK. All costs and probabilities in the influence diagram are just for demonstrational purpose.

6.4.2.2 No measurement

Figure 6.4.2 illustrates the choice of not doing any experiment. This is not an economical decision, but it is still shown. An action must be made and rehabilitating the bridge has the lowest expected cost. This reduces risk by improving the structural condition.

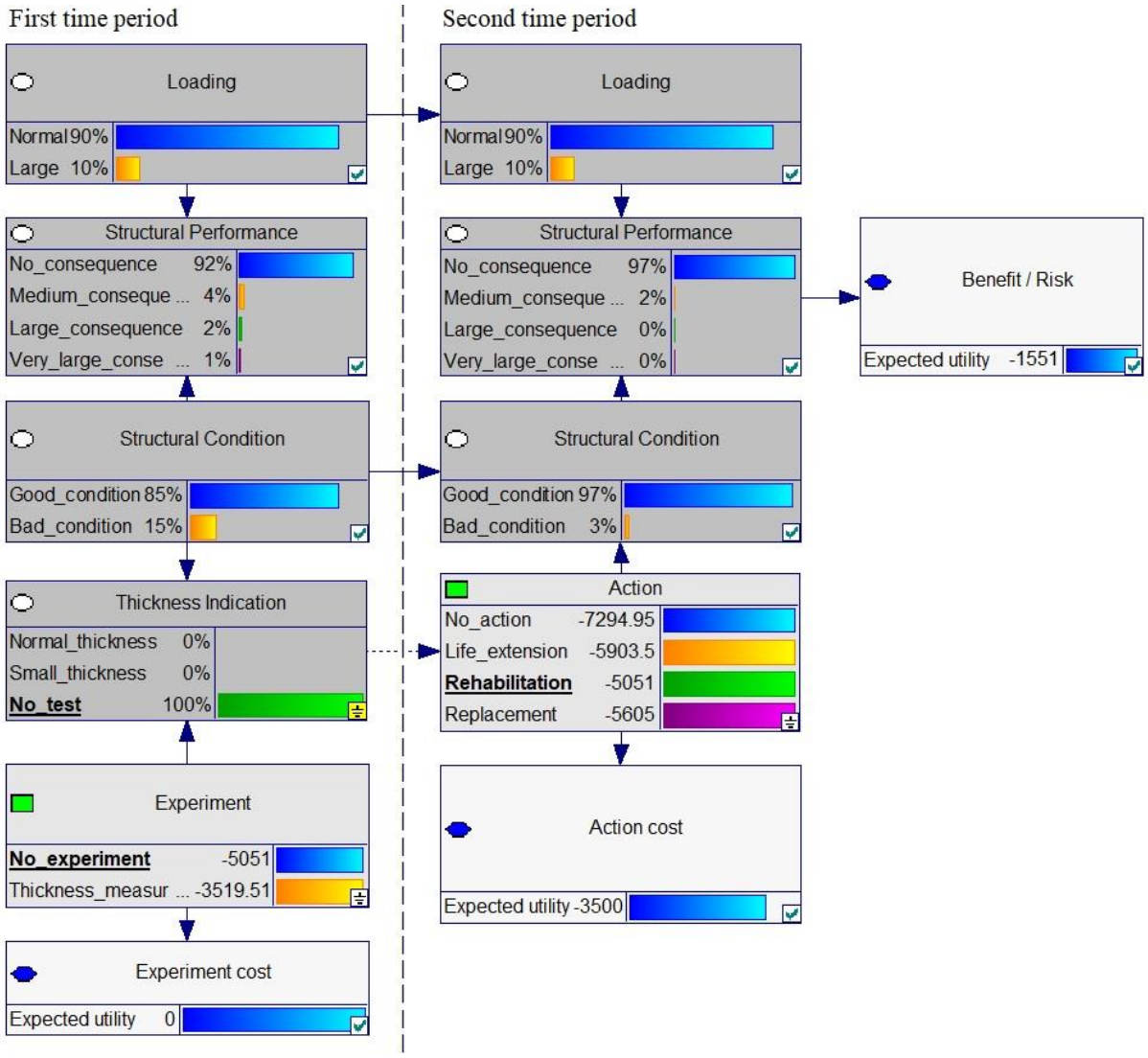

Figure 6.4.2: Inspection of buried pipe with no measurement

6.4.2.3 Thickness measurement with indication of normal thickness

Doing thickness measurement gives a much lower expected cost than no measurement, and it should therefore be performed. Figure 6.4.3 illustrates the case of thickness measurement indicating normal thickness. The most economical action is to do nothing in this case. Life extension is an almost equally good action. Since no action is made, the structural condition is slightly worse in the second time step due to deterioration.

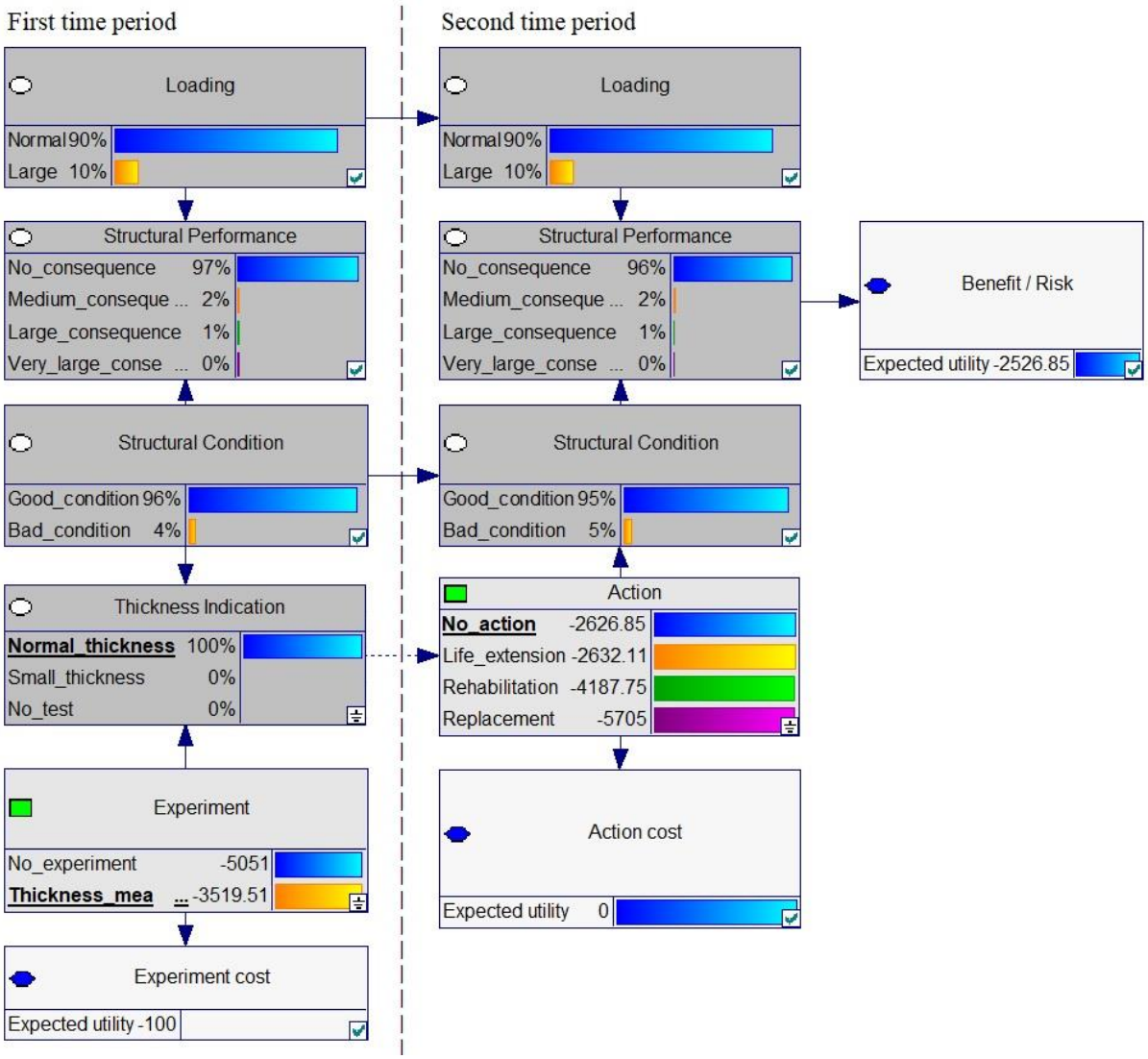

Figure 6.4.3: Inspection of buried pipe with indication of normal wall thickness

6.4.2.4 Thickness measurement with indication of small thickness

In the other case, the measurement indicates small thickness. The best option is to replace the pipe. It reduces risk the most, but it is also the costliest action. The condition for a replaced pipe is assumed to be good. There is still a small chance for some consequence due to chance for the loading being large. Even though the structural condition is good, a flood or an overloaded heavy vehicle might bring some consequence.

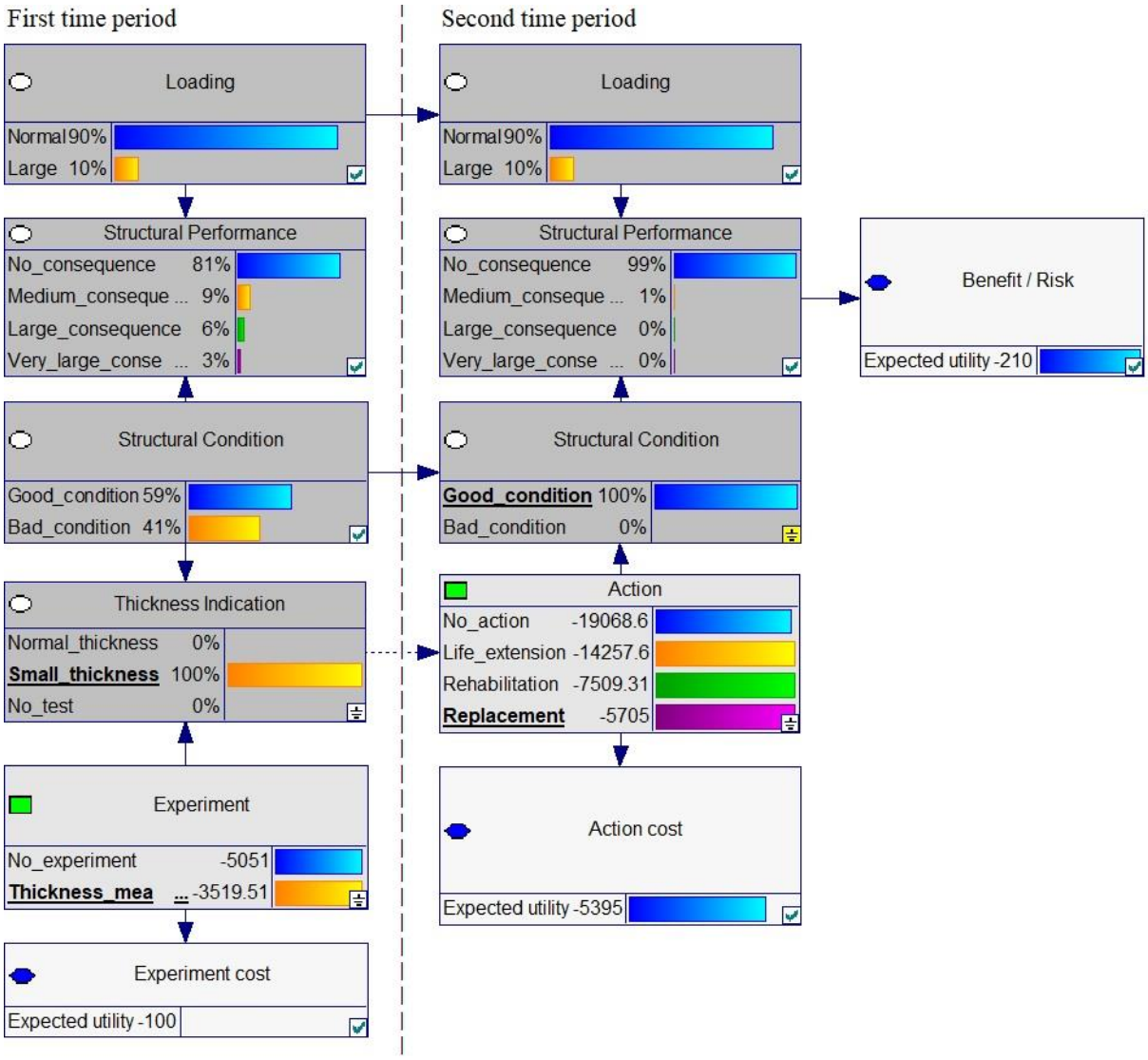

Figure 6.4.4: Inspection of buried pipe with indication of small thickness

6.5 Conclusion

Bayesian network is used to illustrate the structural system's variables and dependencies graphically. This is quite useful in order to truly understand how the variables affect each other. The benefits from different actions are clearly quantified in the decision-making network. With several actions and several indication outcomes, it might be difficult to defend the decision making. Bayesian networks breaks this down and guides the decision procedure to do optimal decisions in a consistent manner. It is also possible to consider change in variables over time with dynamic Bayesian networks. Chapter 8 and 9 focus on deterioration and failure of the pipe bridges over time. In these chapters, aspects of dynamic Bayesian networks are applied.

Chapter 7

Structural reliability analysis

7.1 General

This chapter considers structural reliability analysis, and how it may be used for analysing a buried pipe. The uncertainty for an existing structure might be quite large. By implementing reliability analysis, one might get a better understanding of the condition of the structure. The analysis is used to find the reliability of a structure, but the methods might be applied to other aspects of inspection of existing structures.

First order reliability analysis is used to study the probability of yield of the pipe bridge wall. Attention is also paid towards the sensitivity of variables in the calculations. Finally, a basic Bayesian network shows a connection between the probability of yield and the probability of structural failure. By this, the example also simply illustrates how reliability analysis might be connected with Bayesian networks.

7.2 Limit state

A limit state defines a limit for which a realisation of random variables will enter a certain state. The limit state of consideration is often associated with a consequence. For structural reliability analysis, this might be ultimate failure or serviceability failure. In the management of existing structures, a limit state might also be a certain state which triggers an action as maintenance, rehabilitation or replacement. A Bayesian network might be supported by similar analysis by considering limit states for discrete realisations of variables.

Let the limit state function be defined as $g(\mathbf{X})$, where $\mathbf{X}$ is a vector of the random variables which influence the state. If the limit state considers failure, then the failure domain is $g \leq 0$, and a safe domain is $g > 0$. The probability density function is $f_{\mathbf{X}}$. For the realisations of variables $\mathbf{x}$ which gives $g(\mathbf{x}) < 0$, the probability of failure, P_f, might be calculated by:

$$P_f = \int_{g(\mathbf{x}) \leq 0} f_{\mathbf{X}}(\mathbf{x}) d\mathbf{x} \tag{7.2.1}$$

7.3 Structural reliability methods

7.3.1 General

There are several methods that might be used to solve equation 7.2.1. A fairly simple approach might be applied in case all variables are normal distributed and the limit function is linear. This is shown in chapter 7.3.2. For more complicated limit state functions and distributions, approximate methods might be applied. Some examples are Monte Carlo simulation and first

order reliability method. Monte Carlo simulation is simple to apply, but the method requires a large number of samples. The method might be slow. First order reliability method is a computational effective method, and it also provides some physical interpretation. The method linearizes the failure surface and the method might be less accurate if the problem is strongly nonlinear. A second order reliability method have a better accuracy, but it will not be considered in this paper.

7.3.2 Linear function and normal distribution

A linear limit state function is considered, and the random variables are normal distributed. The resistance of the structure is given as R and the loading S. Failure occur if $S > R$. The limit state function g is defined as:

$$g(R,S) = R - S \tag{7.3.1}$$

Let R and S be normal distributed. The safety margin M is then also normal distributed and defined as:

$$M = R - S \tag{7.3.2}$$

The mean value and the standard deviation of the safety margin are calculated as:

$$\begin{aligned} \mu_M &= \mu_R - \mu_S \\ \sigma_M &= \sqrt{\sigma_R^2 + \sigma_S^2} \end{aligned} \tag{7.3.3}$$

The reliability index is calculated as the mean value of the safety margin divided by the standard deviation of the safety margin:

$$\beta = \frac{\mu_M}{\sigma_M} \tag{7.3.4}$$

The probability of failure is calculated from the cumulative distribution function of the standard normal distribution:

$$P_f = \Phi\left(\frac{0 - \mu_M}{\sigma_M}\right) = \Phi(-\beta) \tag{7.3.5}$$

Figure 7.3.1 shows the normal distributions and their properties for the resistance R and the loading S. The safety margin is shown in figure 7.3.2. The figure illustrates the relation between reliability index, standard deviation and mean value. The grey coloured area of the safety margin distribution is the failure domain.

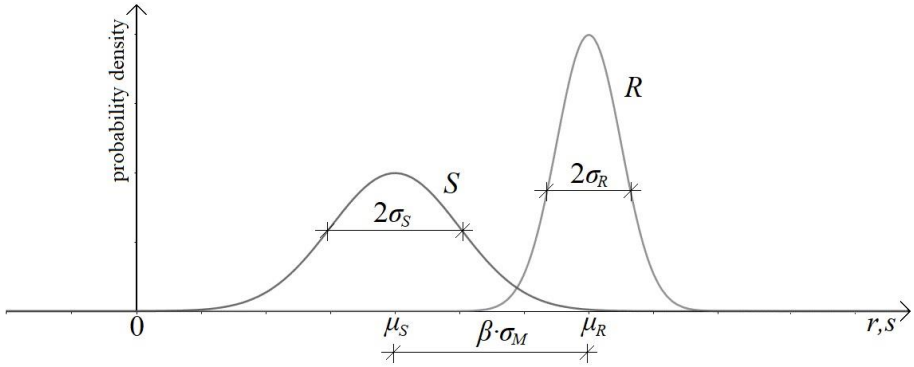

Figure 7.3.1: Resistance and loading distribution

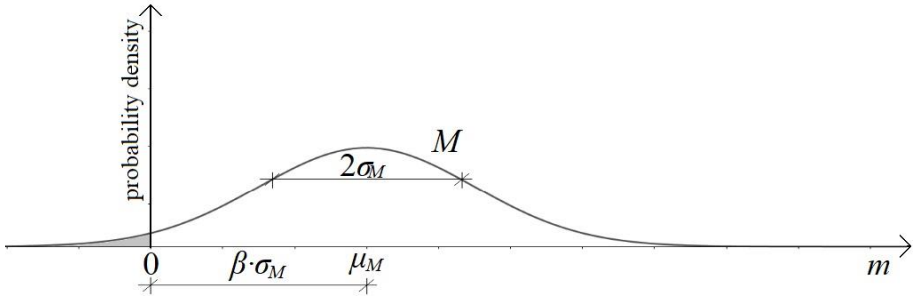

Figure 7.3.2: Safety margin distribution

7.3.3 First order reliability analysis

Some of the main concepts behind first order reliability analysis are introduced. For a more detailed description see Hasofer and Lind (1974).

The standard normal space is considered. For independent normal distributed variables **X**, the transformation to standard normal space is done by:

$$U_i = \frac{X_i - \mu_{X_i}}{\sigma_{X_i}} \tag{7.3.6}$$

where X_i is a normal distributed variable, μ_{Xi} is the mean of the variable, σ_{Xi} is the standard deviation of the variable and U_i is the standard normal distributed variable of X_i.

First order reliability analysis seeks to find the reliability index, β, which gives the smallest distance to the border between the failure domain and the safe domain. This is done by finding for the smallest β which gives the design point $\mathbf{u}^*$ in the standard normal space, for which also $g(\mathbf{u}) = 0$. At the design point, the failure surface is linearized, and this is an approximation.

One approach in finding the reliability index is to express the realisations of the standard normal variables **u** as:

$$\mathbf{u} = \beta \boldsymbol{\alpha} \tag{7.3.7}$$

where $\boldsymbol{\alpha}$ is a normal vector.

Then the reliability index for the design point, is the smallest β which leads to the expression in equation 7.3.8.

$$g(\mathbf{u}^*) = g(\beta\boldsymbol{\alpha}) = 0 \tag{7.3.8}$$

An iterative approach is used to solve this. If the limit state function is differentiable, then for $i = 1, 2, \ldots, n$:

$$\alpha_i = \frac{-\frac{\partial g}{\partial u_i}(\beta\boldsymbol{\alpha})}{k}$$
$$where\ k = \sqrt{\sum_{i=1}^{n}\left(\frac{\partial g}{\partial u_i}(\beta\boldsymbol{\alpha})\right)^2} \tag{7.3.9}$$

By guessing an initial design point, $\beta^{(j)}\boldsymbol{\alpha}^{(j)}$, an updated $\boldsymbol{\alpha}^{(j+1)}$ is calculated from equation 7.3.9. An updated reliability index is then calculated from $g(\beta^{(j+1)}\boldsymbol{\alpha}^{(j+1)}) = 0$, which might be solved with an appropriate fixed-point iteration. The iterative process in finding $\boldsymbol{\alpha}^{(j+1)}$ and then $\beta^{(j+1)}$ should be performed until the difference between $\beta^{(j+1)}$ and $\beta^{(j)}$ is sufficiently small.

The normal vector, $\boldsymbol{\alpha}$, gives information about the sensitivity of the variables. This is an advantage with the first order reliability analysis. The probability of failure calculation is less sensitive to a variable which is associated with a low α-value.

First order reliability analysis can also include non-normal distributed variables and dependent variables.

7.4 Probability of yield of pipe wall

7.4.1 Limit state function

If one considers a pipe with proper support from soil, the failure mechanism of the pipe wall will generally be yield. Buckling capacity should be considered in case there are significant areas with lack of support from backfill.

The limit state function of consideration is:

$$g(r_{wall}, s_{earth}, s_{traffic}) = r_{wall} - s_{earth} - s_{traffic} \tag{7.4.1}$$

where r_{wall} is the yield capacity of the pipe wall, s_{earth} is the ring compression due to earth load and $s_{traffic}$ is the ring compression due to traffic load.

The yield capacity of the wall for a ring compression is:

$$r_{wall} = A \cdot f_y = a \cdot t \cdot f_y \tag{7.4.2}$$

where A is the area of a wall section per length of pipe and f_y is the yield capacity of the pipe. The area of the cross section might also be expressed as $A = at$, where a is the density of cross section per length of pipe and t is the smallest continuous wall thickness of the pipe. This expression therefore assumes that the yield capacity from ring compression is proportional with

the smallest continuous wall thickness. This assumption is based on the findings from El-Taher (2009), and this is discussed in chapter 4.3.2.3 in this document.

Considering a prism load, the ring compression from earth load might be expressed as:

$$s_{earth} = \frac{h\gamma D}{2} k \tag{7.4.3}$$

where h is the depth to the crown of the pipe, γ is the specific weight of the soil, D is the diameter of the pipe and the width of the prism load and k is the prism load constant. This equation is given by QDTMR (2015) together with the assumption that the weight of the soil can be expressed as $W = h\gamma$, Moser (2001).

The compression from traffic load is calculated in accordance with manual V220, NPRA (2010). A line load, $p_{traffic}$, is calculated from the stress from traffic load at the crown of the pipe.

$$p_{traffic} = \frac{\sigma_v \pi h}{2} \tag{7.4.5}$$

σ_v is the pressure at the height of the crown from traffic load, and it may be calculated by Boussinesq equation for point loads at the surface of the road. The line load to compression is calculated as in V220, NPRA (2010):

$$\begin{aligned} s_{traffic} &= p_{traffic}\, for \frac{h}{D} < \frac{1}{4} \\ s_{traffic} &= \left(\frac{5}{4} - \frac{h}{D}\right) \cdot p_{traffic}\, for \frac{1}{4} \leq \frac{h}{D} \leq \frac{3}{4} \\ s_{traffic} &= \frac{p_{traffic}}{2}\, for \frac{h}{D} > \frac{3}{4} \end{aligned} \tag{7.4.4}$$

7.4.2 Variables

7.4.2.1 General

A set of variables are considered for demonstration. Characteristics and assumptions for these variables are discussed. The uncertainties of variables are not deeply studied, and further concern related to this is left for another study.

7.4.2.2 Cross section density

The cross section of consideration is a corrugated profile of 200 x 55 mm from manual V220, NPRA (2010). Figure 7.4.1 shows the cross section. The density of the cross section per length, a, is assumed to be normal distributed, and the mean value is 1.180 m^2/m. Geometrical deviations from damages, installation and accuracy in the making of the steel pipe makes this variable uncertain. The standard deviation is assumed to be 0.05 m^2/m.

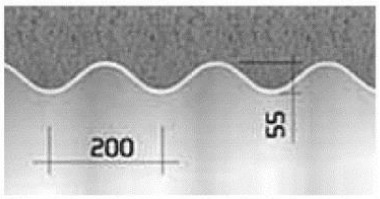

Figure 7.4.1: Steel pipe profile

7.4.2.3 Wall thickness

The smallest continuous thickness of the pipe might be assumed to be normal distributed or log-normal distributed. Modelling the thickness as a normal distribution might have some error. This is because it might have a significant portion of negative values in the representation of the thickness for thicknesses close to 0. A log-normal distribution cannot take values less than 0, and this distribution therefore removes this error in the physical representation.

Uncertainty in the thickness is highly dependent on the method used at inspection. For visual inspection the uncertainty might be relative high. It is difficult to see exactly how thick the wall section is, and there might be corrosion to the external surface which is not visible. The uncertainty is also dependent on the condition of the pipe. If the pipe appears to be as good as new, the uncertainty might be low since the initial condition is known. In case there is no wall thickness or almost nothing, the uncertainty might also be lower because holes indicate total section loss.

If one uses a thickness gauge instrument to measure the thickness, the uncertainty should be lower. The normal standard deviation is assumed to be 0.1 mm for inspection with thickness gauge. In case a thickness gauge is used, there is uncertainty due to the accuracy of the gauge and the sample of thickness measurements representing the true continuous thickness.

7.4.2.4 Yield strength

A steel quality of S235 is assumed. The characteristic yield strength, 5-quantile, is f_{yk} = 235 MPa. If one assumes a normal distribution with a standard deviation of 20 MPa, then the mean is 268 MPa. A log-normal distribution might also be used to describe the yield strength.

7.4.2.5 Crown depth

The depth to the crown is assumed to be normal distributed with a mean value of h. Most buried pipe bridges managed by NPRA have a depth between 1 m and 4 m, but the depth might be as deep as 10 m. There is uncertainty in the depth, as it is difficult to measure the exact depth. The standard deviation is assumed to be $h/20$.

7.4.2.6 Pipe diameter

A normal distribution with a mean value of D is assumed to represent the horizontal diameter. The diameter varies between pipes. A diameter of 3.5 m is chosen for demonstration. The standard deviation is assumed to be $D/100$. Figure 4.2.1 shows that a vertical load might increase the horizontal diameter of the pipe, the ovaling effect. Since the tendency is an increase

in diameter, the uncertainty might be better modelled with a distribution with skewness towards higher diameters. For an even better representation, dependency between loading variables and the diameter might be considered.

7.4.2.7 Specific weight of soil

The specific weight of the soil is assumed to be normal distributed. Specific weight of soil is dependent on type of soil and conditions. According to manual V220, NPRA (2010), a usual range for the specific weight is 15-22 kN/m^3. The mean value is set to 20 kN/m^3 and the standard deviation is set to 3 kN/m^3.

7.4.2.8 Prism load constant

For the prism load constant, a normal distribution is chosen. A mean value of 1 might be conservative, as discussed in chapter 3.3.2.5. Since there are examples of the *k*-value being larger than 1 and without any better estimate of the mean value, the mean value for the prism load constant is set to 1. The standard deviation is assumed to be 0.1.

7.4.2.9 Traffic load

For the traffic load, a Bk10 load is considered, see chapter 4.2.2.6. The critical load is the largest load for the depth of consideration between two lanes loaded with a tandem axle or tridem axle load, given that the road is a two lane road. The ring compression is most sensitive to the traffic load for shallow depths. Even when considering multiple lanes loaded with multiple axles, the load intensity for the shallowest depths are mainly from a wheel load. A wheel load might be considered as an initial simplification. If a wheel load is considered without any reduction for *h*/*D*-ratios, then it gives a quite similar load intensity to a one lane tandem load with *h*/*D*-reduction. For a diameter of $D = 3.5$ m, the comparison for this simplification is shown in figure 7.4.2. For different diameters, the comparison will be a little different, but overall quite similar for typical pipe diameters.

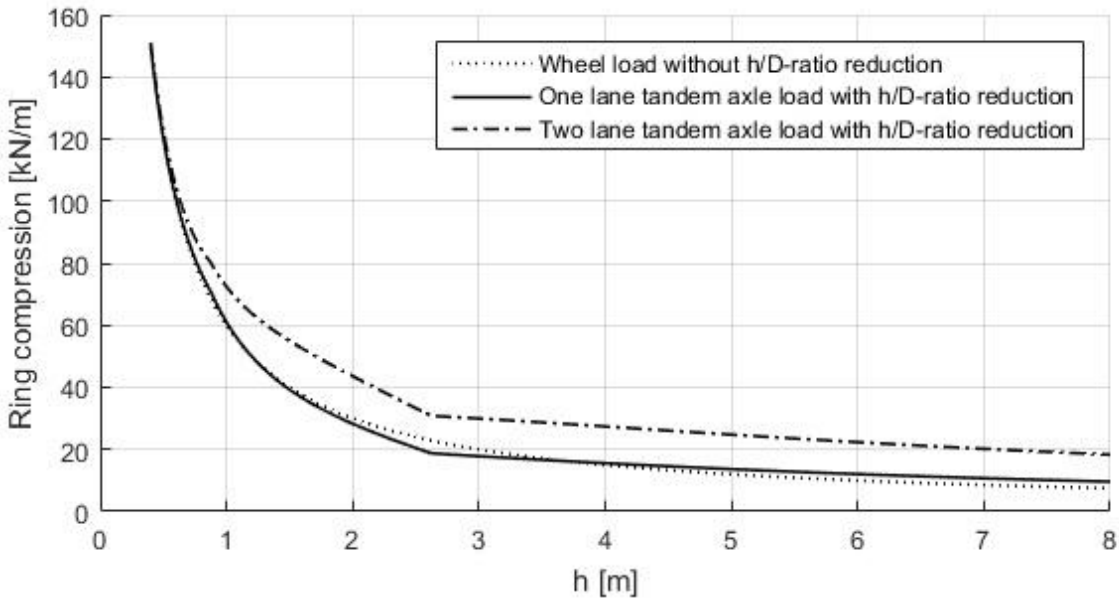

Figure 7.4.2: Simplified traffic load

The ring compression from a wheel load, F, without h/D-reduction might be calculated as in equation 7.4.6. σ_v is calculated with Boussinesq equation at a depth h right under the load F.

$$s_{traffic} = p_{traffic} = \frac{\sigma_v \pi h}{2} = \frac{3Fh^3}{2\pi h^5}\frac{\pi h}{2} = \frac{3F}{4h} \tag{7.4.6}$$

For a Bk10 load, F = 80 kN. A normal distribution is assumed to represent the uncertainty in the load. The annual maximum for the wheel load is assumed to be represented by a mean value of 80 kN and a standard deviation of 10 kN.

The line load for two lanes loaded with tandem Bk10 load might be calculated as:

$$p_{traffic,tandem} = \frac{3\mathrm{F}h^4}{4}\left(\begin{array}{l}\frac{1}{h^5} + \frac{1}{(2^2+h^2)^{\frac{5}{2}}} + \frac{1}{(1^2+h^2)^{\frac{5}{2}}} + \frac{1}{(3^2+h^2)^{\frac{5}{2}}} + \frac{13/64}{(1.3^2+h^2)^{\frac{5}{2}}} \\ + \frac{13/64}{(1.3^2+2^2+h^2)^{\frac{5}{2}}} + \frac{13/64}{(1.3^2+1^2+h^2)^{\frac{5}{2}}} + \frac{13/64}{(1.3^2+3^2+h^2)^{\frac{5}{2}}}\end{array}\right) \tag{7.4.7}$$

where F is the wheel load by Bk10 loading. The largest of this tandem load and the tridem load for depth h could be considered, and in addition it may be multiplied with a reduction factor as shown in equation 7.4.4.

7.4.3 First order reliability analysis

7.4.3.1 Uncertainty in all variables and simplified limit state function

A wheel load without any reduction factor is considered. The limit state function is:

$$g(\mathbf{x}) = atf_y - \frac{h\gamma D}{2}k - \frac{3F}{4h} \tag{7.4.8}$$

The thickness is assessed with a thickness gauge, and it is assumed that the thickness can be represented with a normal distribution for this lower uncertainty. All variables are assumed to be normal distributed and independent for simplicity.

Table 7.4.1: Variables of consideration

#	**Distribution**	X	μ_X	σ_X
1	Normal	a: wall section density	1.180 m^2/m	0.05 m^2/m
2	Normal	t: thickness pipe wall	t	0.1 mm
3	Normal	f_y: yield strength	268 MPa	20 MPa
4	Normal	h: crown depth	h	h/20
5	Normal	γ: specific weight soil	20 kN/m^3	3 kN/m^3
6	Normal	D: diameter pipe	3.5 m	0.035 m
7	Normal	k: prism load constant	1.0	0.1
8	Normal	F: traffic load	80 kN	10 kN

Variables are transformed into the standard normal space. This transformation is shown for *a* from the following equation:

$$u_1 = \frac{a - \mu_a}{\sigma_a}$$
$$a = u_1 \sigma_a + \mu_a \tag{7.4.9}$$

First order reliability analysis is considered with an iterative approach as shown in chapter 7.3.3. The limit state function has a variable in the denominator. An iteration method for the reliability index that might handle this is the Newton Raphson method. The Newton Raphson is a quite fast method, but it may fail to converge. The iterative method is expressed as:

$$\beta^{(j+1)} = \beta^{(j)} - \frac{g\left(\beta^{(j)}\boldsymbol{\alpha}^{(j+1)}\right)}{\frac{d}{d\beta^{(j)}} g\left(\beta^{(j)}\boldsymbol{\alpha}^{(j+1)}\right)} \tag{7.4.10}$$

Expressing the limit state function as a function of $\beta^{(j)}\boldsymbol{\alpha}^{(j+1)}$ is a simplification, but this does not cause any error for the final result due to convergence. No result is obtained if the Newton Raphson method fail to converge for a set of variables and an initial reliability index guess.

The problem is solved in MATLAB. The first order reliability code is shown in appendix A.1. The reliability index is calculated for depths of 0.5 m to 4.5 m. The probability of yield of pipe wall for different heights and wall thicknesses is shown in figure 7.4.3.

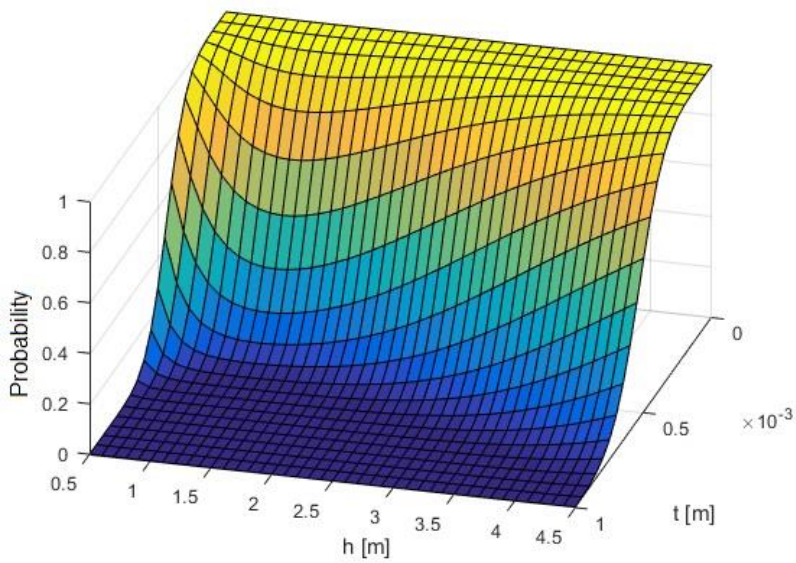

Figure 7.4.3: Probability of yield of pipe wall

A decrease in wall thickness gives a higher probability of yield of pipe wall. The curvature of the probability of yield might be compared with the ring compression figure shown in figure 4.2.7. The ring compression is higher at shallow depths due to traffic load, and for deeper depths, the ring compression gets higher because of larger earth load.

7.4.3.2 Sensitivity analysis

The alpha values give an estimation of the sensitivity to the different variables. A large absolute value of an alpha value indicates that the associated variable has a high importance to the

uncertainty and the reliability index. If the alpha value takes a negative value, then it indicates that a smaller realisation of the variable gives a higher probability of yield. On the other hand, a positive alpha value indicates that a larger realisation of the variable gives a larger probability of yield. Variables that only relate to the resistance of the structure therefore take negative values, and loads take positive values.

The figures below show calculated alpha values. The axes are rotated to give the best view of the surface plot. Thicknesses between 0 to 4 mm and depths between 0 to 10 m are considered. For a reference value, if the reliability index was equally sensitive to all eight variables, then the absolute value of the alpha values would be $\alpha = (1/8)^{0.5} = 0.35$ for all variables.

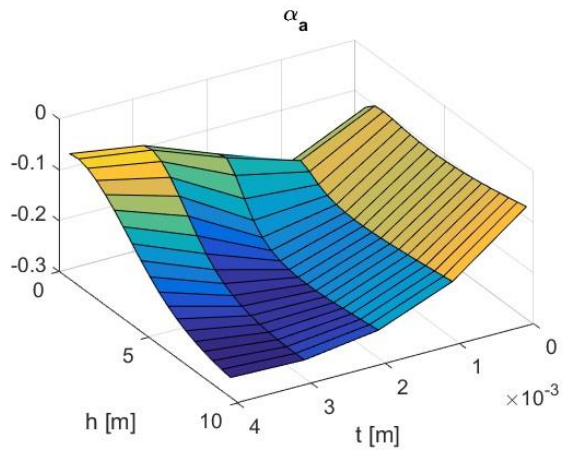

Figure 7.4.4: alpha value wall density

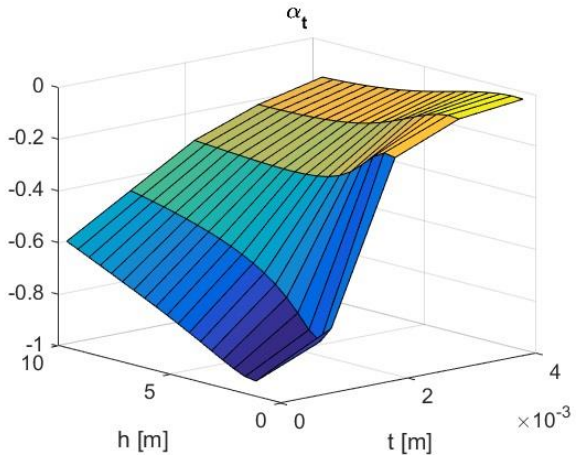

Figure 7.4.5: alpha value thickness

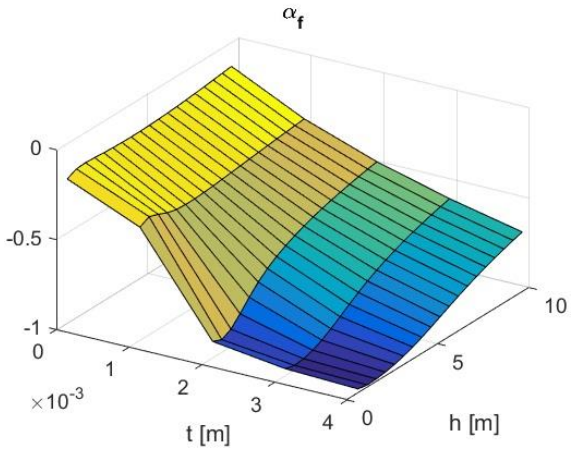

Figure 7.4.6: alpha value yield strength

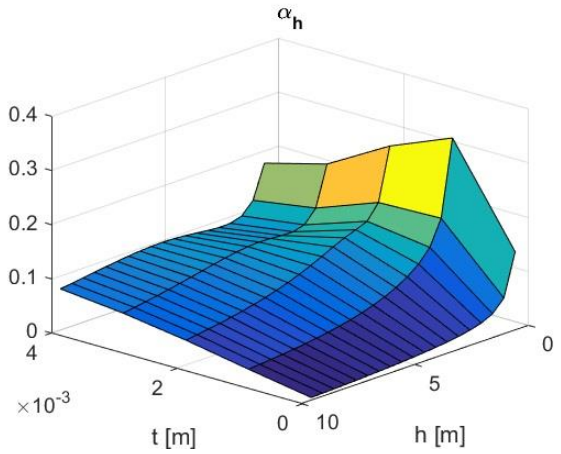

Figure 7.4.7: alpha value depth

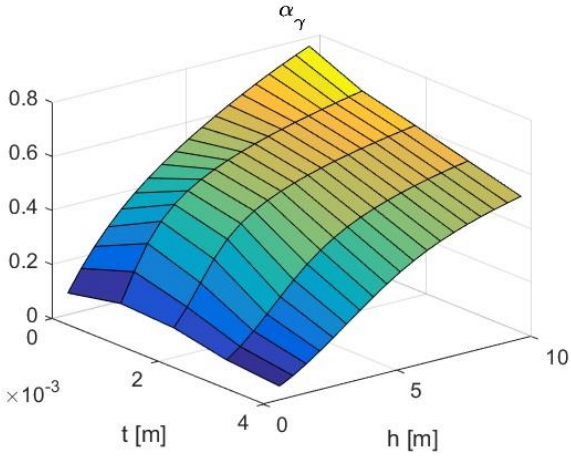

Figure 7.4.8: alpha value specific weight

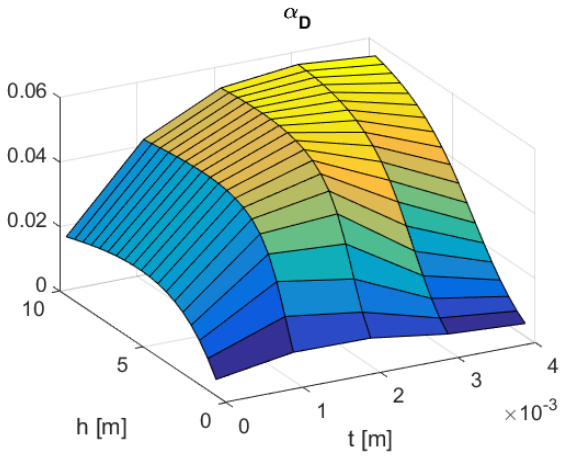

Figure 7.4.9: alpha value diameter

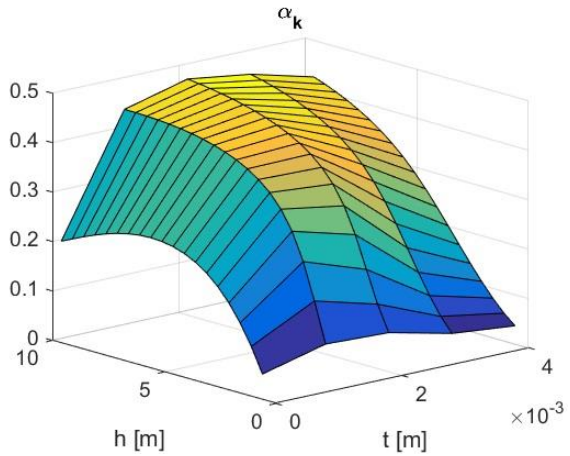

Figure 7.4.10: alpha value prism constant

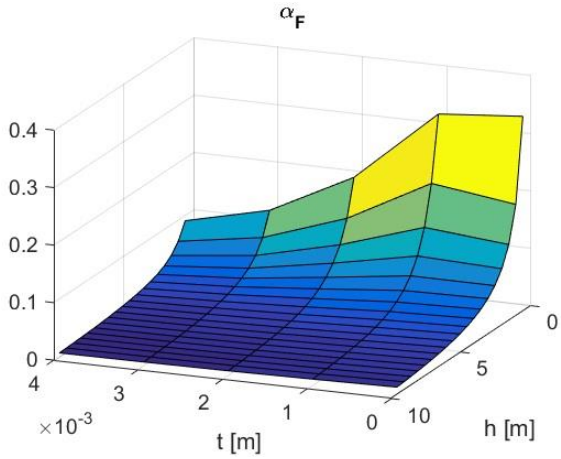

Figure 7.4.11: alpha value traffic load

If one seeks to reduce risk and weigh cost towards risk reduction, then the alpha values might indicate which variables one should focus on. The diameter of the pipe gives alpha values of less than 0.06 for all combinations of wall thicknesses and depths. Reducing the uncertainty of the diameter of the pipe would therefore not reduce the uncertainty in probability of yield that much.

For low wall thicknesses, the alpha value of the wall thickness has a very large absolute value. This indicates that reducing the uncertainty in wall thickness reduces the uncertainty in probability in yield greatly for low thicknesses. For thicker wall sections, the probability of yield is more sensitive to the yield strength.

At a large depth, the specific weight of the soil and the prism load constant are sensitive variables. The traffic load is sensitive at shallow depths. The depth of the pipe has an alpha value of about 0.1 for most combinations of depths and thicknesses, but may take a value of up to about 0.3 for a shallow depth of 0.5 m. Therefore, the probability of yield is in general not that sensitive to the depth, but for a shallower depth it is considerable sensitive to the depth variable.

7.4.3.3 Two lane tandem and tridem axle load

Two lanes loaded by a Bk10 tandem or tridem axle load is considered. The most critical load between the two loads is considered. Tandem axle load is more critical at shallow depths due to a higher concentration in the load and tridem axle load is more critical at deeper depths due to a higher total load.

When considering the tandem and tridem axle load, the limit state function is slightly different, but it is not drastically different. It is assumed that the calculated alpha values for a wheel load without *h/D*-reduction can be used to consider which uncertainties are important for the problem. Assuming the depth of the crown to be discrete makes these calculations much easier. As shown in the sensitive

ity analysis, the uncertainty in depth has never a very important contribution to the uncertainty in probability of yield. At most, the height has a sensitivity close to if all variables were just as significant for the reliability index. The uncertainty in the height is neglected and so is the uncertainty in the diameter.

The variables of consideration are shown in table 7.4.2. Uncertainty in the thickness is assumed to be assessed with a thickness gauge.

Table 7.4.2: Variables of consideration

#	**Distribution**	X	μ_X	σ_X
1	Normal	a: wall section density	1.180 m^2/m	0.05 m^2/m
2	Normal	t: thickness pipe wall	t	0.1 mm
3	Normal	f_y: yield strength	268 MPa	20 MPa
4	Normal	h: crown depth	h	-
5	Normal	γ: specific weight soil	20 kN/m^3	3 kN/m^3
6	Normal	D: diameter pipe	3.5 m	-
7	Normal	k: prism load constant	1.0	0.1
8	Normal	F: traffic load	80 kN	10 kN

The traffic load is given as of equation 7.4.7 for the tandem load, and the expression is quite similar for the tridem load. h/D-reduction for ring compression calculations is included as in equation 7.4.4.

The FORM calculations in MATLAB are shown in appendix A.2. A more stable fixed-point iteration method is used for the calculation of reliability index. The probability of yield is shown in figure 7.4.12. The overall shape is quite similar to the plot for probability of yield from figure 7.4.3, but the probabilities are a little higher for a tandem and tridem axle load compared to the simplified wheel load consideration.

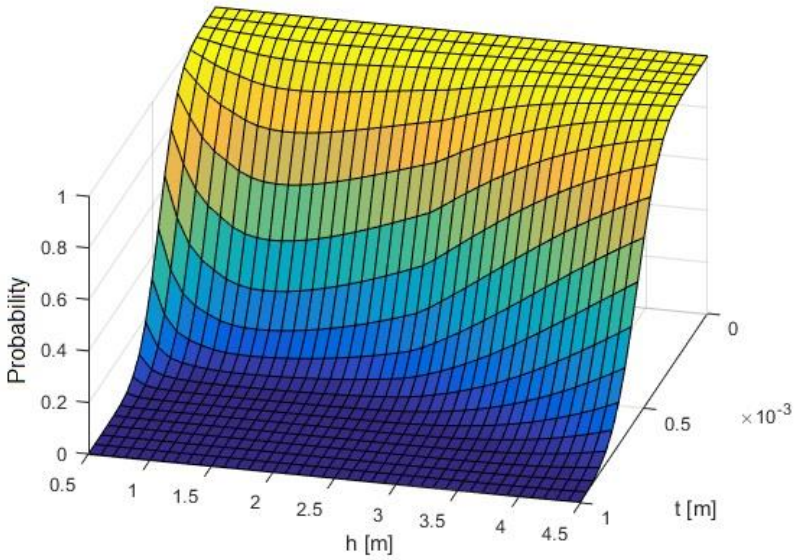

Figure 7.4.12: Probability of yield for the most common depths

Figure 7.4.13 shows the plot for a depth range between 0.5 m and 10 m and thicknesses between 0 and 3 mm. For depths lower than 5 meters, the probability of yield might become large if the thickness is smaller than 1 mm. Pipes at a depth of 10 m has a significant probability of yield for thicknesses smaller than 2 mm.

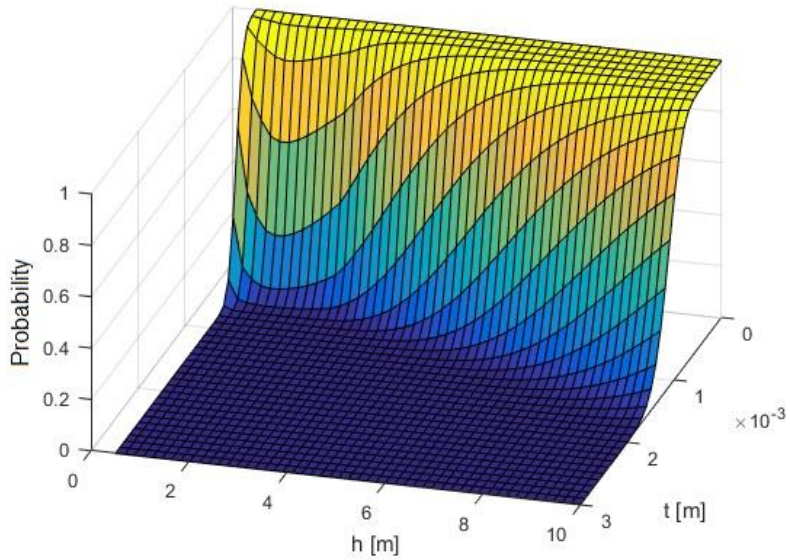

Figure 7.4.13: Probability of yield for a large range of depths

7.4.3.4 Probability of structural failure - Bayesian network

A limit state for yield of pipe wall has been considered. In case of yield or total wall section loss, the pipe will lose its original ring compression. This does not necessarily result in failure of the pipe-soil system. The system might still be standing due to the arching effect. Generally, this effect is highly uncertain, and one may argue that one should not rely on a system that is depending on the arching effect.

This relation between the state for yield of pipe wall, *Y*, and state of failure of the pipe-soil system, *F*, might be modelled as a simple Bayesian network, figure 7.4.14.

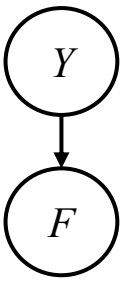

Figure 7.4.14: Bayesian network connecting yield of pipe wall and failure of system

The variable Y can take the discrete states yield or no yield and the variable F can take the states failure or no failure. The probability of failure may then be calculated as:

$$P[F = \text{Failure}] = P[F = \text{Failure}|Y = \text{Yield}] \cdot P[Y = \text{Yield}] + P[F = \text{Failure}|Y = \text{No yield}] \cdot P[Y = \text{No yield}] \tag{7.4.11}$$

There are damage degree 4 pipe bridges with total wall section loss or yield for significant parts of the pipe. Most of these bridges are standing, but some bridges have failed. An attempt to estimate $P[F = \text{Failure}|Y = \text{Yield}]$ can be done with probabilistic analysis, or it can be estimated by the inspector's knowledge.

The probability of failure given there are no yield, $P[F = \text{Failure}|Y = \text{No yield}]$, must also be estimated for finding the total probability of failure. This may be failure of the soil in the soil-pipe system. During a flood the soil might be washed away. Another failure mode of the pipe is a buckling failure mode.

The network in figure 7.4.14 can be extended to include several other variables. The probability of system failure given yield is also dependent on variables as soil condition, type of pipe and location of yield in the pipe. Figure 7.4.15 shows two different types of pipes. Focus has been directed towards the circular pipe. The arch pipe can in many cases have a larger vertical force component at its bottom corners which transfers vertical forces down to the soil, and it might be less affected by section failure at the bottom plate.

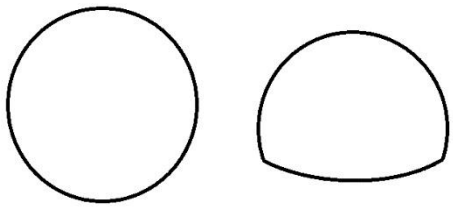

Figure 7.4.15: Circular pipe (left) and arch pipe (right)

7.5 Conclusion

This chapter relates structural reliability analysis to the steel pipe bridges. First order reliability analyses are applied assess the probability of yield. The probability of yield might become large for continuous wall thicknesses of less than 1 mm, depths of 0.5 m to 4.5 m and the given variables and limit state function of consideration. This chapter also illustrates that structural reliability analysis can be connected with Bayesian networks in assessment of existing structures.

Chapter 8

Deterioration prediction

8.1 General

Deterioration is an important aspect in decision making of existing bridges. By modelling the deterioration of a bridge, one may predict the future state of the bridge. This information can support decision making concerning inspection, maintenance, rehabilitation and replacement strategies for a bridge or a bridge stock.

This chapter starts by introducing observed deterioration data for the buried pipe bridge stock in Trøndelag. The Markov process and how it may be used for bridge deterioration is introduced and discussed. Maximum likelihood analysis is used to fit and describe the bridge stock deterioration as a Markov process.

This Markov process might describe the deterioration of the general bridge stock well, but it might not be suitable for decision making for individual bridges. In the end of this chapter, the bridge stock is separated into inland and coastal bridges. Two separate Markovian deterioration models are used to predict the deterioration of bridges in both climates. These models are connected in a simple dynamic Bayesian network.

8.2 Deterioration observation

8.2.1 General

Norwegian Public Roads Administration's database Brutus have information about damage observations for their buried steel pipe bridges. The observations have found place from 1995 until today. The observed damages range from vegetational growth around the bridge to corrosion of the pipe and erosion of surrounding soil. In the following analysis, the condition of the bridge is described by the most critical damage of the bridge. Focus is directed towards deterioration damages which affect the structural system's bearing capacity. These damages are mainly damages as corrosion of the pipe wall, pipe deformation, erosion of surrounding soil and major damages to wingwall. Appendix B shows deterioration data for 157 buried steel pipe bridges.

8.2.2 State discretization

The damage degree division by NPRA is divided into four discrete levels from a small damage to a critical damage, see chapter 2.2.3. These damage degrees are assigned state 1 to 4. In addition, one might include a state for no damage of the bridge, state 0, and failure of the bridge, state 5.

Table 8.2.1: State descriptions

State	Description
0	No damage
1 (damage degree 1)	Small damage
2 (damage degree 2)	Medium damage
3 (damage degree 3)	Large damage
4 (damage degree 4)	Critical damage
5	Failure

The bridge is said to be in the failure state when the bridge loses its functionality and there is no possibility for repair. This involves both a sudden collapse of the pipe and a state of the pipe where immediate actions are required to prevent an ongoing collapse.

The bridges are mainly assigned damage degrees based on visual inspection. The damage degrees are not quantified. Certain conditions are commonly related with the different damage degrees. Based on information by NPRA and an interpretation of the inspection data from Brutus, a selection of images and damage descriptions is used to illustrate some typical conditions related to the damage degrees. This is shown in table 8.2.2. These damages follow a natural decay with corrosion in focus. It is important to point out that the damages and the deterioration stages may be different for other pipes, and it does not need to be centred around corrosion.

There is also a subjective aspect in the assignment of states. The pipes are inspected by different inspectors and the inspectors might assign different states for the same bridge. This subjective aspect might be studied by asking several inspectors to inspect the same bridges. From this, the variation in assigned states can be modelled. Another source of variation is caused by the change in the inspector's experience and knowledge about the pipes' condition. The inspector might get a better understanding about the condition of a pipe based on previous observations. From this updated knowledge, the inspector might assign a different state compared to previous practise.

Table 8.2.2: Examples of damage degrees related to corrosion (photos by Norwegian Public Roads Administration)

Damage	Common conditions related to corrosion	Illustrative photo
Degree 1	There are minor signs of aging. The galvanized layer is present.	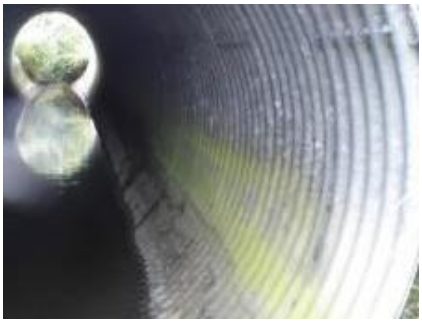
Degree 2	The galvanized layer is worn out. There is no obvious wall thickness reduction.	
Degree 3	There is corrosion with up to 25% continuous wall thickness reduction. Smaller holes from corrosion might be present, and there might be minor erosion through the holes.	
Degree 4	There is corrosion with more than 25% continuous wall thickness reduction. Corrosion might appear at all sections of the pipe. It is likely that there will be holes from corrosion, and there might be larger sections with complete wall thickness reduction. Erosion from these sections can be severe.	

8.2.3 Bridge stock age and present condition

The bridge stock data consists of 157 pipe bridges. Most bridges were constructed between 1960 and 1990. The oldest bridge was constructed in 1961. In 2018, the average age of the bridges in the bridge stock was 41 years.

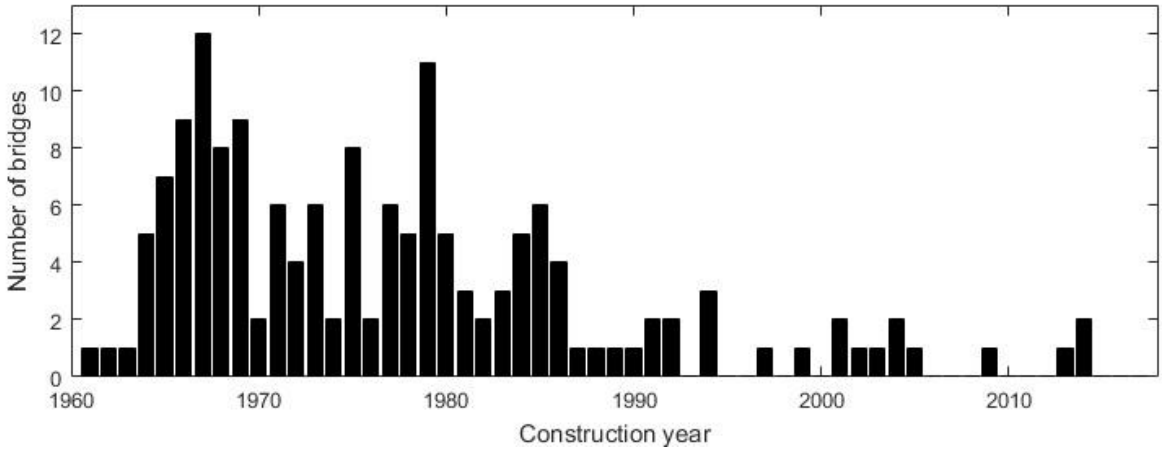

Figure 8.2.3: Construction years for bridge stock

The condition of the bridge stock in April 2018 is shown in figure 8.2.4.

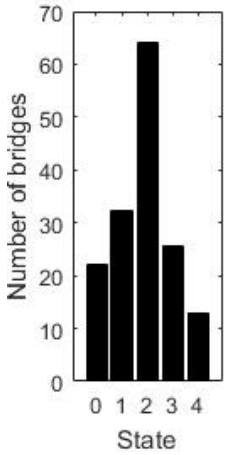

Figure 8.2.4: Condition of the bridge stock in April 2018

8.2.4 Damage observations

There are in total 284 state observations. The number of observations of different states are shown in figure 8.2.5. State 0, no damage, is not included in the observations since the database does not clearly express no damage as an observation. However, it might be assumed that the bridge has no damage right after construction.

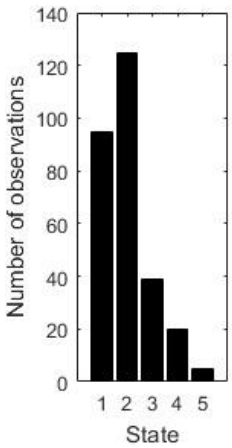

Figure 8.2.5: All observations of states

The inspection interval between two observations are shown in figure 8.2.6. A no damage observation at year 0 is not included. The most common inspection interval is five years. This is because this follows the five-year main inspection interval strategy by NPRA.

Inspection intervals of 10, 15 and 20 years are elevated compared to other nearby inspection intervals. For some main inspections, no state is assigned the bridge, and the inspection interval skips this main inspection. There are examples of bridges staying in the same state for a long inspection interval, and a natural assumption is to assume that one would have observed this state in the skipped inspection. There are, however, also examples of several degrees of decay for a long inspection interval, and then it is difficult to make objective assumptions. To treat the data in a consistent manner, no assumptions are made for skipped inspections.

There is also a higher frequency of inspection intervals shorter than five years. Bridges that are moving into a critical condition might be inspected more frequently.

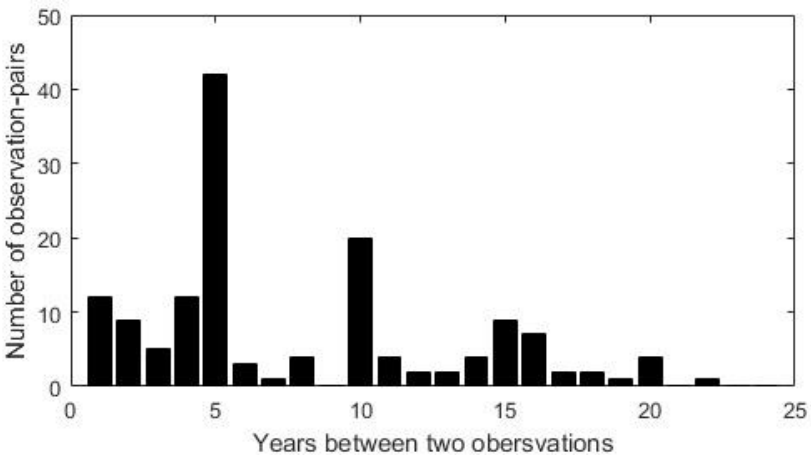

Figure 8.2.6: Interval between two observations

The observations are connected to the age of the bridge at time of observation in figure 8.2.7. This illustrates the density of states for different ages. It also illustrates a pattern of damage decay with increasing bridge age. The smallest dot represents one observation. The largest dot represents eight observations, and this is found for observations of damage degree 2 for 50 years old bridges. Most observations are of damage degree 1 and 2. There are still a

considerable amount of damage degree 3 and 4 observations for older bridges. Five failures have occurred. The bridges were 32, 37, 37, 42 and 49 years at failure.

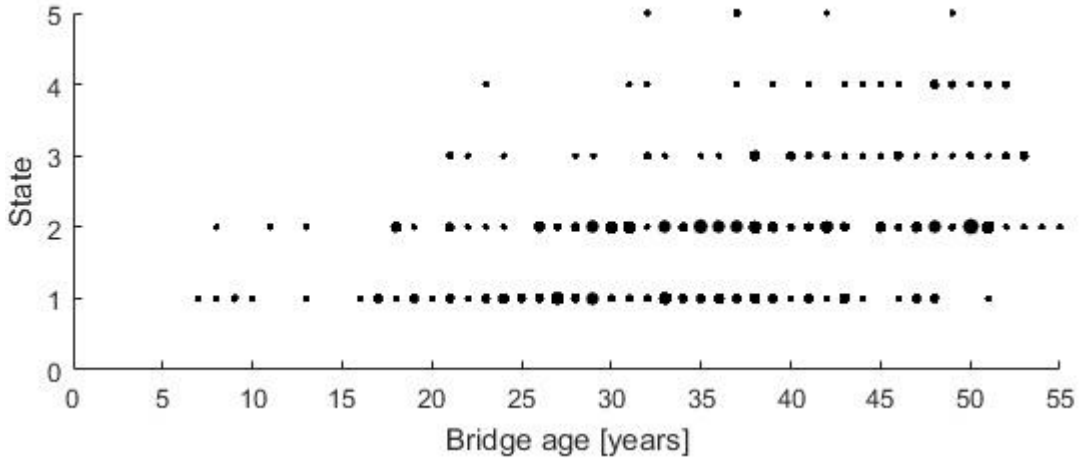

Figure 8.2.7: State observations sorted by bridge age at observation

Figure 8.2.8 shows the average observed state for different bridge ages. The largest dots represent 13 observations, and the smallest dots represent one observation. This plot shows the tendency of increased deterioration for increased age.

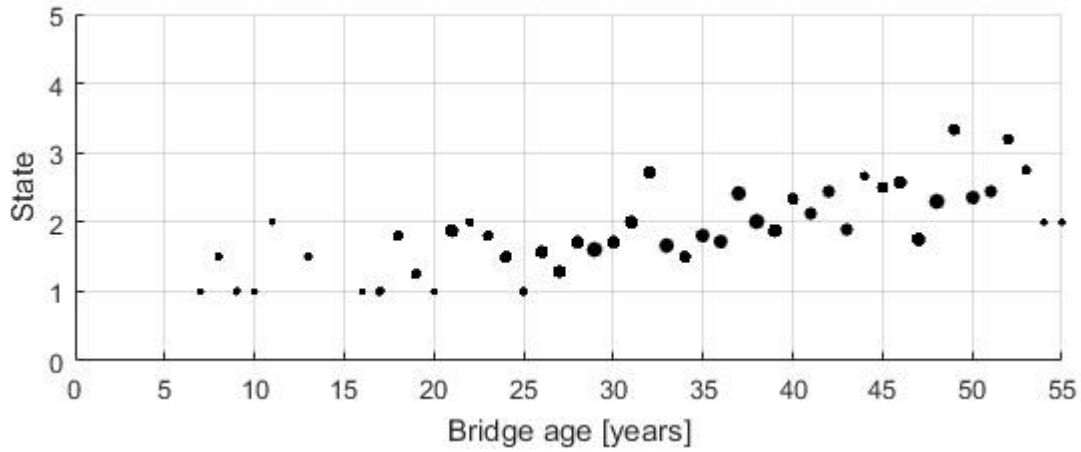

Figure 8.2.8: Average state observation sorted by bridge age at observation

8.3 Markov chain for bridge deterioration

8.3.1 General

Markov chain is a stochastic model that can be used for describing the deterioration of discrete conditional states of bridges. In the inspection of bridges, the conditional state is often divided into discrete states. Norwegian Public Roads Administration describe the severity of a bridge damage with 4 discrete states. A Markov chain might be suitable in the modelling of deterioration between these states.

The Markov chain can be modelled as the most basic dynamic Bayesian network (Straub 2015). The damage development model from a Markov chain is illustrated as a dynamic Bayesian network in figure 8.3.1.

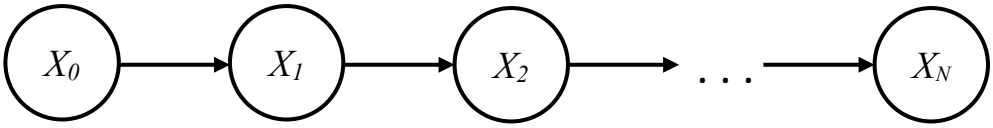

Figure 8.3.1: Markov chain illustrated as a dynamic Bayesian network

The damage degree, *X*, might take six conditional states: no damage, damage degree 1, damage degree 2, damage degree 3, damage degree 4 and failure. In this chapter, deterioration from no damage to damage degree 4 is considered. A deterioration failure consideration is made in chapter 9.

8.3.2 Discrete-time Markov process

A traditional Markov process considers a discrete time step between transitions. The time step, *n*, might be set as a one-year time step or any other preferred time steps. A traditional Markov chain is memoryless. This means that the state in a next time step is only conditional on the current state.

The state probability vector at step *n+1*, $\mathbf{x}_{n+1}$, is calculated by the state probability vector at *n*, $\mathbf{x}_n$, and the transition matrix $\mathbf{\Pi}$ from the following equation:

$$\mathbf{x}_{n+1} = \mathbf{x}_n \cdot \mathbf{\Pi} \tag{8.3.1}$$

A state probability at step *n*, $\mathbf{x}_n$, may be calculated by the initial condition, $\mathbf{x}_0$, from the equation:

$$\mathbf{x}_n = \mathbf{x}_0 \cdot \mathbf{\Pi}^n \tag{8.3.2}$$

8.3.3 Transition matrix for bridge deterioration

Table 8.3.1 shows condition states and transition probabilities in accordance with the discrete states for bridges by NPRA. Failure is not included.

Table 8.3.1: Condition states and transition probabilities

		Condition at $n+1$				
		No damage	**Degree 1**	**Degree 2**	**Degree 3**	**Degree 4**
Condition at n	**No damage**	π_{00}	π_{01}	π_{02}	π_{03}	π_{04}
	Degree 1	π_{10}	π_{11}	π_{12}	π_{13}	π_{14}
	Degree 2	π_{20}	π_{21}	π_{22}	π_{23}	π_{24}
	Degree 3	π_{30}	π_{31}	π_{32}	π_{33}	π_{34}
	Degree 4	π_{40}	π_{41}	π_{42}	π_{43}	π_{44}

The transition matrix is:

$$\mathbf{\Pi} = \begin{bmatrix} \pi_{00} & \pi_{01} & \pi_{02} & \pi_{03} & \pi_{04} \\ \pi_{10} & \pi_{11} & \pi_{12} & \pi_{13} & \pi_{14} \\ \pi_{20} & \pi_{21} & \pi_{22} & \pi_{23} & \pi_{24} \\ \pi_{30} & \pi_{31} & \pi_{32} & \pi_{33} & \pi_{34} \\ \pi_{40} & \pi_{41} & \pi_{42} & \pi_{43} & \pi_{44} \end{bmatrix} \tag{8.3.3}$$

The probability π_{ij} is the probability that a bridge goes from state *i* to state *j* in a time step. The summation of probabilities in a row adds up to one. Each probability has a value between 0 and 1, $0 < \pi_{ij} < 1$.

If one considers natural deterioration, the conditional state can only stay in the same state or decay to a worse state at increasing time step. The criteria will therefore be that there are no improving maintenance, rehabilitation or replacement actions. Maintenance as removing vegetation around the pipe and accumulated stones in the pipe might slow down deterioration, but it is not considered to improve the critical state of the bridge. The no state-improving assumption leads to the following progressive transition matrix:

$$\mathbf{\Pi} = \begin{bmatrix} \pi_{00} & \pi_{01} & \pi_{02} & \pi_{03} & \pi_{04} \\ 0 & \pi_{11} & \pi_{12} & \pi_{13} & \pi_{14} \\ 0 & 0 & \pi_{22} & \pi_{23} & \pi_{24} \\ 0 & 0 & 0 & \pi_{33} & \pi_{34} \\ 0 & 0 & 0 & 0 & 1 \end{bmatrix} \tag{8.3.4}$$

The last state, damage degree 4, can only stay in the last state, and therefore $\pi_{44} = 1$. This state is the absorbing state of the model.

A sequential model is often used to describe bridge deterioration. This model only allows a transition to stay in the same state or decay with one degree. Matrix 8.3.5 shows this model for state 0 to 4.

$$\mathbf{\Pi} = \begin{bmatrix} \pi_{00} & 1-\pi_{00} & 0 & 0 & 0 \\ 0 & \pi_{11} & 1-\pi_{11} & 0 & 0 \\ 0 & 0 & \pi_{22} & 1-\pi_{22} & 0 \\ 0 & 0 & 0 & \pi_{33} & 1-\pi_{33} \\ 0 & 0 & 0 & 0 & 1 \end{bmatrix} \tag{8.3.5}$$

The sequential model might be represented graphically as in figure 8.3.2. The numbers within the circles represent the states and the arrows with probabilities represent the transition probabilities. A similar representation is given by Kallen (2007).

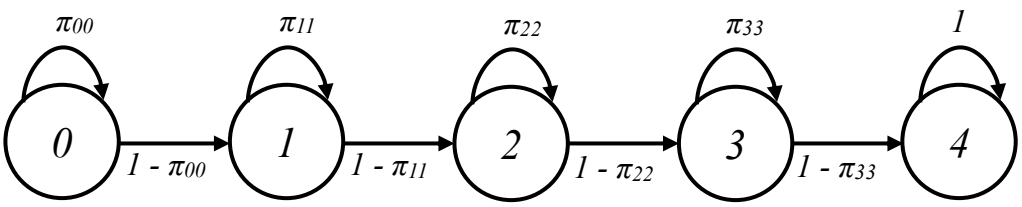

Figure 8.3.2: Sequential Markov process

8.3.4 Semi-Markov process

A semi-Markov process is a stochastic process and it is an extension of the traditional discrete Markov process. The extension of a semi-Markov process includes a time consideration with a probabilistic waiting time for a transition.

Kallen (2007) proposes how a semi-Markov process might relate to infrastructure deterioration. If a bridge moves into state *i* at transition *n*, then the probability for the process to move into state *j* for a time *T* less or equal to *t* is:

$$Q_{ij}(t) = P[T \leq t, X_{n+1} = j | X_n = i] \tag{8.3.6}$$

This probability might be expressed as:

$$Q_{ij}(t) = F_{ij}(t) \cdot \pi_{ij} \tag{8.3.7}$$

where $Fij(t) = P[T \leq t | X_{n+1} = j, X_n = i]$ and $\pi_{ij} = P[X_{n+1} = j | X_n = i]$.

π_{ij} is a transition probability going from state *i* to *j* and F_{ij} is the probability of waiting time *T* being less or equal to *t* given the transition.

The process is called semi-Markov because the waiting time is not necessarily memoryless. If an exponential distribution is chosen to represent the waiting time, then the waiting time distribution has a constant intensity. In that case, the waiting time for a transition is independent from time spent in previous states and the model is still memoryless with Markovian properties. This model is a continuous-time process. The exponential cumulative function for the waiting time, F_i, with transition intensity $\lambda_i > 0$ *is:*

$$F_i(t) = 1 - e^{-\lambda_i t} \tag{8.3.8}$$

For a continuous-time Markov process, the relation between the transition probability matrix, **Π**, and the transition intensity matrix, **Q**, for a transition from time *s* to time *t* may be given as in equation 8.3.9. This relation is explained by Howard (1971).

$$\mathbf{\Pi}(s,t) = \exp(\mathbf{Q} \cdot (t - s)) \tag{8.3.9}$$

The transition intensity matrix, **Q**, for a sequential Markov process with constant transition intensities, λ_i, which only allows decay is given in the matrix below. This matrix considers state 0 to state 4, no damage to damage degree 4, and the last state is the absorbing state.

$$\mathbf{Q} = \begin{bmatrix} -\lambda_0 & \lambda_0 & 0 & 0 & 0 \\ 0 & -\lambda_1 & \lambda_1 & 0 & 0 \\ 0 & 0 & -\lambda_2 & \lambda_2 & 0 \\ 0 & 0 & 0 & -\lambda_3 & \lambda_3 \\ 0 & 0 & 0 & 0 & 0 \end{bmatrix} \tag{8.3.10}$$

This sequential continuous-time Markov process is shown graphically in figure 8.3.3, Kallen (2007). The state of the bridge is given inside the circles.

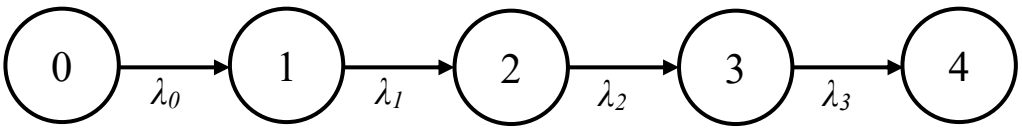

Figure 8.3.3: Sequential continuous-time Markov process

8.4 Predicting deterioration model

8.4.1 General

A transition matrix for a Markov process may be developed by a frequency approach or a regression approach, Ng S. K & Moses F. (1996). The frequency approach requires a set of observation data, and the development of a transition matrix might be poor or impossible for a small amount of data. Regression approaches are more flexible. A common practise is to sort observations by the age of the bridge at inspection and then predict a transition model by minimising the difference from observations by regression.

This paper focus on regression by use of maximum likelihood estimation and a continuous-time Markov process for predicting deterioration. A proposed framework is given by Kallen (2007). The continuous Markov-process follows Markovian properties with a memoryless model. It does not add additional information as exact transition times, which is something many other models do, including the frequency approach. The continuous Markov-process is flexible in dealing with various inspection lengths, and therefore, all the observed deterioration data by NPRA may be used for the prediction model. The maximum likelihood method is a preferred regression approach as it is possible to study the uncertainty of an estimation.

8.4.2 Frequency approach and different time steps

8.4.2.1 Frequency approach

Let n_{ij} be the number of observed transition events in a bridge stock that goes from state i to state j in the next time step and let n_i be the number of transition events being in state i before transition. The probabilities in the transition matrix may then be calculated as:

$$\hat{\pi}_{ij} = \frac{n_{ij}}{n_i} \tag{8.4.1}$$

The frequency approach follows a maximum likelihood estimation of transition probabilities based on a multinomial distribution of observation probabilities, Anderson and Goodman (1957).

The method assumes a constant time step between transitions. Transitions are forced to follow this exact time step, and this adds additional information to the model. This is a weakness with the frequency Markov process model. Another weakness is that the model requires observation pairs. The accuracy for the model increase with a larger data set, but the frequency approach might give a poor estimation for a small data set.

8.4.2.2 Different time steps

It becomes a challenge to use the frequency approach for the data by NPRA, since the inspection intervals vary. Methods have been developed to deal with the challenge of different inspection intervals. This includes a method used by Pontis, a software owned by the American Association of State Highway and Transportation Officials. The method assumes a sequential probability matrix. The transition probabilities for different time steps, n, are transferred into a

reference one-year time step by the relation $\pi_{ii} = \sqrt[n]{\pi_{ii,n}}$ and $\pi_{ij} = 1 - \pi_{ii}$ for $j = i + 1$. $\pi_{ii,n}$ is the probability that state *i* will stay in this state for a transition with time step *n*. The transferred transition matrices for different time steps are then combined to a final transition matrix by the weighted average of the matrices. For further explanation see Pontis 4.4 Techincal Manual (2005).

This method does not differentiate between a transition of one degree or several degrees from observations, and this gives a slower predicted deterioration if there are observations of several degrees of decay. Kallen (2007) also shows that the reference period transformation and average weighting is faulty. Therefore, no more attention will be paid to this combinational method.

8.4.3 Maximum likelihood estimation for a semi-Markov Process

8.4.3.1 Maximum likelihood estimation

Let $f_X(x|\boldsymbol{\theta})$ be the probability density function for the variable *X* given that the distribution is described with parameters $\boldsymbol{\theta}$. For a random sample by inspection $X_0, X_1, \ldots, X_n$, the joint probability distribution becomes:

$$f_{X_0, X_1, \ldots, X_n}(\hat{x}_1, \hat{x}_2, \ldots, \hat{x}_n|\boldsymbol{\theta}) = \prod_{i=1}^{n} f_X\,(\hat{x}_i|\boldsymbol{\theta}) \tag{8.4.2}$$

where $\hat{x}_1, \hat{x}_2, \ldots, \hat{x}_n$ are realisations of the random sample. If one knows the samples from inspection $\hat{\mathbf{x}}$, then one might look at the likelihood of having observed this sample as a function of the parameters $\boldsymbol{\theta}$. The likelihood function is given as:

$$L(\boldsymbol{\theta}|\hat{\mathbf{x}}) = \prod_{i=1}^{n} f_X(\hat{x}_i|\boldsymbol{\theta}) \tag{8.4.3}$$

The maximum likelihood estimation of $\boldsymbol{\theta}$ is given for the set of parameters $\boldsymbol{\theta}^*$ which the likelihood function takes its maxima:

$$\max_{\boldsymbol{\theta}}\{L(\boldsymbol{\theta}|\hat{\mathbf{x}})\} \tag{8.4.4}$$

One might also find the maximum likelihood estimation of $\boldsymbol{\theta}$ by maximising the log-likelihood function. The log-likelihood function has the advantage of dealing with summation rather than multiplication.

$$l(\boldsymbol{\theta}|\hat{\mathbf{x}}) = \sum_{i=1}^{n} \ln(f_X(\hat{x}_i|\boldsymbol{\theta})) \qquad \max_{\boldsymbol{\theta}}\{l(\boldsymbol{\theta}|\hat{\mathbf{x}})\} \tag{8.4.5}$$

For a large observation sample *n*, the distribution of the parameters converges towards a normal distribution. The covariance matrix for the parameters $\boldsymbol{\theta}$, $\mathbf{C}_{\boldsymbol{\theta}\boldsymbol{\theta}}$, is calculated by the inverse of the

Hessian matrix. The Hessian matrix is calculated at the maximization of the parameters $\boldsymbol{\theta}^*$ by the second order partial derivatives of the log-likelihood function.

$$\mathbf{C}_{\boldsymbol{\theta}\boldsymbol{\theta}} = \mathbf{H}^{-1}$$
$$H_{ij} = -\left.\frac{\partial^2 l(\boldsymbol{\theta}|\hat{\mathbf{x}})}{\partial\theta_i \partial\theta_j}\right|_{\boldsymbol{\theta}=\boldsymbol{\theta}^*} \tag{8.4.6}$$

8.4.3.2 Likelihood of bridge observations

The observations from the data set in chapter 7.2 are observations assessed by the inspector. There is an uncertainty in the inspection of the true state of the bridge condition. This is illustrated in the simple dynamic Bayesian network in figure 8.4.1. X_i is the true state of the bridge condition and I_i is the state of the bridge obtained from inspection at step i. Another name for this model is a hidden Markov model.

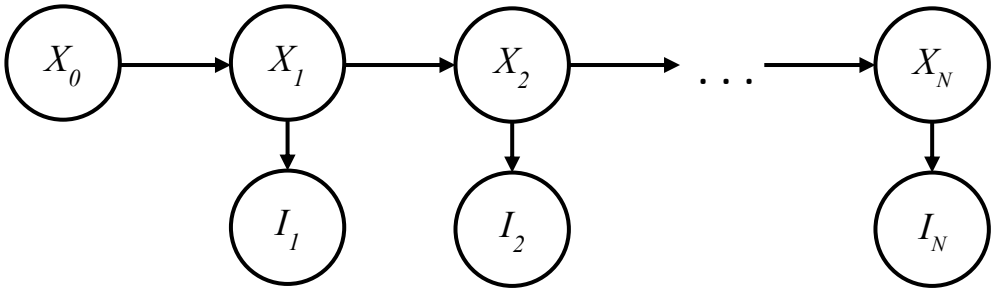

Figure 8.4.1: Bridge deterioration with inspection uncertainty

If the accuracy of the inspections is perfect, then the observed states are the true states of the bridge. In that case, the probability for a sequence of states for a bridge might be expressed as (Kallen 2007):

$$P[X_1, \dots, X_n] = P[X_0] \prod_{i=0}^{n} P[X_{i+1}|X_i] \tag{8.4.7}$$

If imperfect observations are considered, then the probability of a sequence is:

$$P[I_1, \dots, I_N] = \sum_{\forall \boldsymbol{X}} P[\mathbf{I}|\mathbf{X}]\, P[\mathbf{X}] \tag{8.4.8}$$

where $\mathbf{I} = \{I_1, \dots, I_n\}$ *and* $\mathbf{X} = \{X_1, \dots, X_n\}$. If the inspection observations I_i are independent for i = 1, …, n, and inspection observations are only conditional on the true state then $P[\mathbf{I}|\mathbf{X}]$ is calculated as given in equation 8.4.9.

$$P[\mathbf{I}|\mathbf{X}] = \prod_{i=1}^{n} P[I_i|X_i] \tag{8.4.9}$$

Perfect inspections will be considered for analysis of data presented in chapter 7.2. This is because the inspection uncertainty is not known. As discussed in chapter 7.2, the subjective aspect might be studied by asking several inspectors to inspect the same bridges.

The likelihood for a bridge stock of m bridges with n_j transition for each bridge might be calculated as given in equation 8.4.10. This equation assumes the initial condition of the bridges to be certain $P[X_0] = 1$, and for the bridge stock data for the pipe bridges, an initial condition X_0, no damage, will be assumed.

$$L(\boldsymbol{\theta}|\hat{\mathbf{x}}) = \prod_{j=1}^{m}\prod_{i=0}^{n_j} P_j[X_{j,i+1} = \hat{x}_{j,i+1} 1 X_{j,i} = \hat{x}_{j,i}] \tag{8.4.10}$$

With a log-likelihood consideration, the equation becomes:

$$l(\boldsymbol{\theta}|\hat{\mathbf{x}}) = \sum_{j=1}^{m}\sum_{i=0}^{n_j} \ln\left(P_j[X_{j,i+1} = \hat{x}_{j,i+1} |\, X_{j,i} = \hat{x}_{j,i}]\right) \tag{8.4.11}$$

For a time-homogenous sequential semi-Markov process, the parameters to estimate are the transition intensities, λ_i, in the transition intensity matrix:

$$\mathbf{Q} = \begin{bmatrix} -\lambda_0 & \lambda_0 & 0 & 0 & 0 \\ 0 & -\lambda_1 & \lambda_1 & 0 & 0 \\ 0 & 0 & -\lambda_2 & \lambda_2 & 0 \\ 0 & 0 & 0 & -\lambda_3 & \lambda_3 \\ 0 & 0 & 0 & 0 & 0 \end{bmatrix} \tag{8.4.12}$$

The probability for the transition is found by considering the relation between the transformation intensity matrix and the transformation probability matrix. For a continuous time-homogenous semi-Markov process where a transition starts at time s and ends at time t, $\mathbf{\Pi}(s, t) = \mathbf{\Pi}(0, t-s) = \exp(\mathbf{Q}(t-s))$. If i represents the starting condition and j represents the ending condition, then:

$$\pi_{ij}(0, t-s) = P[X(t-s) = j|X(0) = i] \tag{8.4.13}$$

8.5 Buried pipe deterioration

8.5.1 General

Two time-homogenous models for the likelihood maximization of data in chapter 7.2 are considered, model A and model B. Model A assumes a state independent transition intensity model, that is $\lambda_i = \lambda$ for $i = 0, 1, 2, 3$, and model B assumes a state dependent transition intensity matrix, that is $\lambda_i = \lambda_i$ for $i = 0, 1, 2, 3$. There are 5 states of consideration, state 0 to state 4, no damage to damage degree 4. Damage degree 4 is the absorbing state. All damage development observations are sorted into a table as shown in table 8.5.1. Failure observations are not included, and all bridges are assumed to be in state 0 in year 0.

Table 8.5.1: Sorted damage observations

Data storage, D

t_i	t_{i+1}	X_i	X_{i+1}
0	43	0	1
43	54	1	2
0	41	0	2
0	31	0	1
31	38	1	1
38	52	1	3
52	53	3	3
…	…	…	…

The maximum likelihood estimation of the parameters λ_i are found for both model A and B. Numerical calculations are performed in MATLAB for this maximization. The procedure is shown in appendix C. Instead of maximizing the log-likelihood, the procedure minimizes the negative of the log-likelihood.

8.5.2 Result for state independent model A

A maximum likelihood consideration for model A with state independent transition intensities is made in appendix C.1. This leads to the following result:

Table 8.5.2: Estimated parameter for bridge stock deterioration, model A

Parameter	**Mean,** μ	**Coefficient of variation,** $c_v = \sigma/\mu$
λ	0.0555	0.0440

This gives the following maximization of the transition intensity matrix:

$$\mathbf{Q} = \begin{bmatrix} -0.0555 & 0.0555 & 0 & 0 & 0 \\ 0 & -0.0555 & 0.0555 & 0 & 0 \\ 0 & 0 & -0.0555 & 0.0555 & 0 \\ 0 & 0 & 0 & -0.0555 & 0.0555 \\ 0 & 0 & 0 & 0 & 0 \end{bmatrix} \tag{8.5.1}$$

The transition probability matrix for a one-year time step is:

$$\mathbf{\Pi} = \exp(\mathbf{Q} \cdot 1) = \begin{bmatrix} 0.9460 & 0.0525 & 0.0015 & 0.0000 & 0.0000 \\ 0 & 0.9460 & 0.0525 & 0.0015 & 0.0000 \\ 0 & 0 & 0.9460 & 0.0525 & 0.0015 \\ 0 & 0 & 0 & 0.9460 & 0.0540 \\ 0 & 0 & 0 & 0 & 1 \end{bmatrix} \tag{8.5.2}$$

This transition probability matrix follows the sequential damage development even though it appears to skip states in the one-year reference period. This is because there is a possibility that there are several degrees of sequential decay within one year.

The predicted distribution of deterioration over the years is shown in figure 8.5.1. In year 0, the initial state is no damage. The lines are continuous for the time period where prediction is fitted to observations. Striped lines show a prediction of deterioration outside years of observation.

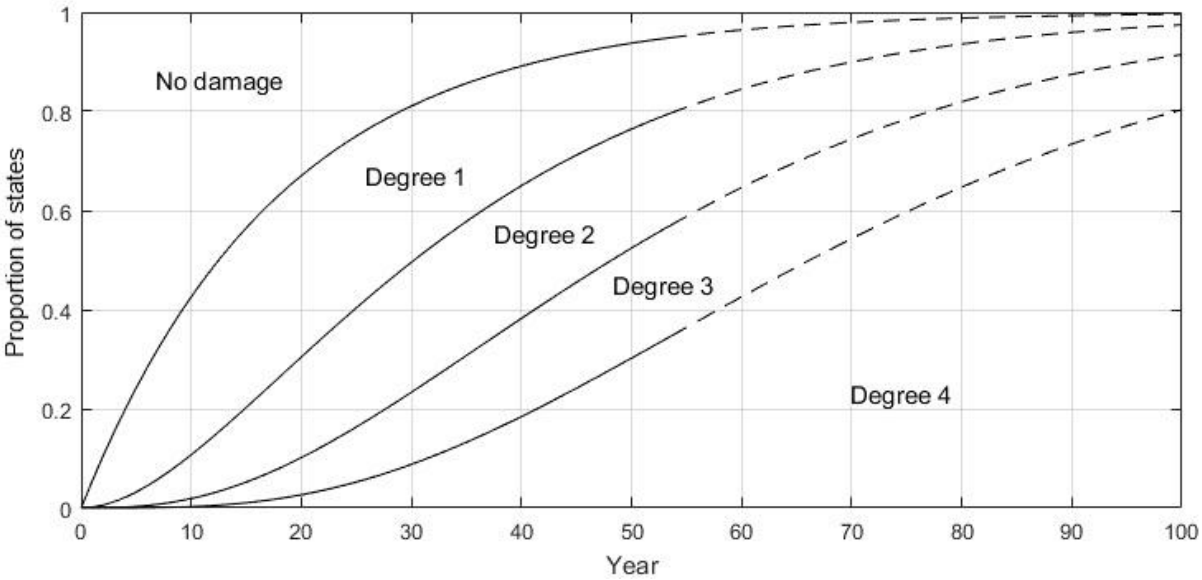

Figure 8.5.1: Predicted deterioration for a new bridge with model A

8.5.3 Result for state dependent model B

Calculations for model B is shown in appendix C.2. Table 8.5.3 shows the estimated parameters for model B:

Table 8.5.3: Estimated parameters for bridge stock deterioration, model B

Parameter	**Mean,** μ	**Coefficient of variation,** $c_v = \sigma/\mu$
λ_0	0.1811	0.1995
λ_1	0.0356	0.0880
λ_2	0.0268	0.1295
λ_3	0.0636	0.2291

For the mean value of the predicted parameters, the transition intensity matrix becomes:

$$\mathbf{Q} = \begin{bmatrix} -0.1811 & 0.1811 & 0 & 0 & 0 \\ 0 & -0.0356 & 0.0356 & 0 & 0 \\ 0 & 0 & -0.0268 & 0.0268 & 0 \\ 0 & 0 & 0 & -0.0636 & 0.0636 \\ 0 & 0 & 0 & 0 & 0 \end{bmatrix} \tag{8.5.3}$$

The transition probability matrix for a one-year time step is given in matrix 8.5.4.

$$\mathbf{\Pi} = \begin{bmatrix} 0.8343 & 0.1627 & 0.0030 & 0.0000 & 0.0000 \\ 0 & 0.9650 & 0.0346 & 0.0004 & 0.0000 \\ 0 & 0 & 0.9735 & 0.0256 & 0.0008 \\ 0 & 0 & 0 & 0.9384 & 0.0616 \\ 0 & 0 & 0 & 0 & 1 \end{bmatrix} \tag{8.5.4}$$

The correlation coefficients for the parameters are shown in table 8.5.4.

Table 8.5.4: Correlation coefficient between estimated parameters

Correlation coefficient, ρ	λ_0			
λ_0	1	λ_1		
λ_1	−0.4530	1	λ_2	
λ_2	−0.1144	−0.0161	1	λ_3
λ_3	−0.0284	−0.0013	−0.0263	1

The correlation is negative between all parameters. This implies that increase in one parameter gives decrease in other parameters. Some parameters have quite small correlations and are almost independent. The correlation is especially strong between λ_0 and λ_1, where $\rho_{\lambda 0 \lambda 1} = -0.45$, and λ_0 and λ_2, where $\rho_{\lambda 0 \lambda 2} = -0.11$. An increase in the estimation of transition intensity going from no damage to damage degree 1 will give significant decrease in the estimation of transition intensity going from damage degree 1 to damage degree 2.

Figure 8.5.2 shows the predicted distribution of damage degrees per year by model B.

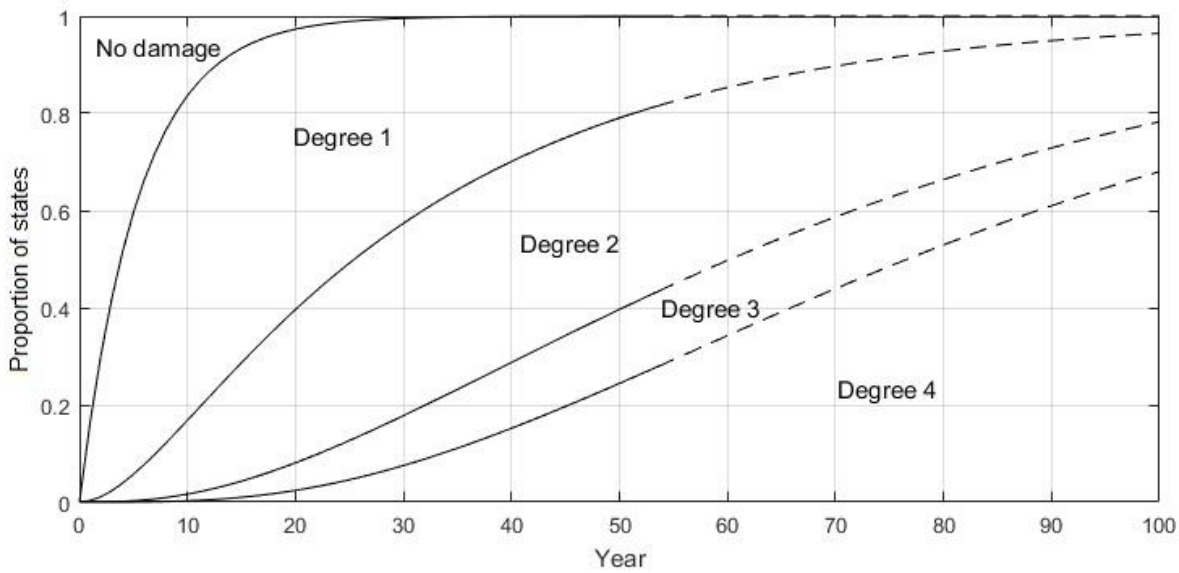

Figure 8.5.2: Predicted deterioration for a new bridge with model B

8.5.4 Comparison of models and quality of fit

The average value of the predicted deterioration is plotted for both models together with the observed states. Model B shows a more flexible curve than model A, and it appears that model B has a higher goodness of fit based on the average value of the predicted states.

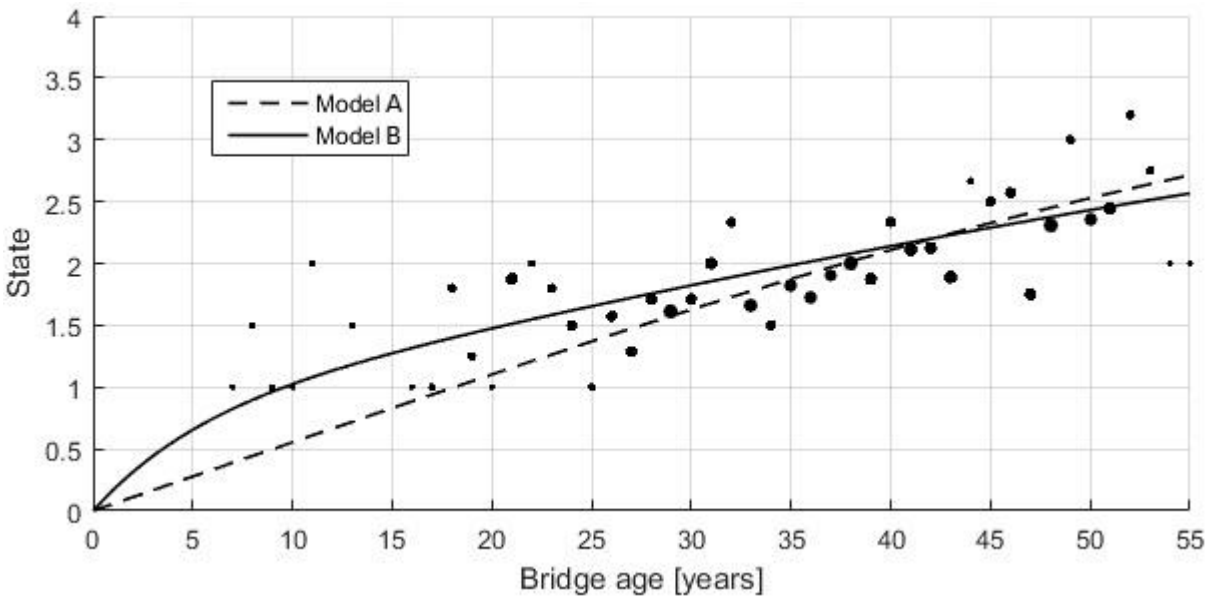

Figure 8.5.3: Average observations and average predictions

A likelihood ratio test may be used to test the significance of the better fit of model B compared to model A. Table 8.5.5 shows the number of parameters of the models and the log-likelihood value for the considered data set.

Table 8.5.5: Log-likelihood and number of parameters for the bridge stock models

Model	Parameters	Log-likelihood
A	1	−587.3
B	4	−529.6

The models are nested, which implies that the more general model B can be transformed into model A. The transformation constraint which transforms model B into model A is $\lambda_i = \lambda$ for $i = 0, 1, 2, 3$.

The more general model B is assumed to give a correct distribution for the population which the damage degree observations are from. This is the H hypothesis. An alternative hypothesis is considered, H_0, which is a hypothesis that model A describes the observations.

H_0: The observations are from a population with a model A-distribution

H: The observations are from a population with model B-distribution

L_A^* represent the maximum likelihood for model A and L_B^* represent the maximum likelihood for model B. Model A has $m = 1$ degrees of freedom and model B has $h = 4$ degrees of freedom. By using results from Wilks (1938), one might express the relation between these likelihoods in a way that is χ^2-distributed with $h - m$ degrees of freedom, equation 8.5.5.

$$-2\ln\left(\frac{L_A^*}{L_B^*}\right) = -2(\ln(L_A^*) - \ln(L_B^*)) \tag{8.5.5}$$

If one considers a desired statistical significance level, one might use equation 8.5.5 to decide whether to reject hypothesis H_0. This is done by comparing the value from equation 8.5.5 with the value of the χ^2-distribution with $h - m$ degrees of freedom for the statistical significance. If the value from equation 8.5.5 is larger than this, then H_0 is rejected. The 0.01-quantile of χ^2-distribution is considered:

$$-2\ln\left(\frac{L_A^*}{L_B^*}\right) > \chi^2_{0.01,3} \qquad (8.5.6)$$
$$-2\big(-587.3 - (-529.6)\big) = 115.4 > 11.3$$

Since the expression is true, the H_0 hypothesis is rejected. Model B describes the deterioration of the bridge stock better than model A.

8.5.5 Bridge stock deterioration from today

Based on the current condition of the buried pipe bridges, a prediction is made for the future states with damage degree 4 being the absorbing state. Model B transition probabilities are used. The prediction assumes the bridges to continue to deteriorate as they have done, and no replacements or major actions are made. It also does not consider failure of bridges. The expected distribution of states per year for the bridge stock within the next 50 years is shown in figure 8.5.4.

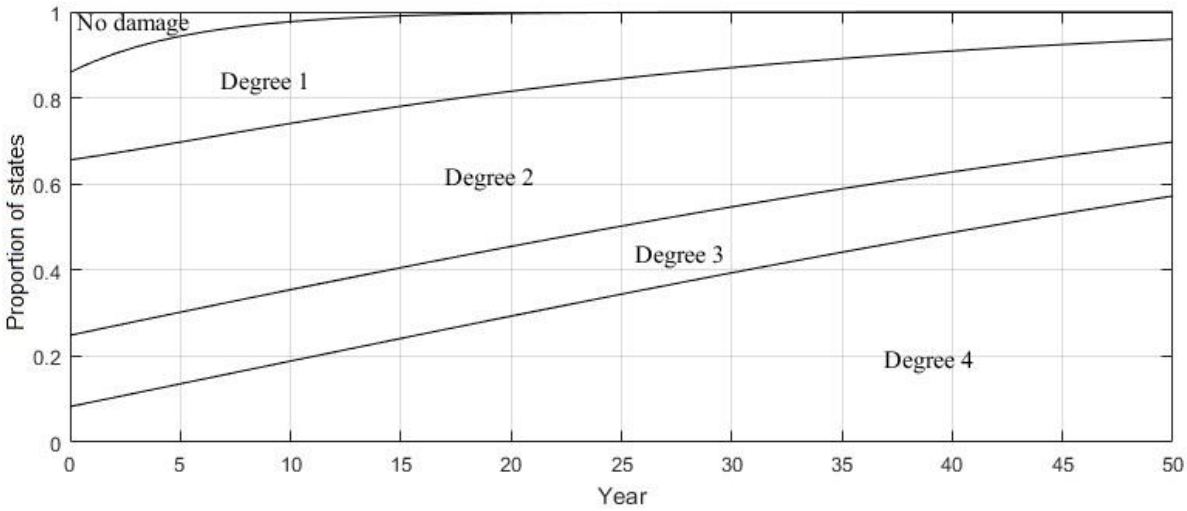

Figure 8.5.4: Deterioration of the bridge stock with model B

The bridge stock has 157 bridges. The expected number of bridges in each state is calculated from this prediction. Figure 8.5.5 to figure 8.5.9 show the prediction for number of bridges in the different states. The vertical axis is adjusted for the best fit. Number of bridges with damage degree 4 is predicted to increase a lot in number over the years. This prediction is unlikely since failures and renewals are not considered. See chapter 9.4 for a prediction of failures and chapter 10.5 for a consideration of renewals.

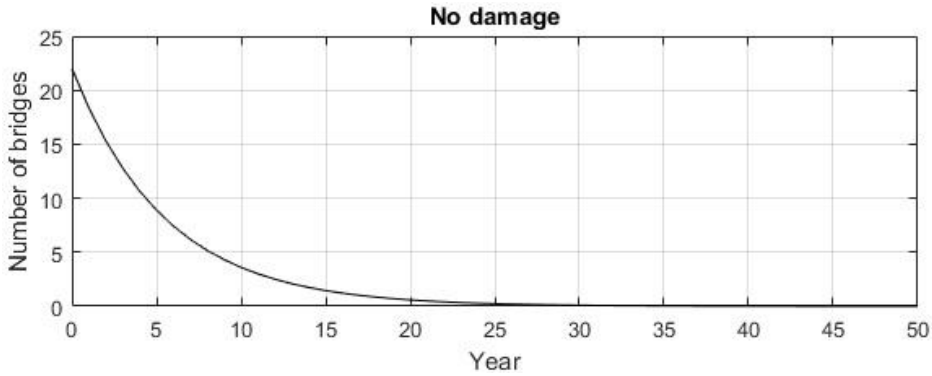

Figure 8.5.5: Predicted number of bridges with no damage

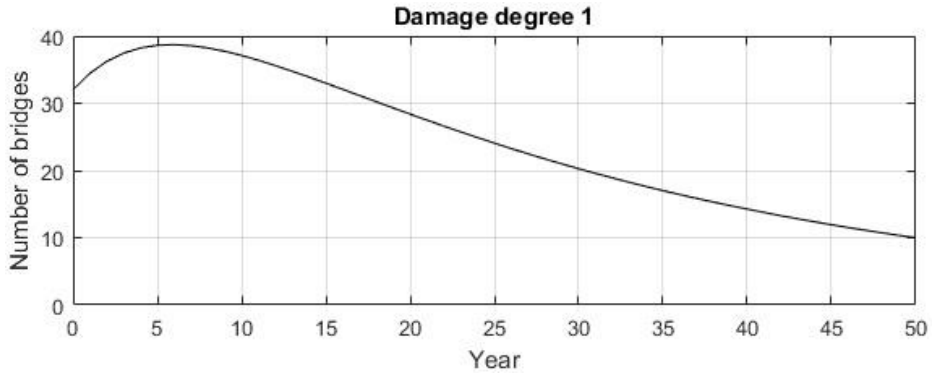

Figure 8.5.6: Predicted number of damage degree 1 bridges

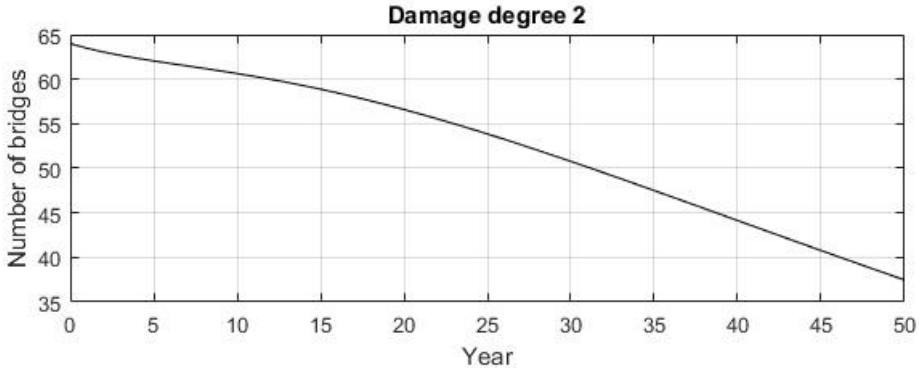

Figure 8.5.7: Predicted number of damage degree 2 bridges

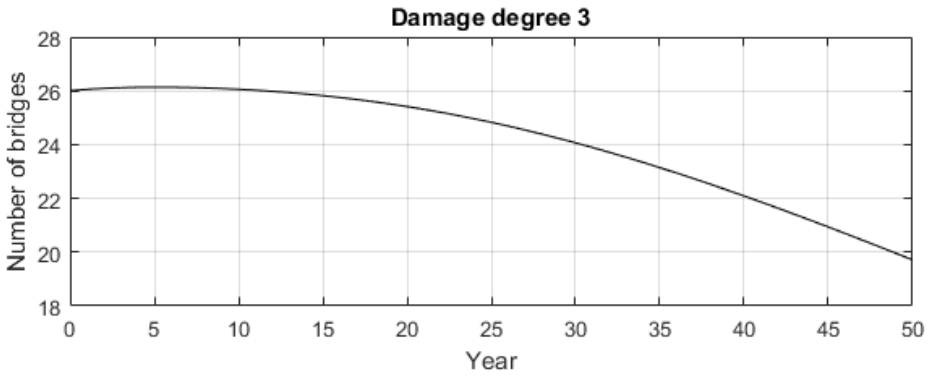

Figure 8.5.8: Predicted number of damage degree 3 bridges

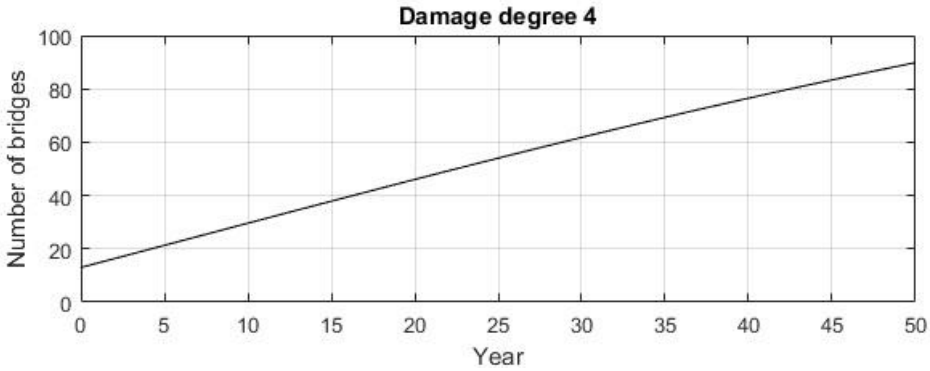

Figure 8.5.9: Predicted number of damage degree 4 bridges

8.6 Deterioration dependent on variables

8.6.1 General

The predicted deterioration in chapter 7.4 considers deterioration for the whole bridge stock. For individual bridge decision making, the predicted deterioration might not be accurate. A dynamic Bayesian network which considers the deterioration to depend on variables will give a model that is better suited for decision making for individual bridges.

There are several ways to approach this problem. In this section, prediction of deterioration will be done based on data from a selection of bridges with similar properties. For buried steel pipe bridges, this can for example be properties as age or environmental conditions. This will, however, probably not be an accurate prediction for an individual bridge, but it is a step in the direction of making deterioration dependent on variables. One variable is considered, and it is whether the bridge is in a coastal or inland environment.

8.6.2 Coast and inland

For the buried pipe bridges of consideration, appendix B, 16 out of 157 bridges are in a coastal environment and climate. The coastal climate for these bridges varies in intensity, but a general coastal category is considered. The other 141 brides are situated inland.

Bridges that are in a coastal climate are expected to generally deteriorate faster than inland bridges. One reason for this is a higher likelihood of chlorides being present, which increase the likelihood and rate of corrosion. The coastal climate in Norway is also generally harsher with more wind and rain.

8.6.3 Bridges in coastal climate

The methodology used to estimate transition intensities in chapter 8.4 is applied to damage development data for the coastal bridges. There are in total 21 state observations for the coastal bridges.

Model A is first considered. Table 8.6.1 shows the result from the maximum likelihood calculations. The transition intensity is higher than for the whole bridge stock, and this indicates

the deterioration rate for coastal bridges being faster than for the whole bridge stock. As the number of observations are smaller for coastal bridges compared to the whole bridge stock, the uncertainty in the estimated model parameter is larger.

Table 8.6.1: Estimated parameter for coastal bridge stock deterioration, model A

Parameter	**Mean,** μ	**Coefficient of variation,** $c_v = \sigma/\mu$
λ	0.0695	0.1827

The equivalent transition probability matrix for a one-year time step is calculated.

$$\mathbf{\Pi} = \begin{bmatrix} 0.9362 & 0.0617 & 0.0020 & 0.0000 & 0.0000 \\ 0 & 0.9362 & 0.0617 & 0.0020 & 0.0000 \\ 0 & 0 & 0.9362 & 0.0617 & 0.0021 \\ 0 & 0 & 0 & 0.9362 & 0.0638 \\ 0 & 0 & 0 & 0 & 1 \end{bmatrix} \tag{8.6.1}$$

Model B is also considered, and the result is shown in table 8.6.2. All transition intensities except for λ_0 are higher for the coastal bridge stock compared to the whole bridge stock. The uncertainty is very large for this model, as many parameters are estimated but the number of observations is lower. Overall, the mean values of the parameters follow a relative similar pattern to the whole bridge stock, but with a faster overall deterioration.

Table 8.6.2: Estimated parameters for inland bridge stock deterioration, model B

Parameter	**Mean,** μ	**Coefficient of variation,** $c_v = \sigma/\mu$
λ_0	0.1416	1.0274
λ_1	0.0471	0.4444
λ_2	0.0439	0.5253
λ_3	0.0882	0.8184

The one-year transition probability matrix is:

$$\mathbf{\Pi} = \begin{bmatrix} 0.8679 & 0.1289 & 0.0031 & 0.0000 & 0.0000 \\ 0 & 0.9540 & 0.0450 & 0.0010 & 0.0000 \\ 0 & 0 & 0.9571 & 0.0411 & 0.0019 \\ 0 & 0 & 0 & 0.9156 & 0.0844 \\ 0 & 0 & 0 & 0 & 1 \end{bmatrix} \tag{8.6.2}$$

Table 8.6.3 shows the summary of the log-likelihood calculations for each model.

Table 8.6.3: Log-likelihood and number of parameters for the coastal bridge stock models

Model	**Parameters**	**Log-likelihood**
A	1	−31.0
B	4	−30.0

A log likelihood ratio test as in chapter 7.4.3.5 is carried out to compare the models. In this case, a less strict criterium is made by comparing it to the 0.05-quantile of the χ^2-distribution:

$$-2\ln\left(\frac{L_A^*}{L_B^*}\right) = 2.0 < \chi^2_{0.05,3} = 7.8 \tag{8.6.3}$$

Since the χ^2-expression for the likelihoods is less than the significance criteria, the hypothesis H_0 cannot be rejected. Model A is therefore a better representation of the observations because of the smaller sample size.

Because of the smaller sample size, there is a probability that the observations do not represent the population they belong to well. One should therefore be careful with using a smaller sample size. In this case, the result agrees with the overall expectations. The coastal bridges deteriorate slightly faster than the whole bridge stock.

8.6.4 Bridges in inland climate

There are 263 state observations to represent the deterioration for 141 inland pipe bridges. Most bridges in the bridge stock are inland bridges. The deterioration analysis is expected to be quite similar to the analysis of the whole bridge stock, but the deterioration should be slightly slower.

The result for model A is shown in table 8.6.4.

Table 8.6.4: Estimated parameter for inland bridge stock deterioration, model A

Parameter	**Mean,** μ	**Coefficient of variation,** $c_v = \sigma/\mu$
λ	0.0552	0.0452

This gives the transition probability matrix:

$$\mathbf{\Pi} = \begin{bmatrix} 0.9463 & 0.0522 & 0.0014 & 0.0000 & 0.0000 \\ 0 & 0.9463 & 0.0522 & 0.0014 & 0.0000 \\ 0 & 0 & 0.9463 & 0.0522 & 0.0015 \\ 0 & 0 & 0 & 0.9463 & 0.0537 \\ 0 & 0 & 0 & 0 & 1 \end{bmatrix} \tag{8.6.4}$$

Observations are also fitted to model B and the result is:

Table 8.6.5: Estimated parameters for inland bridge stock deterioration, model B

Parameter	**Mean,** μ	**Coefficient of variation,** $c_v = \sigma/\mu$
λ_0	0.1825	0.2430
λ_1	0.0354	0.1145
λ_2	0.0264	0.1648
λ_3	0.0613	0.2726

The one-year transition probability matrix for model B is:

$$\mathbf{\Pi} = \begin{bmatrix} 0.8332 & 0.1638 & 0.0030 & 0.0000 & 0.0000 \\ 0 & 0.9652 & 0.0343 & 0.0004 & 0.0000 \\ 0 & 0 & 0.9739 & 0.0253 & 0.0008 \\ 0 & 0 & 0 & 0.9406 & 0.0594 \\ 0 & 0 & 0 & 0 & 1 \end{bmatrix} \tag{8.6.5}$$

Overall, the results are quite similar to the results for the whole bridge stock and the deterioration is slightly slower for inland bridges.

A comparison of model A and model B is made:

Table 8.6.6: Log-likelihood and number of parameters for the inland bridge stock models

Model	Parameters	Log-likelihood
A	1	−558.3
B	4	−502.0

The log likelihood ratio is tested with the 0.01-quantile criteria:

$$-2\ln\left(\frac{L_A^*}{L_B^*}\right) = 112.6 > \chi^2_{0.01,3} = 11.3 \tag{8.6.6}$$

Model B represent the deterioration best.

8.6.5 Modelled in a dynamic Bayesian network

The result for coastal and inland bridges are modelled in a dynamic Bayesian network. 10.2% of the bridges in the bridge stock are situated in a coastal climate. Transition probabilities for bridges in coastal climate are represented with model B transitions. Due to the low sample size, model A is an advised model for coastal bridge deterioration data. Model B is still used because model B is a better model for the inland data set. Using the same model makes comparison easier.

Deterioration for a new bridge is considered and the state is 0 in year 0. The time frame is 40 years, and the predicted states are displayed in year 40. First, predictions are made for the whole bridge stock, and the climate is unknown. This is displayed with the use of GeNIe, figure 8.6.1. Inside the temporal plate, there is a series of damage degrees from time step 0 until 40. This is similar to the simple dynamic Bayesian network in figure 8.3.1. In addition, the transitions are dependent on the climate.

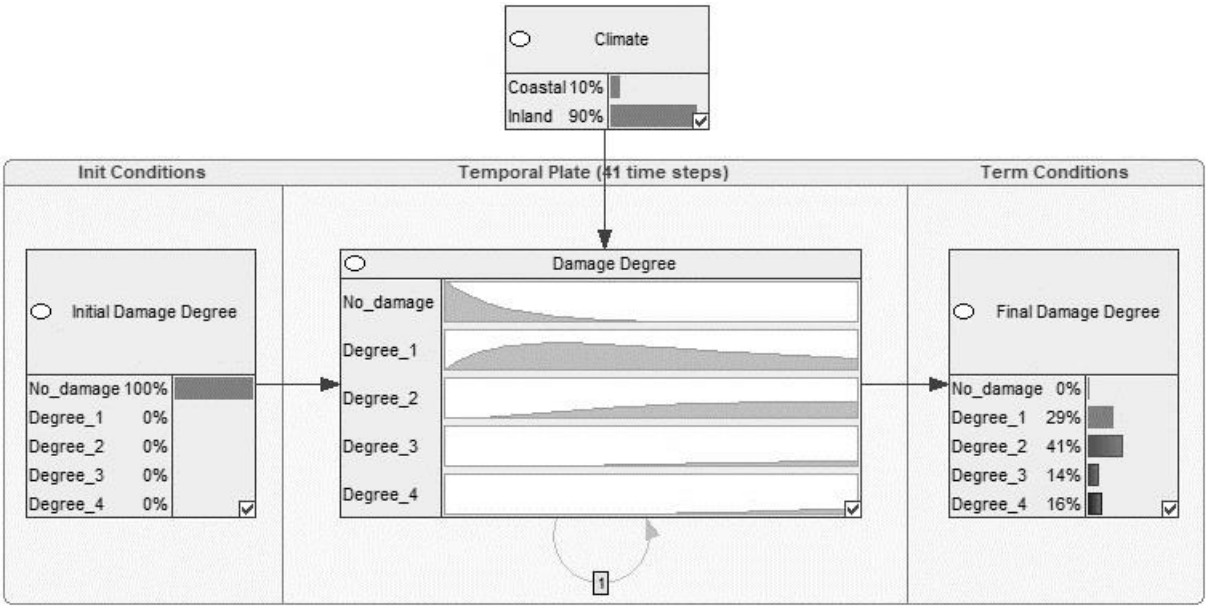

Figure 8.6.1: Deterioration with no climate evidence

This prediction is similar but slightly different from a prediction based on transition probabilities for the whole bridge stock, chapter 7.4.3.5. The model for the transition probabilities based on the whole bridge stock is shown in figure 8.6.2. One reason for the small difference is that coastal bridges are given more importance in the model differentiating between coastal and inland bridges. Coastal bridges make up for 16/157 = 10.2% of the bridge stock, but only 21/284 = 7.4% of the state observations from the bridge stock are from coastal bridges.

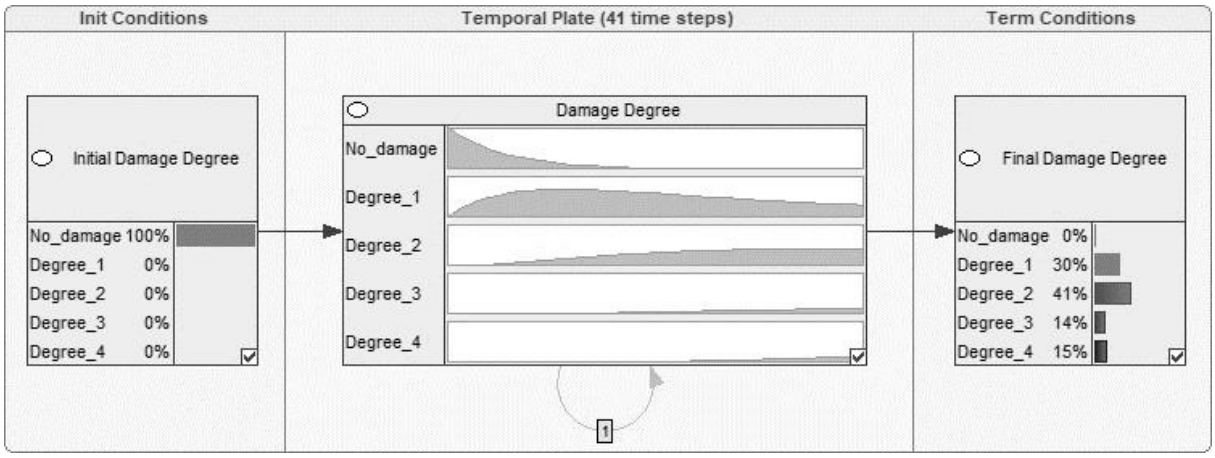

Figure 8.6.2: Deterioration with transition probabilities for the whole bridge stock

If the climate for a bridge is known, then the deterioration prediction might be calculated based on the transition probabilities for this climate. In case the bridge belongs to a coastal climate the prediction will be as shown in figure 8.6.3.

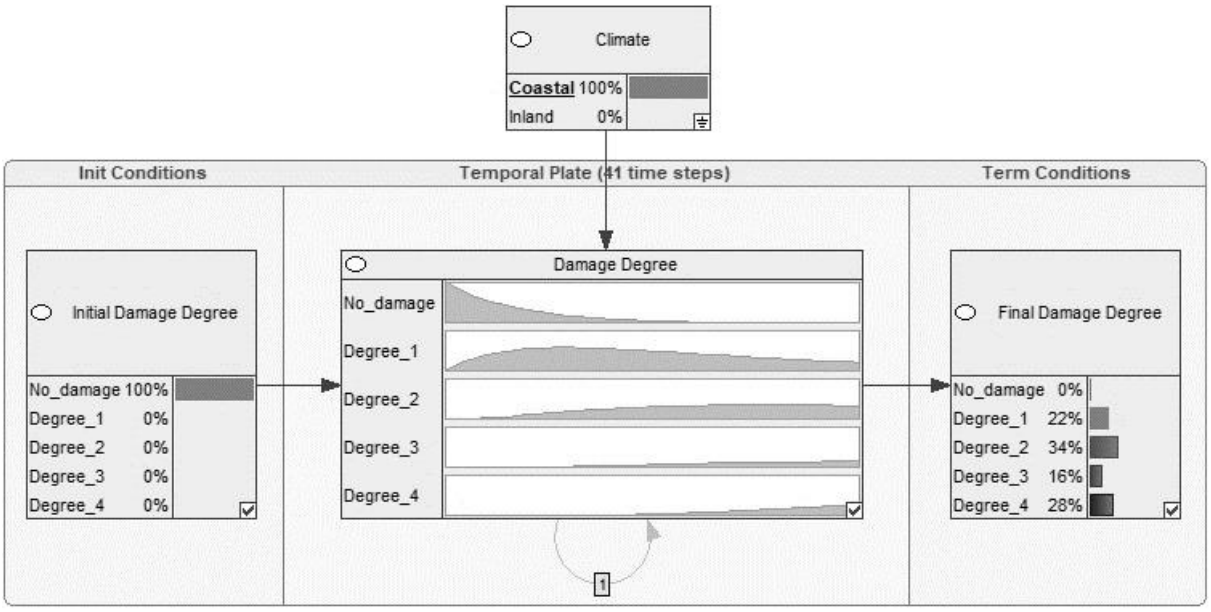

Figure 8.6.3: Deterioration with coastal evidence

For an inland bridge, the deterioration prediction is shown figure 8.6.4.

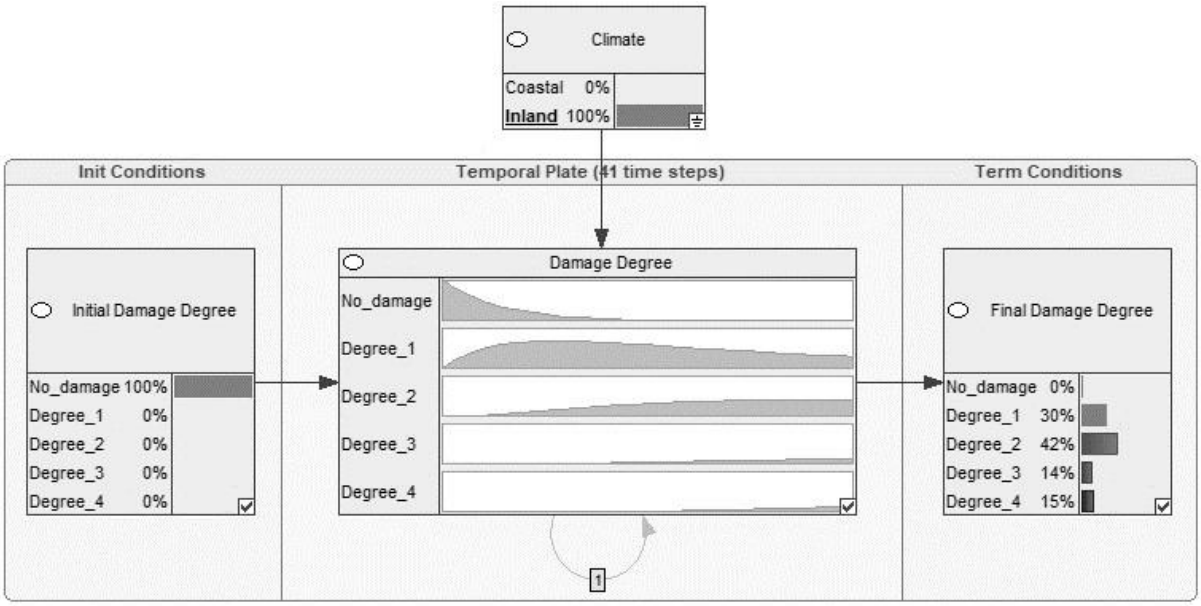

Figure 8.6.4: Deterioration with inland evidence

While an inland bridge is predicted to be in damage degree 4 after 40 years with 15% probability, a coastal bridge is predicted to be in this state with 28% probability.

8.7 Conclusion

The condition of the bridges in the bridge stock has been observed and stored for a period of 24 years. A statistical approach is well suited for predicting the deterioration of the pipe bridge stock. It is possible to use a Markov process to describe the uncertainty in development of discrete states in the bridge stock over time. The semi-Markov process is used to model the deterioration. It can easily handle different inspection intervals and it also does not add or remove any information from the observations in its predictions. Combining a semi-Markov process model with maximum likelihood analysis makes it possible to study the uncertainty in the prediction of deterioration.

The deterioration prediction is also made dependent on a variable. A method by selection of deterioration data is shown, and the bridges are divided into coastal and inland bridges. The method has a weak spot as the number of observations becomes less for each property, and the uncertainty that the observations represents the true deterioration becomes less.

A method with selection might not be accurate enough for individual bridge assessment. For prediction of individual bridge deterioration, physical theory might need to be included in the deterioration model. A dynamic Bayesian network can combine information from probabilistic and physical assessments, as well as the expert's knowledge. In the next chapter, failure prediction is studied. In chapter 9.5, an illustrative Bayesian network example is shown for predicting failure of an individual bridge. This approach has connection to deterioration.

Chapter 9

Failure prediction

9.1 General

Failure prediction is important for the decision making. This chapter considers probability of failure over time. Focus is directed towards probability of failure for deteriorating structures without any major improvement as life extension or rehabilitation. The failure prediction might be used to study when a deteriorating structure should be replaced. If life extension or rehabilitation is to be considered, then the probability of failure should be studied for these actions.

For the buried steel pipe bridges, the probability of failure can be relatively high. Based on previous events, failure is likely to occur within the bridge stock in the future. A sequential continuous-time Markov model with a final failure state will be considered for the bridge stock of buried steel pipe bridges. Failure is then the absorbing state and it is assumed that failure has to go through damage degree 4 before failure. This is a simplification, and the failures must be deterioration failures.

A different approach is necessary for failure prediction for an individual bridge. For an individual bridge, variables that are unique for that bridge should be considered in the failure prediction. A dynamic Bayesian network can give a more complex failure prediction model. It can be suitable for predicting failure for the whole bridge stock as well as for an individual bridge. In this chapter, an example model will be presented.

9.2 Time dependent probability of failure

Recall the reliability analysis in chapter 7. If R is the resistance of the structure and S is the load, the limit state function for a structure is:

$$g(R,S) = R - S \tag{9.2.1}$$

Existing structures are subject to deterioration and a time consideration is important in analysis of existing structures. Time may be included in the reliability analysis. The limit state function can be defined as:

$$g(R,S,t) = R(t) - S(t) \tag{9.2.3}$$

Failure occur at time t if the limit state function is less than 0 at time t, equation 9.2.4.

$$g(R,S,t) \leq 0 \tag{9.2.4}$$

Figure 9.2.1 illustrates concepts of deterioration and uncertainty. The load varies over time with some randomness. The resistance of the structure generally decreases over time, as the structure is subject to deterioration. Over time the probability of failure increases.

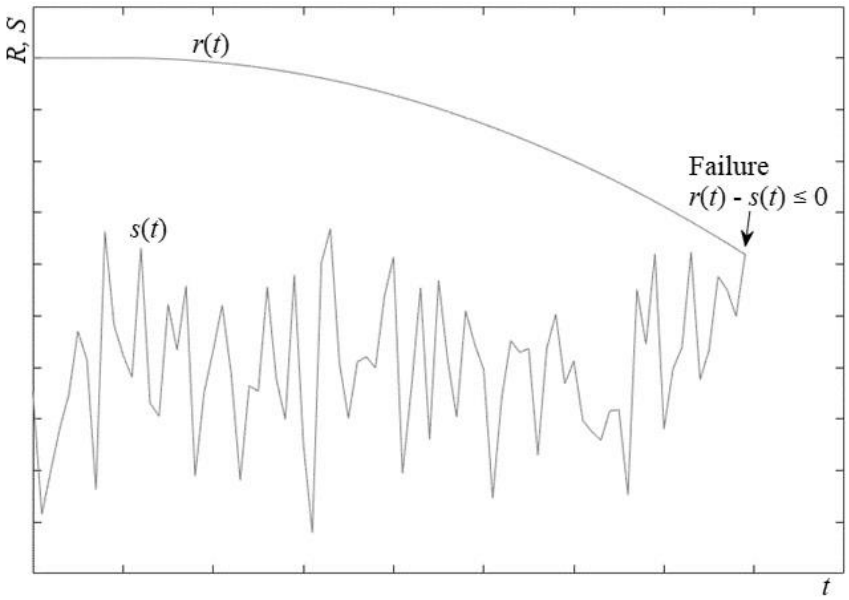

Figure 9.2.1: Time dependent resistance and loading

9.3 Failure and reliability function

There are several available methods for analysis of reliability of structures over time. A Poisson process might be used to describe structural loads as pulses. The Poisson distribution is memoryless, and events occur independently. The rate of occurrence is also constant. For structural reliability the Poisson process can be used by considering a mean failure rate of λ, a length of time of consideration t and number of failures within the time period of x. The density function of failures is:

$$f(\lambda, x, t) = \frac{(\lambda t)^x e^{-\lambda t}}{x!} \tag{9.3.1}$$

The reliability function R is the probability that no failures have occurred, $x = 0$, within the time period. For the Poisson distribution with constant failure rates λ, the reliability function becomes:

$$R(t) = e^{-\lambda t} \tag{9.3.2}$$

This is related to the exponential distribution. In some cases, the reliability function may be described better by other distributions as for example the Weibull distribution or lognormal distribution.

The cumulative failure function describes the probability that failure has occurred within a time reference t, and this function can be defined as in equation 9.3.3.

$$F(t) = 1 - R(t) \tag{9.3.3}$$

For an exponential distribution, the failure function becomes the cumulative density function of the exponential distribution:

$$F(t) = 1 - e^{-\lambda t} \tag{9.3.4}$$

9.4 Failure prediction for bridge stock

9.4.1 General

A sequential continuous-time Markov process is used to predict failure for the bridge stock. Since a sequential model is used, failure has to go through all damage degrees before the final absorbing failure state. There are 5 failures in the bridge stock deterioration table in appendix B.

9.4.2 Model fitting

The general transition table with condition states and transition probabilities is shown in the table below.

Table 9.4.1: Condition states and transition probabilities

		Condition at $n + 1$					
		No damage	**Degree 1**	**Degree 2**	**Degree 3**	**Degree 4**	**Failure**
Condition at n	**No damage**	π_{00}	π_{01}	π_{02}	π_{03}	π_{04}	π_{05}
	Degree 1	π_{10}	π_{11}	π_{12}	π_{13}	π_{14}	π_{15}
	Degree 2	π_{20}	π_{21}	π_{22}	π_{23}	π_{24}	π_{25}
	Degree 3	π_{30}	π_{31}	π_{32}	π_{33}	π_{34}	π_{35}
	Degree 4	π_{40}	π_{41}	π_{42}	π_{43}	π_{44}	π_{45}
	Failure	π_{50}	π_{51}	π_{52}	π_{53}	π_{54}	π_{55}

A sequential deterioration assumption as introduced in chapter 8.3 is assumed. The final absorbing failure state is included, and the 5 observations of failure are included in the prediction.

$$\mathbf{Q} = \begin{bmatrix} -\lambda_0 & \lambda_0 & 0 & 0 & 0 & 0 \\ 0 & -\lambda_1 & \lambda_1 & 0 & 0 & 0 \\ 0 & 0 & -\lambda_2 & \lambda_2 & 0 & 0 \\ 0 & 0 & 0 & -\lambda_3 & \lambda_3 & 0 \\ 0 & 0 & 0 & 0 & -\lambda_4 & \lambda_4 \\ 0 & 0 & 0 & 0 & 0 & 0 \end{bmatrix} \tag{9.4.1}$$

Again, model A describes state independent transitions, while model B describes state dependent transitions. The result for model A is shown in table 9.4.2.

Table 9.4.2: Estimated parameter, model A

Parameter	**Mean,** μ	**Coefficient of variation,** $c_v = \sigma/\mu$
λ	0.0563	0.0433

This gives the transition probability matrix:

$$\mathbf{\Pi} = \begin{bmatrix} 0.9453 & 0.0532 & 0.0015 & 0.0000 & 0.0000 & 0.0000 \\ 0 & 0.9453 & 0.0532 & 0.0015 & 0.0000 & 0.0000 \\ 0 & 0 & 0.9453 & 0.0532 & 0.0015 & 0.0000 \\ 0 & 0 & 0 & 0.9453 & 0.0532 & 0.0015 \\ 0 & 0 & 0 & 0 & 0.9453 & 0.0547 \\ 0 & 0 & 0 & 0 & 0 & 1 \end{bmatrix} \tag{9.4.2}$$

Observations are also fitted to model B and the result is:

Table 9.4.3: Estimated parameters, model B

Parameter	**Mean,** μ	**Coefficient of variation,** $c_v = \sigma/\mu$
λ_0	0.1796	0.1987
λ_1	0.0358	0.0879
λ_2	0.0283	0.1263
λ_3	0.0748	0.2118
λ_4	0.0509	0.4675

Correlations for the transition intensities are given in the table below.

Table 9.4.4: Correlation coefficient between estimated parameters

Correlation coefficient, ρ	λ_0	λ_1	λ_2	λ_3	λ_4
λ_0	1				
λ_1	−0.4548	1			
λ_2	−0.1173	−0.0168	1		
λ_3	−0.0282	−0.0017	−0.0284	1	
λ_4	0.0021	−0.0016	−0.0031	−0.0288	1

The transition probability matrix for model B is:

$$\mathbf{\Pi} = \begin{bmatrix} 0.8356 & 0.1614 & 0.0030 & 0.0000 & 0.0000 & 0.0000 \\ 0 & 0.9648 & 0.0347 & 0.0005 & 0.0000 & 0.0000 \\ 0 & 0 & 0.9721 & 0.0269 & 0.0010 & 0.0000 \\ 0 & 0 & 0 & 0.9280 & 0.0702 & 0.0018 \\ 0 & 0 & 0 & 0 & 0.9503 & 0.0497 \\ 0 & 0 & 0 & 0 & 0 & 1 \end{bmatrix} \tag{9.4.3}$$

A comparison of model A and model B is made.

Table 9.4.5: Log-likelihood and number of parameters for the models

Model	Parameters	Log-likelihood
A	1	−611.5
B	5	−555.5

The log likelihood ratio is tested with the 0.01-quantile criteria:

$$-2\ln\left(\frac{L_A^*}{L_B^*}\right) = 112.0 > \chi^2_{0.01,4} = 13.3 \tag{9.4.4}$$

Model B represent the failure deterioration best, since this expression is true.

9.4.3 Model fitting discussion

Most transition intensities are similar to the previous predictions for the bridge stock in chapter 8. Transition intensity λ_3 is slightly larger for the model including failure. Since the model is sequential, final failure state is forced to deteriorate through all damage degrees before reaching failure. Several of the failure events had an observation of a damage degree of less than 4 at the last observation. These damages will then contribute to a relatively rapid deterioration to failure. This is in particular the case for damage degree 3 transiting through damage degree 4 before reaching failure. λ_3 is therefore estimated to be slightly higher for the deterioration model included failure compared to the previous deterioration model.

The transition intensity λ_4, damage degree 4 transiting to failure, is quite uncertain. This might also indicate that future failure events are quite uncertain. The correlations between λ_4 and other transition intensities are relatively low.

9.4.4 Failure prediction

A failure prediction is carried out based on model B transition intensities. The five non-failure states are considered as initial conditions in year 0. Failure prediction for each initial state is given in figure 9.4.1. This is the case if no actions as replacement and rehabilitation is made, and the bridges continue to deteriorate.

An initial damage degree of 4 can either stay in damage degree 4 or go into failure. The annual failure probability for damage degree 4 is 0.0497. The failure function for an initial damage degree 4 follows an exponential function as the failure rate is constant.

For other initial states, the failure function is not exponential. This is because a lower damage degree will have an increasing probability of being in damage degree 4 by time. Since only damage degree 4 is considered to go into failure in the sequential model, the increasing probability of being in damage degree 4 also gives an increasing probability of going into failure for initial states which are not damage degree 4. In these cases, the increasing probability of failure might be illustrated as in figure 9.2.1.

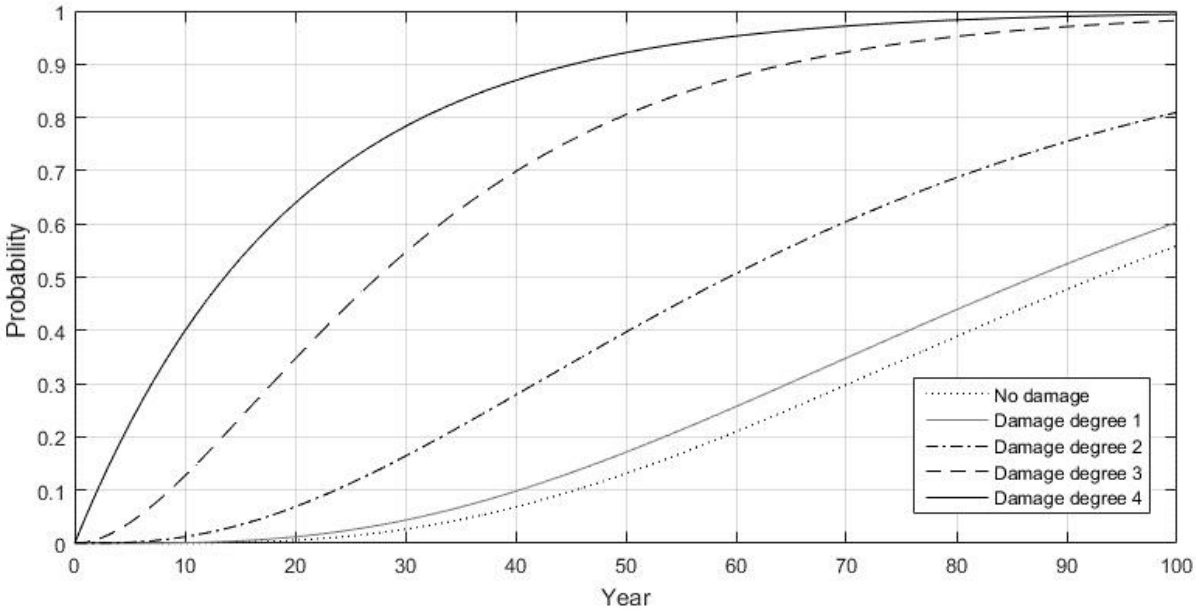

Figure 9.4.1: Failure function for different initial states

A future failure prediction is made for the 157 bridges in the bridge stock. This failure prediction is shown for the next 20 years, given that no replacements or major actions are made.

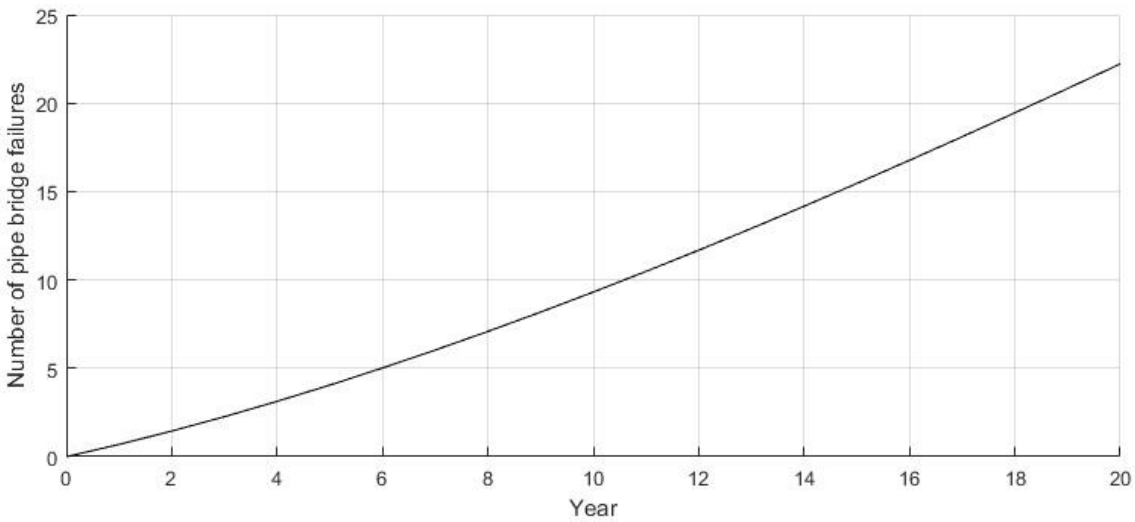

Figure 9.4.2: Predicted number of failures in bridge stock

Within the next 6 years, about 5 failures are expected. This number seems quite large, but there have been 5 failures within the last 5 years. The bridges will continue to deteriorate to even worse conditions, and in this perspective the prediction seems reasonable.

9.5 Dynamic Bayesian network for failure prediction

9.5.1 General

The failure prediction is dependent on variables, and when considering an individual bridge, several properties for the bridge should be known. A dynamic Bayesian network might be suitable for predicting failure for an individual bridge.

9.5.2 Prediction with dynamic Bayesian network

The Bayesian network for a buried pipe presented in figure 6.4.1 might be expanded into a dynamic Bayesian network. This is shown as an illustrative example in figure 9.4.3. Variables that change over time can be modelled with a time consideration. Deterioration of variables should be modelled.

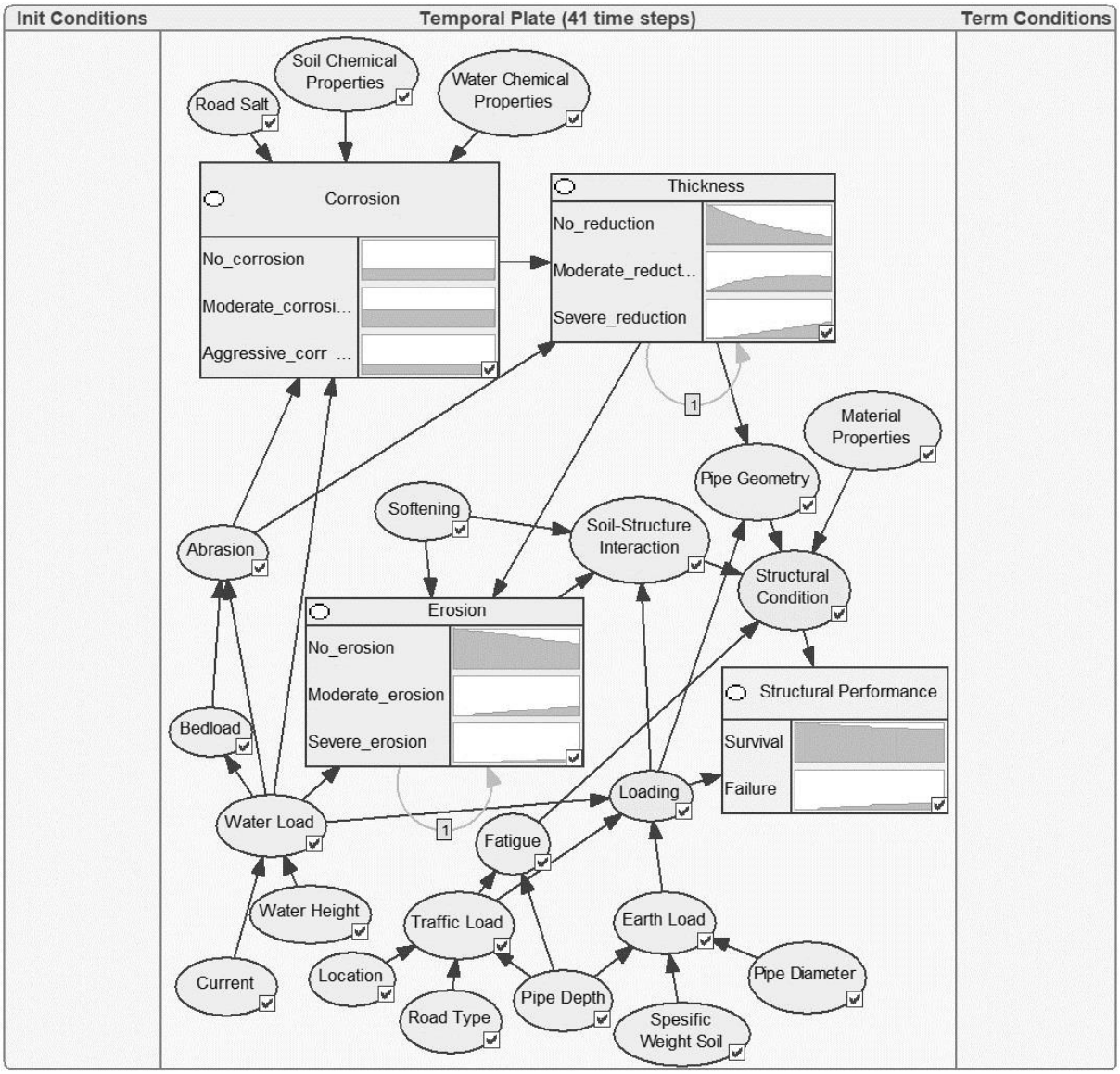

Figure 9.5.1: Dynamic Bayesian network for failure prediction

For the general consideration, the variables should be modelled with distributions that represent the bridge stock's conditions. This dynamic Bayesian network will therefore be an extension to the previous bridge stock consideration that does not take variables into account. The corrosion variable is shown in figure 9.4.3, and it is assumed to have a discrete distribution of states that represent the states in the bridge stock. This distribution could also be continuous. All other variables should also be modelled.

Deterioration of the thickness of the wall is dependent on corrosion and abrasion as well as the current condition of the thickness. The decay is modelled as memoryless, and only the current

condition of the thickness is considered for decay to the next time step. This is considered for 41-time steps, which gives a prediction of condition from year 0 to year 40. Erosion is modelled in a similar way. The whole model gives a failure prediction for the general bridge stock condition.

When assessing an individual bridge, realisations of the variables for that bridge are assessed. The prediction becomes more accurate when many variables are assessed. Figure 9.4.4 shows an example displaying the corrosion variable. A bridge is assumed to have aggressive corrosion over all time steps, and there is made evidence of this in the model. Alternatively, if there is information about the corrosion's parent variables, this could be given evidence instead of the corrosion variable. A new failure prediction is calculated and since the bridge have more aggressive corrosion compared to the whole bridge stock, the bridge is more likely to fail than the general case.

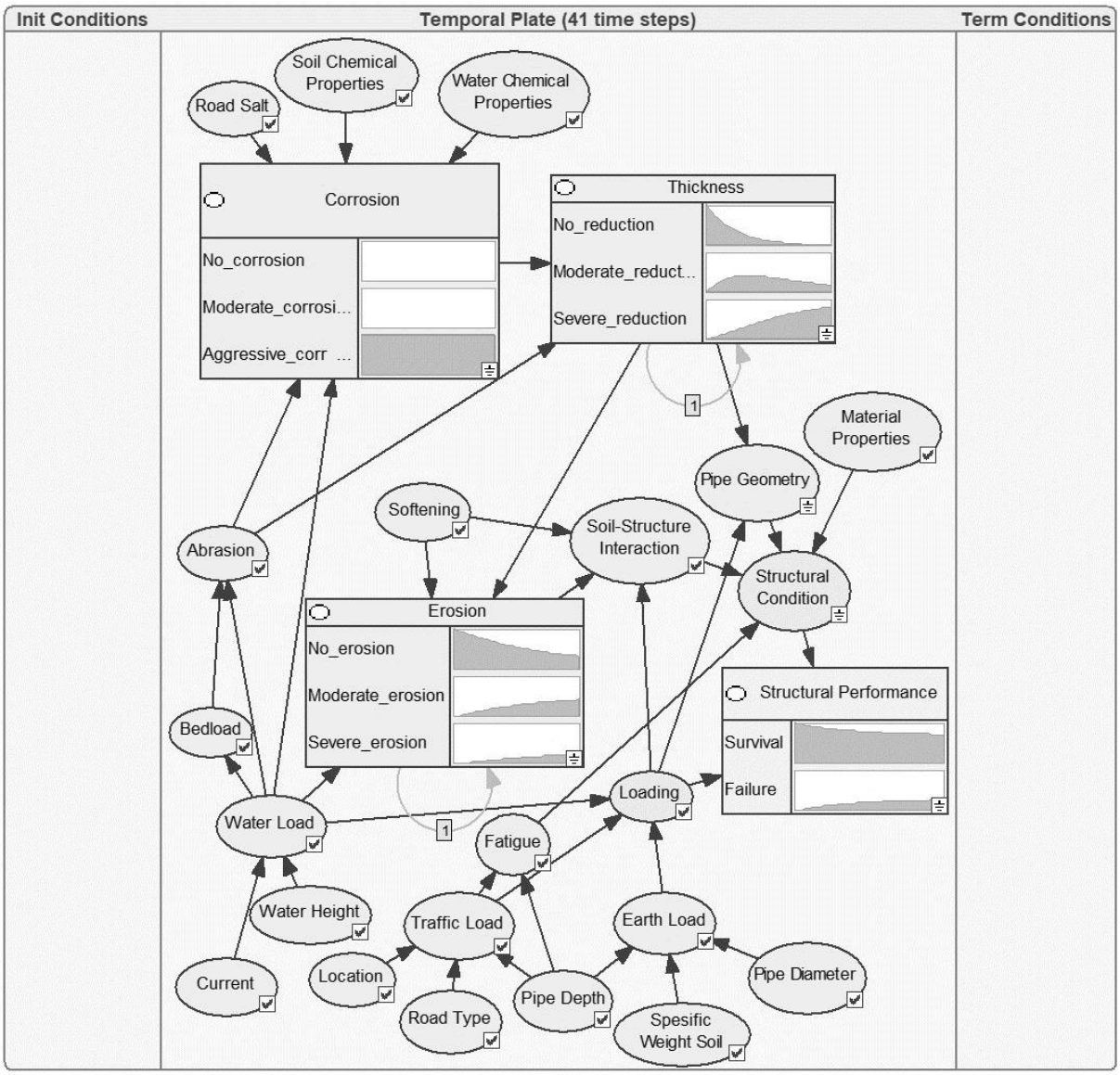

Figure 9.5.2: Failure prediction with evidence of aggressive corrosion

The variables might also take different values over time. This might be change in the use of road salt because of future change in snow and ice management of roads. It might also be a change in traffic load if a new road classification is considered in the future.

9.6 Conclusion

In this chapter, a sequential Markov process is used to predict failures in the bridge stock. If all failures are deterioration failures and go through damage degree 4 before failure, then this is a valid assumption. This might not be the case, and the assessment should be performed carefully. Based on the predictions, if no actions are made, then five failures are expected to occur within the bridge stock for the next six years.

The model that is used to predict failure in the bridge stock is not suitable for individual bridge assessment. More variables must be considered. A dynamic Bayesian network is an extension to the Markovian model. This dynamic Bayesian network is more powerful as it can assess the whole bridge stock, but also give a prediction for individual bridges when there are evidences of variables.

Failure predictions are useful for replacement strategies. This is considered in the next chapter.

Chapter 10

Replacement strategies

10.1 General

This chapter considers replacement of individual bridges and the bridge stock. When studying an individual bridge, cost will be considered. This cost is divided into cost for the user and the owner of the bridge. Understanding risk is important for estimating these costs. Risk and benefit-cost analysis is presented in early parts of this chapter. A methodology for estimating when an individual bridge should be replaced is shown. For the bridge stock, some different replacement strategies are briefly discussed. These strategies are illustrated by modifying the Markov chain deterioration model from chapter 8.5.

10.2 Risk and cost-benefit analysis

10.2.1 Risk

Risk is a measure considering consequences and probabilities of undesirable events. The risk for an action, R_A, is usually described as the sum of risk of all possible events from the action. The risk for each event is the product of the probability of the event, P_{Ei}, and the consequence of the event, C_{Ei}.

$$R_A = \sum_{i=1}^{N} P_{Ei} \cdot C_{Ei} \tag{10.2.1}$$

10.2.2 Risk acceptance

A risk acceptance criterium can be used to set an absolute limit to the accepted condition of a bridge. A limit for the highest tolerable risk, R_{limit}, may be defined. The highest tolerable probability of failure, $P_{f,limit}$, may then be calculated if the consequence of a failure, C_f, is known.

$$P_{f,limit} = \frac{R_{limit}}{C_f} \tag{10.2.2}$$

This acceptance criterium illustrates that a higher probability of failure may be accepted if the consequence is low, while for a higher consequence, a lower probability of failure is accepted.

10.2.3 Weighing risk and cost

Risk and cost may be weighted towards each other in risk management. Figure 10.2.1 shows three bridges, 1, 2 and 3. Bridge 3 is the best option among these bridges, because both the cost and risk are lower than for bridge 1 and 2. Comparing bridge 1 and 2, however, can be more challenging. Bridge 1 has a higher cost than bridge 2, but it also has a lower risk. This is one of

the main elements in decision assessment of whether to replace an existing bridge. The new bridge will have a lower risk than the existing bridge, but there are costs related to replacing the existing bridge.

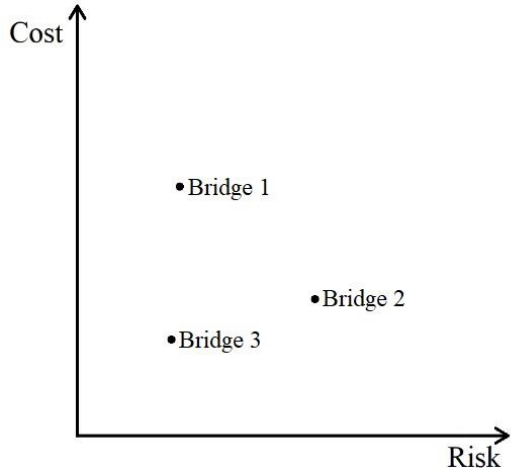

Figure 10.2.1: Cost and risk for different bridges

The risk decreases with investment in maintenance and design. Commonly, the benefit from risk reducing investment is great at small effort, but as the effort increases, the cost for reducing risk also increases. The optimal cost-benefit condition is found at the minimum of total cost. This point has an optimal design and maintenance strategy associated with it. Figure 10.2.2 shows this optimum at the lowest total cost. A similar illustration is given by Straub (2004).

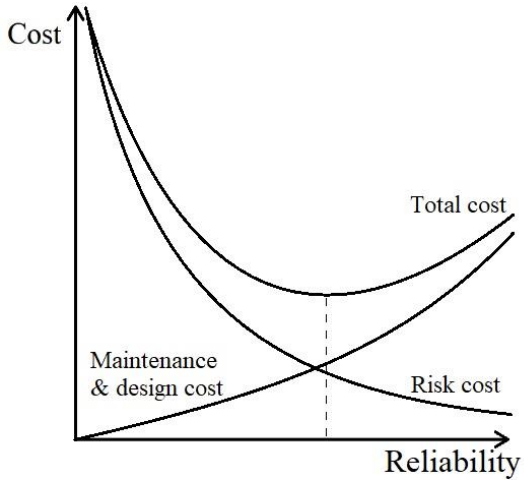

Figure 10.2.2: Risk, maintenance and design costs as function of reliability

10.2.4 Benefit of risk reduction, operational savings and life extension

Ayuub (2014) introduces a contributing factor diagram for replacement of an existing bridge, figure 10.2.3. The diagram considers three benefits: benefits of risk reduction, benefits from operation and maintenance savings and benefits of life extension. For risk reduction, a new bridge will generally have a lower probability of failure and lower risk. A new bridge is also expected to have lower operational and maintenance costs. However, replacing the bridge is a major cost. If the life of the existing bridge can be extended, then there will be a benefit from the life extension.

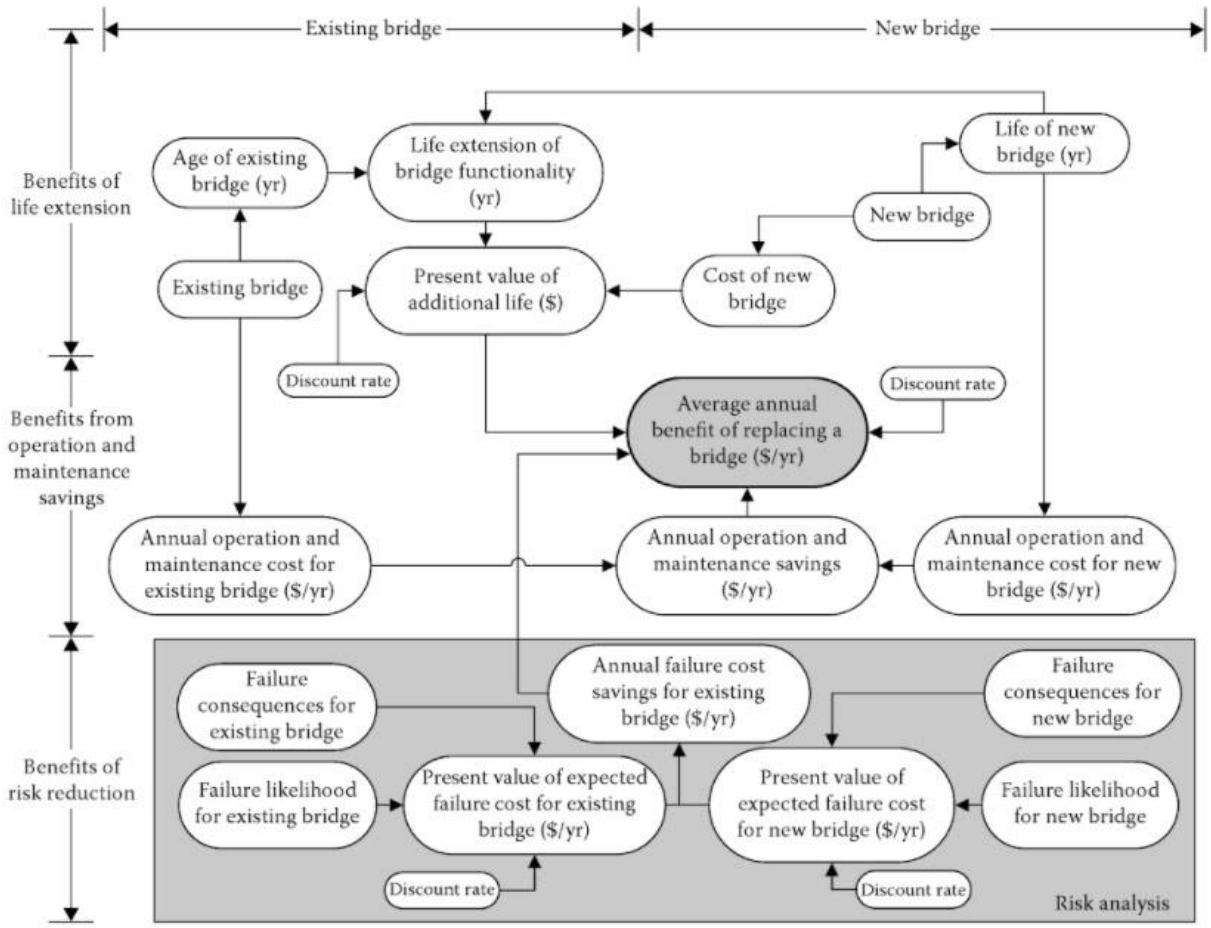

Figure 10.2.3: Cost-benefit consideration for bridge replacement (Ayuub 2014)

10.2.5 Optimal design

Rackwitz (2000) proposes an optimisation scheme for design of a structure based on benefit, cost and risk. Let Z be the objective function for a structure as given in equation 10.2.3. B is the benefit from the structure, C is the cost of design and construction and D is the expected damage cost. $\mathbf{p}$ is a vector with all parameters related to safety. The structural design is optimal when this function has its maximum.

$$Z(\mathbf{p}) = B(\mathbf{p}) - C(\mathbf{p}) - D(\mathbf{p}) \tag{10.2.3}$$

If one assumes failure upon construction or never, and the structure is abandoned after the first failure, the equation might be expressed as:

$$Z(\mathbf{p}) = B^*(1 - P_f(\mathbf{p})) - C(\mathbf{p}) - H(\mathbf{p})P_f(\mathbf{p}) \tag{10.2.4}$$

where P_f is the failure probability and H is the direct failure cost.

With failure due to time-variant loads or resistance, systematic reconstruction and infinite time, the equation becomes:

$$Z(\mathbf{p}) = \frac{b}{\gamma} - C(\mathbf{p}) - \big(C(\mathbf{p}) + H(\mathbf{p})\big)\frac{\lambda(\mathbf{p})}{\gamma} \tag{10.2.5}$$

where b is the annual benefit, γ is the interest rate and λ is the parameter of a Poisson failure process with exponential failure rate.

Rackwitz gives an extended form of the objective function that may be written as:

$$Z(\mathbf{p}) = B^* - C(\mathbf{p}) - I(\mathbf{p}) - U(\mathbf{p}) - M(\mathbf{p}) - A(\mathbf{p}) - D(\mathbf{p}) \tag{10.2.6}$$

where the variable I is inspection and maintenance cost, U is serviceability failures, M is aging failures, A is obsolescence and D is ultimate limit state failure.

10.3 Individual bridge replacement analysis

10.3.1 General

This section presents a method that is used to consider when a bridge should be replaced. The method is inspired by bridge life-cycle analysis as well as the elements from the extended objective function by Rackwitz.

In the analysis of optimal design by Rackwitz (2000), infinite time is considered. For replacement analysis of an existing bridge, it may be of interest to limit the time frame. Information about the state of the bridge and other conditions are greatest for the nearest future. The decision may also be taken within near future. The reference period may be set to T years. One can analyse whether the bridge should be replaced within T years, and if so, in which year.

Thoft-Christiansen (2006) considers benefit, repair and failure costs in a life-cycle perspective. The repair cost for an existing bridge is multiplied with its survival function. Repair will only occur in case the bridge is there.

In the method of this section, the costs associated with the existing bridge or the bridge replaced by planning are assumed to take place with certainty for each year. This is a simplification. It is not considered that the costs, as maintenance cost, might change due to a probability of failure resulting in a bridge reconstruction. When considering replacement for each year, it is also not considered that there is a probability that the existing bridge has failed and already been reconstructed. A failure function is only applied to the failure cost.

10.3.2 Method

The expected value of the bridge in year $t = 0$ for the time period $t = 0$ to $t = T$ may be expressed as:

$$V(T) = B(T) - C_I(T) - C_U(T) - C_R(T) - C_F(T) + V_{ERP}(T) \tag{10.3.1}$$

B is the benefit from the bridge, C_I is inspection, maintenance and operational cost, C_U is serviceability failure cost, C_R is replacement cost, C_F is failure cost, and V_{ERP} is an end of reference period value. V_{ERP} is included in order to take account for the value of the bridge functionality after the reference period of consideration.

The existing bridge may be replaced with a new bridge for any year within the time period of consideration.

The annual benefit from the bridge being operational in year t-1 to t is b_t. The discount rate is i. The total expected benefit in present value, B, is then as shown in equation 10.3.2, Thoft-Christiansen (2006).

$$B(T) = \sum_{t=1}^{T} b_t \frac{1}{(1+i)^t} \tag{10.3.2}$$

Let $c_{I,t}$ be the annual inspection, maintenance and operation cost in year t for the existing bridge or the bridge which is replaced by planning. This cost must be updated in the year of replacement. The expected present value cost for inspection, maintenance and operation, C_I, may be calculated as shown in equation 10.3.3.

$$C_I(T) = \sum_{t=1}^{T} c_{I,t} \frac{1}{(1+i)^t} \tag{10.3.3}$$

The expected cost for serviceability failures, C_U, is related to costs as traffic detour cost and accidental cost due to reduced road safety. The expected present value of the cost is the sum of serviceability costs, $c_{U,t}$, for all years, equation 10.3.4. $c_{U,t}$ must be updated in the year of replacement if the new bridge has different expected annual serviceability failures.

$$C_U(T) = \sum_{t=1}^{T} c_{U,t} \frac{1}{(1+i)^t} \tag{10.3.4}$$

The expected replacement cost, C_R, in present value is:

$$C_R(T) = c_{R,t_r} \cdot \frac{1}{(1+i)^{t_r}} \tag{10.3.5}$$

where $c_{R,tr}$ is the replacement cost that finds place at the year of replacement, t_r.

The expected cost for failure, C_F, is:

$$\begin{aligned} C_F(T) &= \sum_{t=1}^{T} c_{f,t} \cdot (F(t) - F(t-1)) \frac{1}{(1+i)^t} \\ &= \sum_{t=1}^{T} c_{f,t} \cdot P_f(t) \frac{1}{(1+i)^t} \end{aligned} \tag{10.3.6}$$

$c_{f,t}$ is the cost for failure in year t, $P_f(t)$ is the probability of failure in year t and $F(t)$ is the failure function. Thoft-Christiansen (2006) gives a similar expression for the failure cost.

The expected end of reference period value, V_{ERP}, in present value is:

$$V_{ERP}(T) = V_{ERP,T} \cdot \frac{1}{(1+i)^T} \tag{10.3.7}$$

where $V_{ERP,T}$ is the value of the bridge in year T.

C is the expected present cost which is calculates as the present value without considering the benefit variable. The average expected annual cost for each year in the reference period, AC, can then be calculated from the present cost as shown in equation 10.3.8.

$$\begin{aligned} C(T) &= -C_I(T) - C_U(T) - C_R(T) - C_F(T) + V_{ERP}(T) \\ AC(T) &= C(T) \cdot \frac{i(1+i)^T}{(1+i)^T - 1} \end{aligned} \tag{10.3.8}$$

10.3.3 Connection to dynamic influence diagram

The replacement analysis has a connection to the dynamic influence diagram shown in figure 6.3.4. A decision on replacing the bridge is made each year. This decision affects the condition of the pipe and the condition is considered until the end of a reference period time. Here, the expected annual cost is considered, because it makes it easy to compare the result from different years of replacement.

10.3.4 Example calculation

An example case is used to demonstrate the model. The reference period is set to 20 years. The replacement and failure cost for the bridge are based on examples from chapter 3. These costs are divided into cost for the owner and the user.

Table 10.3.1: Replacement and failure costs

		Cost NOK (2016)
Replacement	**Owner**	-5,000,000
	User	-395,000
Failure	**Owner**	-5,200,000
	User	-12,055,000

An initial damage degree 3 bridge is considered. The failure function, $F(t)$, and the annual probability of failure, $P_f(t)$, for the existing bridge is based on the failure prediction from chapter 9. This is just for demonstrational purpose. For a new bridge, the failure function is based on estimations for a new bridge in the general bridge stock, which is also a simplification. The failure function and annual probability of failure for the existing bridge is shown in figure 10.3.1.

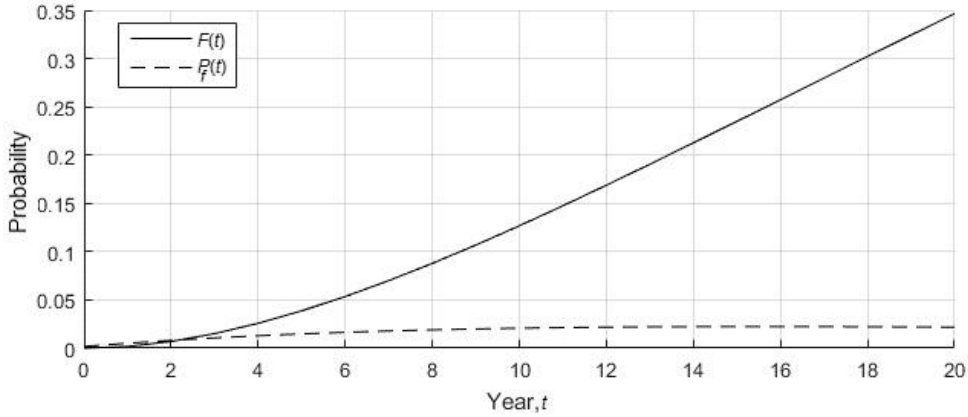

Figure 10.3.1: Failure function and annual probability of failure for the existing bridge

Some assumptions are made for the end of reference period value of a new bridge. The new bridge is assumed to deteriorate as the general bridge stock. The remaining value of the bridge is expressed with relative values to its initial cost. The relative value is assumed to be 100% of the initial value for a no damage condition. For damage degree 1, 2, 3 and 4, the remaining value of the initial value is assumed to be 75%, 50%, 25% and 0, respectively. The probability distribution of states for different ages of the new bridge is calculated by the general bridge stock deterioration model, chapter 8.5. The expected remaining value is calculated and shown in figure 10.3.2. No end of reference period value is assigned the existing bridge.

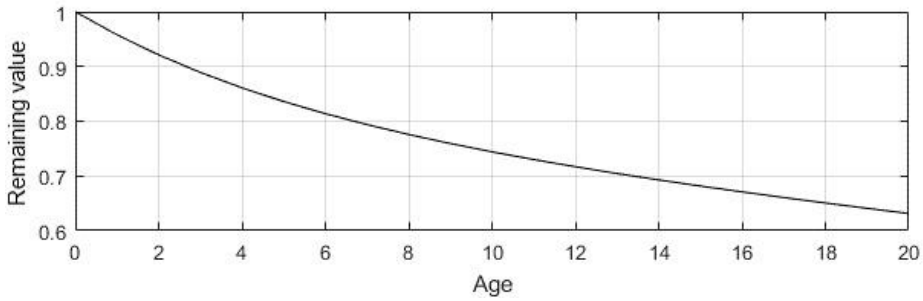

Figure 10.3.2: Remaining value of a new bridge

The discount rate is set to i = 4%. This discount rate is to be used for all types of public investment in Norway with a reference period of 40 years or less according to Norwegian Ministry of Finance, report R-109/2014. This rate consists of a rate without risk of 2.5% and an additional rate of 1.5% to take care of systematic investment risk.

An existing bridge with a higher maintenance and operational cost than a new bridge is considered. This will often be the case. An existing bridge will often require more frequent inspections. It might also need more maintenance in order to serve its function. The maintenance and operational cost is assumed to be constant in the period of consideration.

Table 10.3.2: Annual costs

		Annual Cost NOK (2016)
Maintenance and operation, $c_{I,t}$	**Existing bridge**	-100,000
	Replacement bridge	-50,000
Serviceability failure, $c_{U,t}$		0

The expected average annual cost for the user and owner is shown for different years of replacement in figure 10.3.3.

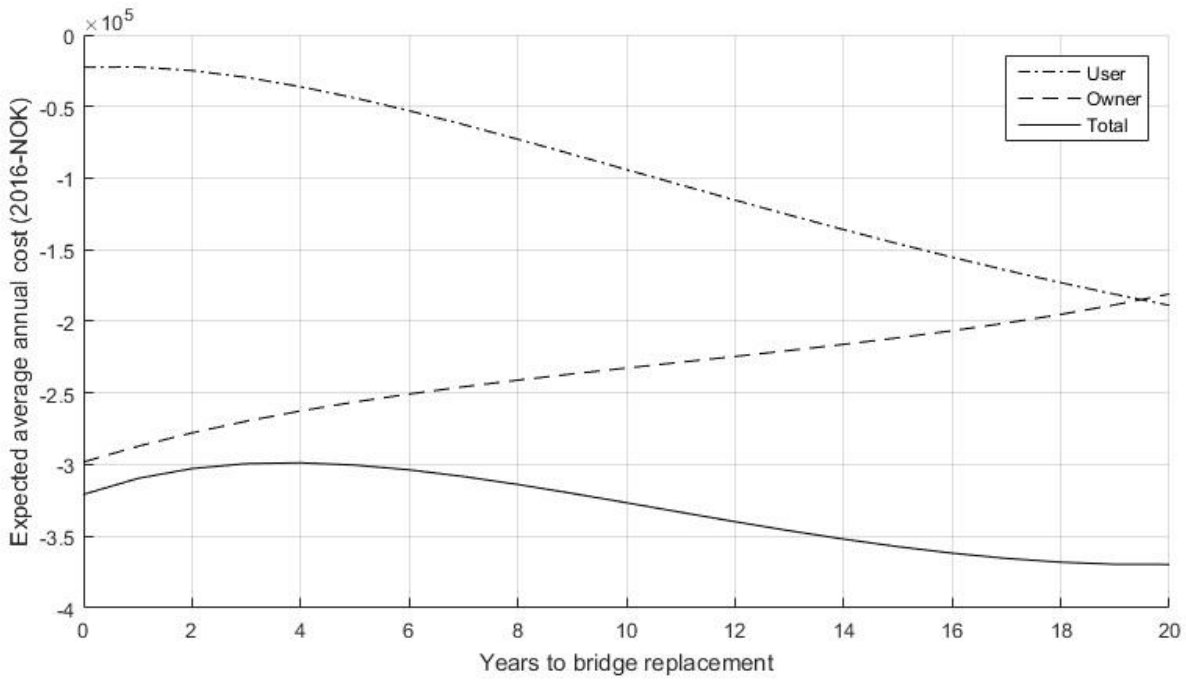

Figure 10.3.3: Expected annual cost for different years of replacement

From the owner's perspective, it is beneficial to not replace the bridge within the period of consideration. The user's perspective is different, and it would be beneficial to replace the bridge today. This reduces accidental and traffic disruption costs. When considering the total cost, the lowest expected annual cost is obtained by replacing the bridge in four years from now.

10.4 Bridge stock replacement strategies

10.4.1 General

This chapter briefly discusses the effect of different replacement strategies for the whole bridge stock. Deterioration is considered, and the deterioration model B from chapter 8.5 is used.

10.4.2 Worsening bridge stock condition

The deterioration of the bridge stock as discussed in chapter 8.5.5 is presented. Failure, replacement and improving actions are not considered. The expected condition of the bridge stock is shown in figure 10.4.1.

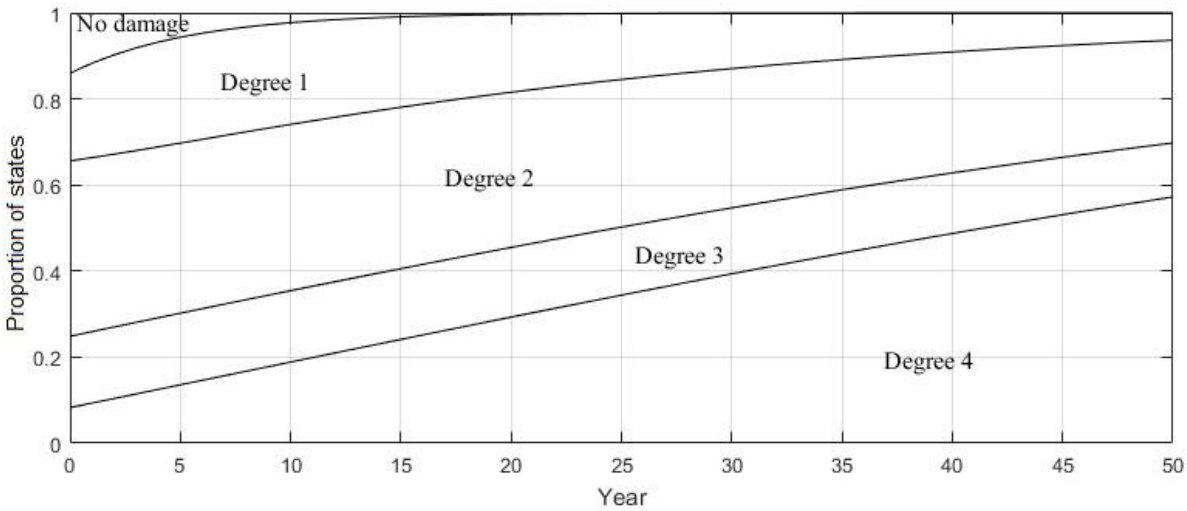

Figure 10.4.1: Worsening bridge stock condition

With this strategy, the bridges will continue to deteriorate until failure, and the bridges must be reconstructed after failure. Following this strategy will especially affect the user in a bad way. The roads are expected to be frequently closed with frequent failures, and accidents are likely to happen. As shown in chapter 3, the consequences related to failure are much larger than consequences related to planned replacement.

10.4.3 Maintaining bridge stock condition

Replacement of bridges in the bridge stock is considered. New bridges are assumed to deteriorate in a similar way to the existing bridges. The bridge stock deterioration model from chapter 8.3 is used. If 13% of the bridges with damage degree 4 are replaced every year, then the bridge stock will maintain a condition which is quite similar to toady's condition. The transition probability matrix for this replacement strategy is shown in matrix 10.4.1.

$$\mathbf{\Pi} = \begin{bmatrix} 0.8343 & 0.1627 & 0.0030 & 0.0000 & 0.0000 \\ 0 & 0.9650 & 0.0346 & 0.0004 & 0.0000 \\ 0 & 0 & 0.9735 & 0.0256 & 0.0008 \\ 0 & 0 & 0 & 0.9384 & 0.0616 \\ 0.13 & 0 & 0 & 0 & 0.87 \end{bmatrix} \tag{10.4.1}$$

Figure 10.4.2 shows the development of bridge stock condition with this replacement strategy. As the condition of the bridge stock reaches a steady state, 8% of the bridge stock will be stay in damage degree 4 and 17% of the bridge stock will stay in damage degree 3. With 157 bridges in the bridge stock and 13% of the damage degree 4 bridges being replaced annually, the average time between replacements will be 7.3 months.

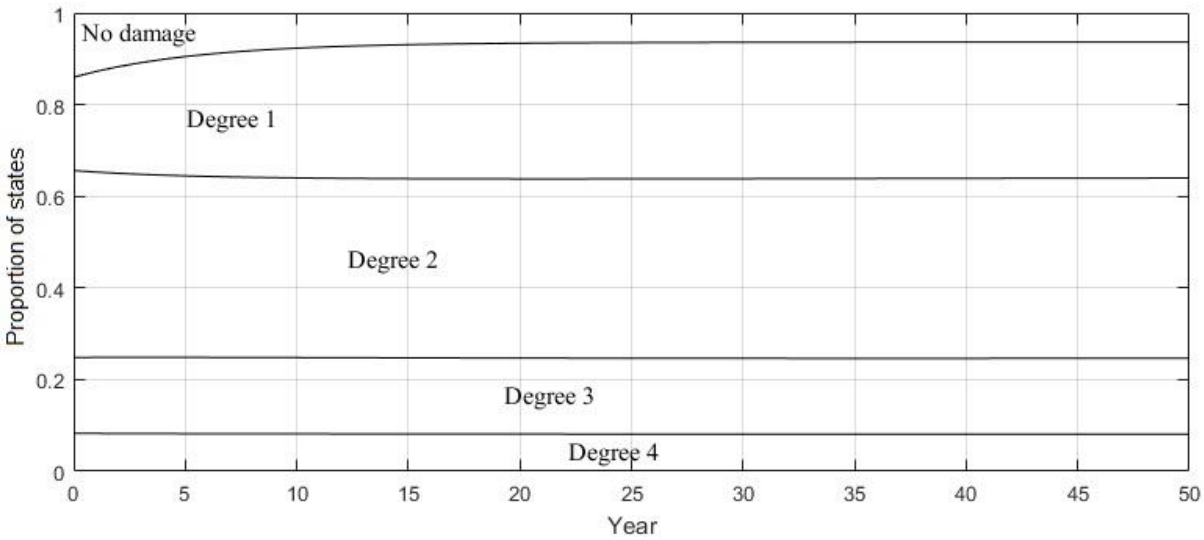

Figure 10.4.2: Maintaining bridge stock condition

There have been several failures for today's bridge stock. It is therefore expected that some of the replacements will be reconstructions after bridge failures if this strategy is followed. In case the yearly probability of failure for damage degree 4 bridge is 5%, then about 40% of the replacements are replacement after failure and 60% of the replacements are planned replacements.

10.4.4 Improving bridge stock condition

A stricter replacement strategy is considered. All damage degree 4 bridges are replaced within one year and 10% of damage degree 3 bridges are replaced within one year. The ratio of damage degree 3 bridges staying in damage degree 3 or transiting to damage degree 4 is assumed to be similar to the deterioration of chapter 8.5.5. If the damage degree 3 bridges with the worst conditions are replaced, then the probability for a damage degree 3 bridge to decay to damage degree 4 could be less. It is assumed to be the same for now. The transition probability matrix for the bridge stock condition is shown in matrix 10.4.2.

$$\mathbf{\Pi} = \begin{bmatrix} 0.8343 & 0.1627 & 0.0030 & 0.0000 & 0.0000 \\ 0 & 0.9650 & 0.0346 & 0.0004 & 0.0000 \\ 0 & 0 & 0.9735 & 0.0256 & 0.0008 \\ 0.1 & 0 & 0 & 0.9 \cdot 0.9384 & 0.9 \cdot 0.0616 \\ 1 & 0 & 0 & 0 & 0 \end{bmatrix} \tag{10.4.2}$$

The distribution of states in the bridge stock over time is shown in figure 10.5.3. With this replacement strategy, the bridge stock reaches a steady state where 8% of the bridges are expected to stay in damage degree 3 and 0.5% of the bridges are expected to stay in damage degree 4. The average time between replacements is expected to be 6.1 months.

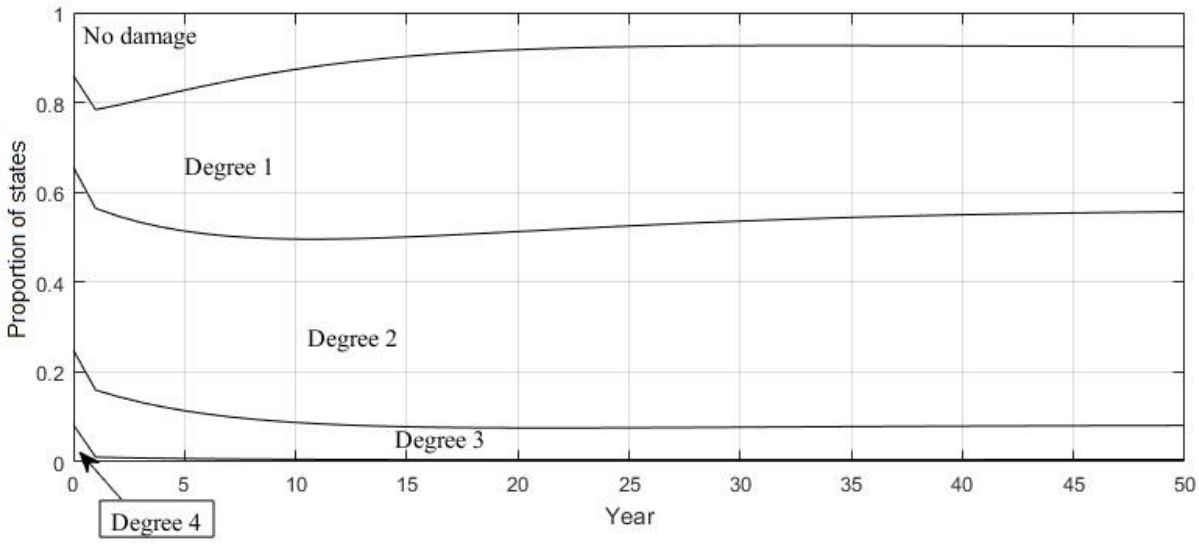

Figure 10.4.3: Improving bridge stock condition

This strategy will require large resources to improve the bridge stock condition within the next few years. Alternatively, the improvement could take place over several years before following the strategy that gives the steady state of figure 10.4.3.

10.5 Conclusion

Assessment of the bridge stock can guide budgeting and overall strategies for management of bridges. For optimal management of the bridge stock, individual bridges should also be assessed in order to support right prioritisation.

The assessment of individual bridge replacement looks at both the user and owner cost. It is important to notice how the cost is different for the user and owner. In management and budgeting of bridges, the user cost might not be quantified towards owner cost. The user cost might therefore be overseen to some degree. Figure 10.3.3 shows a case where it would not be beneficial to replace the bridge during the time of consideration from the owner's perspective. The user's perspective is completely different, and the risk and cost increase over time for the user.

When considering bridge stock strategies, it seems like a bad strategy to let the bridges continue to deteriorate without any actions. This strategy is likely to bring large consequences to the user, and it might also bring large consequences to the owner. It is not easy to plan the budget with this strategy.

Maintaining today's condition will lead to less consequences than doing nothing. As several bridges are failing with today's condition, occasional failures will still be expected with this strategy. If only replacements are considered, then the time between replacements might be 7.3 months for maintaining today's condition.

Improving today's condition will clearly lead to less failures, and failures might even be avoided. The strategy in chapter 10.4.3 might avoid failures, and the average time between replacements is estimated to be 6.1 months. There will probably be less serviceability failures.

When considering the large difference in consequence from a planned replacement and a failure, this improving strategy seems better than maintaining today's condition. The expected frequency of replacements is not that large between this more risk adverse strategy and the strategy for maintaining today's condition.

Delaying actions gives an increase in risk and damages. There might be large unforeseen costs and consequences associated with a highly deteriorated bridge stock. There will, however, be a balance where the cost for reducing risk will not be beneficial, also for the bridge stock. This is what figure 10.2.2 illustrates. Accurate calculations for the most optimal strategy is not given in this paper, but the study indicates that an improvement in the bridge stock condition seems to be beneficial.

Chapter 11

Conclusions and recommendations

11.1 Probabilistic methods in inspection and management of bridges

The goal with this study was to show how probabilistic methods can support inspection and management of bridges, and the focus has been directed towards buried steel pipe bridges. Norwegian Public Roads Administration manages more than 17,500 bridges. With such a large bridge stock, any improvement in management and inspection can have a great positive impact. Probabilistic methods have the potential to support better decision making for inspections and better strategies for management. It might also give a better understanding of the condition of the bridges, and therefore reduce risk.

Bayesians decision trees and influence diagrams show a great potential for guiding decision making and inspection of bridges. The decision making is consistent, and this might optimise the decision making. Such methods might also give the inspectors better confidence in their prioritisations and decisions. This can support good habits and understanding in the inspection practise. Influence diagrams are illustrative and can deal with higher complexity problems. As the complexity of the problem becomes larger, it might be more requiring to create a large influence diagram. When an influence diagram can support decisions for large bridges involving large costs, or when it can be applied for several bridges within a bridge stock, it might give large savings from optimal decisions. Developing a good influence diagram can therefore be a good strategy.

A Bayesian network can be useful for developing an understanding of the structural condition and loading. The variables and dependencies are presented graphically. Bayesian networks can be especially useful for structural systems with complex relations between variables. This is the case for buried steel pipe bridges. Some variables relate to both loading and structural resistance.

Reliability analysis is used to evaluate the condition of the bridges and the uncertainties of variables are taken account. For complex problems, reliability analysis may be connected with Bayesian networks for assessment of structural performance. First order reliability analysis makes it possible to study variables' importance for the uncertainty of structural performance.

Norwegian Public Roads Administration has a large amount of damage observations in their database of Brutus. These are discrete damage degree observations, ranging from small to critical damages. Prediction of deterioration is performed based on previous observations. A prediction is made in this document for the bridge stock of buried steel pipe bridges in Trøndelag. This is done with maximum likelihood estimation of transition intensities of a continuous Markov process. The Markov process is memoryless, and this is a model assumption that is often used to describe bridge stock deterioration. The model is also

sequential and progressive. Improvement of the bridges are therefore not considered, and in case this is to be studied, an alternative model must be used.

In this study, the deterioration of the bridge stock has been the main concern. A Markov chain is sufficient for analysis of the bridge stock. A dynamic Bayesian network can extend this further and consider more variables in the deterioration assessment. Such a network might be used to predict deterioration of individual bridges as well as the whole bridge stock. Creating good estimations in a complex dynamic Bayesian network might be requiring, and it might be necessary to combine probabilistic analyses with physical theories.

Failure predictions will often be relevant for decision making. This could be useful for management of a whole bridge stock and also for an individual bridge. A sequential continuous-time Markov process is used for failure prediction for the pipe bridge stock. As for deterioration, a dynamic Bayesian network might be suitable for failure prediction for an individual bridge.

Replacement of buried steel pipe bridges is studied. Several strategies are considered for the bridge stock. The strategies are studied by modifying the predicted deterioration model. In order to make a prioritisation for improving actions as replacement within the bridge stock, individual bridges should be studied. This is done in this document by considering cost and risk over time.

The final conclusion from these studies is that probabilistic analyses have a good potential for benefiting management and inspection of bridges. The expert's experience and knowledge together with physical theory and probability theory are all important elements for optimal management. The benefits and limitations of the current inspection and management practise as well as benefits and limitations for alternative approaches should be realistic.

11.2 Buried steel pipe bridges

A buried steel pipe bridge is a quite complex structure. The condition of the structure is both dependent on the condition of the corrugated steel pipe and the condition of the surrounding soil. Geotechnical engineering includes many uncertainties, and it might be difficult to predict the behaviour of the soil. A Bayesian network is made to illustrate the variables and dependencies that affect the structural performance of a buried steel pipe bridge. The network shows that there are many dependencies between loading variables and structural condition variables. The surrounding soil contributes to an earth load on the pipe, but the soil is also supporting the pipe.

There exist simplified formulas to calculate the performance of corrugated steel pipe bridges. Corrugated steel pipes have a flexible bending stiffness relative to the soil, but the stiffness in ring compression is very large for the pipes, Moser (2001). The earth load might be considered to act as a prism load, Moore (2001). All the soil above the pipe is carried by the walls of the pipe, and this is assumed to create a ring compression in the pipe.

Deterioration affects the structural capacity. Corrosion reduces the wall thickness. El-Taher's study (2009) shows that the relation between the yield capacity of the pipe wall and the smallest

continuous wall thickness of the pipe is almost proportional. This is the case if the pipe has proper support from the soil. Erosion might strongly reduce the buckling capacity of the pipe, El-Taher (2009).

First order reliability analysis is used to assess the probability of yield of the pipe wall. A set of assumed variables are given. The probability of yield might become significant for depths of less than 4.5 meters with wall thicknesses of less than 1 mm. The traffic load is most critical at shallow depths since the pipe carries a larger portion of the traffic load at shallow depths. At deeper depths, the earth load becomes more critical. The pipe bridge might be standing even though there is yield of the pipe wall. This is because the loads might be transferred through the soil rather than the pipe. The effect of loads being transferred through the soil is called the arching effect, Moser (2001).

A prediction of deterioration is made for the buried steel pipe bridges. All bridges are assumed to be in state 0, no damage, right after construction. A continuous-time Markov process is fitted to the observations with a maximum likelihood estimation. This procedure is based on a proposed framework by Kallen (2007). Based on the current condition of the bridge stock, a future prediction is made. This prediction assumes that there are no actions nor failures, and damage degree 4 is the absorbing state. It is calculated that the number of damage degree 4 bridges will more than double within the next ten years when no actions nor failures are considered. By the damage development prediction of a bridge with no damage in year 0, it is seen that a 100-year design life is unrealistic, and a 50-year design life might be more realistic.

A failure prediction is also made for the bridge stock. This is modelled with a sequential deterioration failure model which assumes that a bridge goes through all states before failure occur. The model is a continuous-time Markov process. A damage degree 4 bridge is predicted to have an annual probability of failure of 0.05. It is predicted that there will occur five failures within the bridge stock for the six next years. Five failures have occurred during the past five years, and this prediction seems realistic.

The costs for a planned replacement and a failure including reconstruction is studied. To quantify the benefit of reducing risk, these costs should be known. The costs are divided into costs to the owner of the bridge and to the users of the bridge. Owner costs mainly include design cost and construction cost, while user costs mainly include traffic disruption cost and accidental cost. The user cost may be seen from the society's point of view. A failure might bring especially large consequences to the users.

Since the risk associated with failures are high, the benefit from risk reduction can be great. Some replacement strategies are studied for the bridge stock. These strategies are studied by modifying the Markovian deterioration model. It is seen that today's bridge stock condition can be maintained by replacing 13% of damage degree 4 bridges every year. With this strategy, there will be a significant amount of damage degree 4 bridges in the bridge stock. On average, one bridge must be replaced every 7.3 months.

A strategy that improves the bridge stock condition is also studied. It is assumed that all bridges deteriorating to damage degree 4 are replaced within a year. 10% of damage degree 3 bridges are replaced every year, and ideally, these should be the most critical damage degree 3 bridges.

This strategy maintains a bridge stock condition with far less damage degree 3 and 4 bridges. When the bridge stock condition has reached a steady state, then the average time between replacements is 6.1 months This is not very different from the replacement frequency that maintains today's condition. An improvement of the bridge stock condition seems to be beneficial. Increased investment in improving bridge stock condition can strongly reduce failures.

11.3 Recommendations and outlook

The condition of the pipe bridge stock should be improved. Further studies are required for finding an optimal strategy. Other actions in addition to replacement might be studied. It could also be interesting to study how limited budget affects strategies and decisions.

It is advised for inspectors to study the simple concepts of Bayesian decision trees. These trees are simple to set up, and they can help quantifying and compare options among measurements and actions for bridges.

There is potential benefit from creating a software that can predict deterioration based on the large amount of damage observations in Norwegian Public Roads Administration's database. The observations are holding a lot of information. With statistical analysis, one might take better use of this information. If damage degrees are stored in a structured way, the predictions might be made effortless and automatic. The predictions can then support budgeting and management of the bridge stock.

Perfect observations are assumed for the prediction of deterioration of buried pipe bridges. It could be interesting to do further studies on imperfect observations. A hidden Markov-process, a simple dynamic Bayesian network, might be used to model imperfect observations. The subjective aspect of observations can be estimated by making several inspectors evaluate the same bridges and then study the variance of their assessment. For further studies, a model that also allows lower damage degree bridges to go directly into failure might be considered.

It is of interest to develop the studies further in the direction of dynamic Bayesian networks. A well-established dynamic Bayesian network can be very powerful for deterioration and failure prediction. This makes it possible to study the whole bridge stock and individual bridges. To create such a network, statistics, physical theory and the experts' knowledge might be combined to a greater extent. Combining Bayesian networks with reliability analysis to assess probabilities could be a good approach.

References

AASHTO (2005). *Pontis Release 4.4 Technical Manual.* AASHTO, Washington, DC, USA.

Ayuub, B.M. (2014). *Risk Analysis in Engineering and Economics, Second Edition*. Chapman & Hall/CRC, Boca Raton, FL, USA.

BayesFusion, LLC. (2018). *GeNIe Modeler, Version 2.2.4, Built on 4/3/2018.* Available at: http://support.bayesfusion.com/docs/ Accessed 22.05.18. BayesFusion, LLC, Pittsburgh, PA, USA.

BayesFusion, LLC. (2018). *GeNIe Modeler, USER MANUAL Version 2.2.4.* BayesFusion, LLC, Pittsburgh, PA, USA.

Benjamin, J.R. & Cornell, C.A. (1970). *Probability, Statistics, and Decisions for Civil Engineers*. McGraw-Hill Book Company, New York, NY, USA.

Chen, J., Ooi, J. & Teng, J. (2008). *Structures and Granular Solids*. Taylor & Francis, London, United Kingdom.

Chen, W.F. & Duan, L. (2014). *Bridge Engineering Handbook: Construction and Maintenance.* Taylor & Francis, Boca Raton, FL, USA.

El-Taher, M. (2009). *The Effect of Wall and Backfill Soil Deterioration on Corrugated Metal Culvert Stability.* Queen's University, Kingston, Ontario, Canada.

Haggag, A.A. (1989). *Structural backfill design for corrugated-metal buried structures.* PhD thesis, University of Massachusetts Amherst, MA, USA.

Hasofer, A.M. & Lind, N.C. (1974). *Exact and invariant second-moment code format.* Journal of the Engineering Mechanics division, ASCE.

Howard R.A. (1971). *Dynamic Probabilistic Systems, Volume II: Semi-Markov and Decision Processes.* John Wiley & Sons, New York, NY, USA.

Jensen, F.V. & Nielsen, D.N. (2007). *Bayesian Networks and Decision Graphs.* Springer, New York, NY, USA.

Kallen, M.J. (2007). *Markov processes for maintenance optimization of civil infrastructure in the Netherlands.* PhD thesis, Delft University of Technology, Delft, Netherlands.

Moore, I.D. (2001). *Buried Pipes and Culverts*. In: Rowe R.K. *Geotechnical and Geoenvironmental Engineering Handbook*. Springer, Boston, MA, USA.

Moser, A.P. (2001). *Buried Pipe Design.* 2nd edition. McGraw-Hill, New York, NY, USA.

Ng, S.K. & Moses, F. (1996). *Prediction of Bridge Service Life Using Time-Dependent Reliability Analysis.* University of Pittsburgh, PA, USA.

NPRA (2003). *Bruklassifisering, Manual R412.* Norwegian Public Roads Administration, Directorate of Public Roads, Oslo, Norway.

NPRA (2015). *Bruprosjektering, Manual N400.* Norwegian Public Roads Administration, Directorate of Public Roads, Oslo, Norway.

NPRA (2010). *Geoteknikk i vegbygging, Manual V220.* Norwegian Public Roads Administration, Directorate of Public Roads, Oslo, Norway.

NPRA (2000). *Inspeksjonshåndbok for bruer, Manual V441.* Norwegian Public Roads Administration, Directorate of Public Roads, Oslo, Norway.

NPRA (2018). *Konsekvensanalyser, Manual V712.* Norwegian Public Roads Administration, Directorate of Public Roads, Oslo, Norway.

QDTMR (2015). *Criteria for Inspection, Life Extension and Rehabilitation of Circular Corrugated Metal Culverts, Manual.* Queensland Department of Transport and Main Roads, Brisbane, Australia.

Rackwitz, R. (2000). *Optimization – the basis of code-making and reliability verification.* Technische Universität München, München, Germany.

Samstad, H. (2017). *Oppdatering av enhetskostnader i nytte-kostnadsanalyser i Statens vegvesen.* COWI, Depertment of Economics, Oslo, Norway.

Straub, D. (2004). *Generic approaches to risk based inspection planning for steel structures.* PhD thesis, Institute of Structural Engineering, ETH Zurich, Switzerland.

Straub, D. (2015). *Lecture Notes in Engineering Risk Analysis*. Technische Universität München, Engineering Risk Analysis Group, Munich, Germany.

Thoft-Christensen, P. (2006). *Life-cycle cost-benefit (LCCB) analysis of bridges from user and social point of view*. Aalborg University, Aalborg, Denmark.

Wilks, S.S. (1938). *The Large-Sample Distribution of the Likelihood Ratio for Testing Composite Hypotheses.* Ann. Math. Statist. 9.

Østli, V., Halse, A. & Killi, M. (2015). *Verdsetting av tid, pålitelighet og komfort tilpasset NTM6, TØI report 1389*. Norwegian Institute of Transport Economics, Oslo, Norway.

Appendix

Appendix A: Yield of pipe wall - FORM analysis with MATLAB

A.1: Chapter 7.4.4.1

```
function [b] = form1(ma,sa,mt,st,mf,sf,mh,sh,mg,sg,mD,sD,mk,sk,mF,sF)

a = [-1,-1,-1,1,1,1,1,1]/sqrt(8);
b1 = 1; diff = 1;

while abs(diff)>= 10^-6
    u = a*b1;
    dg(1) = sa*(st*sf*u(2)*u(3)+st*mf*u(2)+mt*sf*u(3)+mt*mf);
    dg(2) = st*(sa*sf*u(1)*u(3)+sa*mf*u(1)+ma*sf*u(3)+ma*mf);
    dg(3) = sf*(sa*st*u(1)*u(2)+sa*mt*u(1)+ma*st*u(2)+ma*mt);
    dg(4) = sh*(-(sg*sD*sk*u(5)*u(6)*u(7)+sg*sD*mk*u(5)*u(6)+...
                sg*mD*sk*u(5)*u(7)+mg*sD*sk*u(6)*u(7)+sg*mD*mk*u(5)+...
                mg*sD*mk*u(6)+mg*mD*sk*u(7)+mg*mD*mk)/2-3*(sF*u(8)+...
                mF)/4/(u(4)*sh+mh)^2);
    dg(5) = -sg*(sh*sD*sk*u(4)*u(6)*u(7)+sh*sD*mk*u(4)*u(6)+...
                sh*mD*sk*u(4)*u(7)+mh*sD*sk*u(6)*u(7)+sh*mD*mk*u(4)+...
                mh*sD*mk*u(6)+mh*mD*sk*u(7)+mh*mD*mk)/2;
    dg(6) = -sD*(sh*sg*sk*u(4)*u(5)*u(7)+sh*sg*mk*u(4)*u(5)+...
                sh*mg*sk*u(4)*u(7)+mh*sg*sk*u(5)*u(7)+sh*mg*mk*u(4)+...
                mh*sg*mk*u(5)+mh*mg*sk*u(7)+mh*mg*mk)/2;
    dg(7) = -sk*(sh*sg*sD*u(4)*u(5)*u(6)+sh*sg*mD*u(4)*u(5)+...
                sh*mg*sD*u(4)*u(6)+mh*sg*sD*u(5)*u(6)+sh*mg*mD*u(4)+...
                mh*sg*mD*u(5)+mh*mg*sD*u(6)+mh*mg*mD)/2;
    dg(8) = -sF*3/(4*(u(4)*sh+mh));
    k = sqrt(sum(dg.^2));
    a = -dg/k;
    u = a*b1;

    g = (u(1)*sa+ma)*(u(2)*st+mt)*(u(3)*sf+mf)-...
        (u(4)*sh+mh)*(u(5)*sg+mg)*(u(6)*sD+mD)*(u(7)*sk+mk)/2-...
        3*(u(8)*sF+mF)/(4*(u(4)*sh+mh));
    dgb = 3*b1^2*sa*st*sf*a(1)*a(2)*a(3)+2*b1*(sa*st*mf*a(1)*a(2)+...
          2*sa*mt*sf*a(1)*a(3)+2*ma*st*sf*a(2)*a(3))+sa*mt*mf*a(1)+...
          ma*st*mf*a(2)+ma*mt*sf*a(3)-...
          1/2*(4*b1^3*sh*sg*sD*sk*a(4)*a(5)*a(6)*a(7)+...
          3*b1^2*(sh*sg*sD*mk*a(4)*a(5)*a(6)+sh*sg*mD*sk*a(4)*a(5)*a(7)+...
          sh*mg*sD*sk*a(4)*a(6)*a(7)+mh*sg*sD*sk*a(5)*a(6)*a(7))+...
          2*b1*(sh*sg*mD*mk*a(4)*a(5)+sh*mg*sD*mk*a(4)*a(6)+...
          sh*mg*mD*sk*a(4)*a(7)+mh*sg*sD*mk*a(5)*a(6)+...
          mh*sg*mD*sk*a(5)*a(7)+mh*mg*sD*sk*a(6)*a(7))+...
          sh*mg*mD*mk*a(4)+mh*sg*mD*mk*a(5)+mh*mg*sD*mk*a(6)+...
          mh*mg*mD*sk*a(7))-3*sF*mh/(4*(b1*a(4)*sh+mh))^2*a(8)+...
          3*mF*sh*a(4)/(4*(b1*a(4)*sh+mh))^2;

    b2 = b1 - g/dgb;

    diff = b2-b1;
    b1 = b2;
end

b = b2;
end
```

A.2: Chapter 7.4.4.3

```
function [b] = form2(ma,sa,mt,st,mf,sf,mg,sg,mk,sk,mF,sF,h,D)

tridem = 3/4*h^4*(70/mF*(1/h^5+1/sqrt(h^2+2^2)^5+1/sqrt(h^2+1^2)^5+...
     1/sqrt(h^2+3^2)^5)+2*35/mF*(1/sqrt(h^2+1.3^2)^5+...
     1/sqrt(h^2+2^2+1.3^2)^5+1/sqrt(h^2+1^2+1.3^2)^5+...
     1/sqrt(h^2+3^2+1.3^2)^5));
tandem = 3/4*h^4*(1/h^5+1/sqrt(h^2+2^2)^5+1/sqrt(h^2+1^2)^5+...
     1/sqrt(h.^2+3^2)^5+32.5/mF*(1/sqrt(h^2+1.3^2)^5+...
     1/sqrt(h^2+2^2+1.3^2)^5+1/sqrt(h^2+1.3^2+1^2)^5+...
     1/sqrt(h^2+3^2+1.3^2)^5));

if h/D < 0.25
    red = 1;
elseif h/D < 0.75
    red = 1.25-h/D;
else
    red = 0.5;
end

tF = red*max(tridem,tandem);

a = [-1,-1,-1,1,1,1]/sqrt(6);
b1 = 1; diff = 1;

while abs(diff)>= 10^-6

    u = a*b1;
    dg(1) = sa*(st*sf*u(2)*u(3)+st*mf*u(2)+mt*sf*u(3)+mt*mf);
    dg(2) = st*(sa*sf*u(1)*u(3)+sa*mf*u(1)+ma*sf*u(3)+ma*mf);
    dg(3) = sf*(sa*st*u(1)*u(2)+sa*mt*u(1)+ma*st*u(2)+ma*mt);
    dg(4) = -h*D/2*sg*(sk*u(5)+mk);
    dg(5) = -h*D/2*sk*(sg*u(4)+mg);
    dg(6) = -sF*tF;

    k = sqrt(sum(dg.^2));
    a = -dg/k;

    b2 = (h*D*mg*mk/2+mF*tF-ma*mt*mf)/(b1^2*sa*st*sf*a(1)*a(2)*a(3)+...
        b1*(sa*st*mf*a(1)*a(2)+sa*mt*sf*a(1)*a(3)+ma*st*sf*a(2)*a(3)-...
        h*D/2*(sg*sk*a(4)*a(5)))+sa*mt*mf*a(1)+ma*st*mf*a(2)+...
        ma*mt*sf*a(3)-h*D/2*(sg*mk*a(4)+mg*sk*a(5))-sF*tF*a(6));

    diff = b2-b1;
    b1 = b2;
end

b = b2;
end
```

Appendix B: Bridge stock deterioration observations

Table B.1: Bridge stock deterioration

Bridge			Damage degree by observation year																							
Identity	**Constr. year**	**Climate**	1995	1996	1997	1998	1999	2000	2001	2002	2003	2004	2005	2006	2007	2008	2009	2010	2011	2012	2013	2014	2015	2016	2017	2018
16-0604	1963	Coastal												1											2	
16-0611	1964	Coastal											2													
16-0613	1964	Inland	1							1														3	3	
16-0634	1964	Coastal																							2	
16-0637	1964	Inland													2					2				3	3	
16-0640	1965	Inland											2										2			
16-0643	1965	Inland																		1				2		
16-0644	1965	Inland		2																				2		
16-0646	1965	Coastal												1										2		
16-0649	1965	Inland	2						2		2												4	4	4	
16-0652	1965	Inland						3					3								4			4	4	
16-0664	1966	Inland							2															2		
16-0665	1966	Inland																		2				3		
16-0667	1966	Inland								1											1				2	
16-0670	1966	Inland																1				1				
16-0688	1967	Inland																					2			
16-0694	1967	Inland																					2			
16-0697	1967	Inland												2										2		
16-0704	1967	Inland								2															2	
16-0709	1967	Inland																							3	
16-0715	1967	Inland		2																		2				
16-0727	1967	Inland							2																2	
16-0733	1967	Inland																							2	
16-0739	1967	Inland										2										3		5		
16-0742	1967	Inland																							2	
16-0745	1968	Inland																						1		
16-0746	1968	Inland																	1						3	
16-0754	1968	Inland							1																2	
16-0760	1969	Coastal				2				3												4			4	
16-0764	1969	Inland							3														3		4	
16-0770	1969	Coastal																				2				
16-0771	1969	Inland													1										3	
16-0773	1969	Inland																							2	
16-0775	1968	Inland										2										4				
16-0776	1969	Inland																					1			
16-0791	1970	Inland														1					1					
16-0795	1971	Inland	1																						2	
16-0798	1971	Inland																			3					
16-0801	1971	Inland			2																5					
16-0807	1971	Inland																			2					
16-0819	1972	Inland																						3	3	
16-0820	1972	Inland								2															2	
16-0829	1973	Inland																2					2			
16-0833	1973	Inland														2						3		4	4	
16-0834	1973	Inland			1																	1				
16-0837	1973	Coastal																				1				
16-0844	1973	Inland																1					1			

Table B.2: Bridge stock deterioration

Bridge			**Damage degree by observation year**																							
Identity	**Constr. year**	**Climate**	1995	1996	1997	1998	1999	2000	2001	2002	2003	2004	2005	2006	2007	2008	2009	2010	2011	2012	2013	2014	2015	2016	2017	2018
16-0851	1975	Inland									1											1				
16-0860	1974	Inland													2										3	
16-0872	1975	Inland																				1			3	
16-0875	1975	Inland																		1					2	
16-0879	1970	Inland											2								2		2			
16-0892	1975	Inland										1										1				
16-0898	1975	Inland																	1					2		
16-0905	1976	Inland																	2					3		
16-0926	1977	Coastal											1								2			4		
16-0935	1977	Inland																					3			
16-0937	1977	Inland													2										3	
16-0959	1978	Inland										2										2				
16-0965	1978	Inland				1																			2	
16-0973	1978	Inland																	2					2		
16-0992	1979	Inland				1								1										2	3	
16-0994	1979	Inland																							2	
16-0996	1979	Inland																		1				2		
16-0997	1979	Inland												1										2	3	
16-988	1979	Inland						3																5		
16-1004	1980	Inland			1																	1				
16-1019	1980	Coastal							3																5	
16-1031	1981	Inland																							3	
16-1058	1967	Inland																				2				
16-1100	1983	Inland																		1				2		
16-1103	1983	Inland																		1				2		
16-1106	1973	Inland																						1		
16-1157	1984	Inland																							1	
16-1160	1985	Inland																				1				
16-1165	1984	Coastal							1														2			
16-1174	1985	Inland																						2		
16-1177	1985	Inland																								
16-1187	1985	Inland									2															
16-1193	1985	Inland																					2			
16-1196	1985	Coastal																				3				
16-1211	1991	Inland																							1	
16-1216	1986	Inland																		2					2	
16-1217	1986	Inland																	1					1		
16-1218	1986	Inland																							2	
16-1226	1987	Inland																	1					2		
16-1238	1988	Inland																		1				2		
16-1271	1989	Inland			2			2													3				3	
16-1281	1994	Inland																		2				3	4	
16-1284	1994	Inland							1		1										1		2			
16-1322	1992	Inland																1					1			
16-1344	1990	Inland																							2	
16-1367	1991	Inland																				1				
16-1375	1992	Inland																	2					2		
16-1395	1994	Coastal																								
16-1514	1997	Inland																								
16-1573	2001	Inland																								

Table B.3: Bridge stock deterioration

Bridge			**Damage degree by observation year**																							
Identity	**Constr. year**	**Climate**	1995	1996	1997	1998	1999	2000	2001	2002	2003	2004	2005	2006	2007	2008	2009	2010	2011	2012	2013	2014	2015	2016	2017	2018
16-1576	1999	Inland																							2	
16-1620	2001	Coastal																								
16-1621	2002	Coastal																					3			
16-1625	2003	Coastal																								
16-1635	2005	Inland																			1					
16-1637	2004	Inland																				1				
16-1638	2004	Inland																			1					
16-1852	2014	Inland																								
16-1923	2014	Inland																								
17-0482	1961	Inland																			2					
17-0547	1962	Inland			2					2					2					2					2	
17-0640	1964	Inland			1															2					3	
17-0673	1965	Inland																								
17-0690	1966	Inland																				1				
17-0700	1966	Inland																							2	
17-0703	1966	Inland								1															1	
17-0709	1966	Inland																								
17-0718	1966	Inland													2					3					3	
17-0742	1967	Inland								1															2	
17-0754	1968	Inland								1															4	
17-0757	1968	Inland																								
17-0805	1968	Inland						1																2		
17-0819	1969	Inland		1																				1		
17-0821	1969	Inland		1															2					2		
17-0831	1969	Inland																						2		4
17-0867	1971	Inland										2					2					2				
17-0872	1971	Inland																							3	
17-0885	1972	Inland						2														2				
17-0888	1968	Inland																								
17-0892	1972	Inland																								
17-1000	1974	Inland									2										2					
17-1001	1978	Inland					2																		2	
17-1030	1975	Inland																								
17-1039	1975	Inland		1																				3		
17-1051	1975	Inland		1																				4		
17-1060	1976	Inland							1															1		
17-1089	1977	Inland															1					1				
17-1093	1977	Inland									1										1					
17-1097	1977	Inland											1										1			
17-1147	1978	Inland									1					2					2					
17-1148	1979	Inland											1											2		
17-1153	1979	Inland								2					2					2					2	
17-1154	1979	Inland						2					2										2		3	
17-1156	1979	Inland		1					2					2					3					4		
17-1159	1979	Inland																								
17-1162	1979	Inland														2					2					
17-1172	1980	Inland															1					1				
17-1174	1980	Inland									1										1					
17-1179	1980	Inland					1										2					2				

Table B.4: Bridge stock deterioration

Bridge			**Damage degree by observation year**																							
Identity	**Constr. year**	**Climate**	1995	1996	1997	1998	1999	2000	2001	2002	2003	2004	2005	2006	2007	2008	2009	2010	2011	2012	2013	2014	2015	2016	2017	2018
17-1193	1981	Inland																						1		
17-1198	1981	Inland																	1					1	2	
17-1213	1982	Inland									1										1					
17-1225	1983	Inland		2					2													4	5			
17-1261	1984	Inland																			1					
17-1278	1984	Inland						1																4		
17-1281	1982	Inland										1					1					2				
17-1571	1984	Coastal																								
17-1575	1986	Inland																								
17-1578	2009	Inland																								
17-1666	2013	Inland																								

Appendix C: Bridge stock deterioration prediction with MATLAB

C1: Model A, chapter 8.5.2

```
function [logl] = ModelA(a)
D = importdata('DamageDev.txt');
Q = [-a a 0 0 0;
     0 -a a 0 0;
     0 0 -a a 0;
     0 0 0 -a a;
     0 0 0 0 0];
logl = 0;
for i = 1:length(D)
    P = expm(Q*(D(i,2)-D(i,1)));
    logl = logl - log(P(D(i,3)+1,D(i,4)+1));
end
end
```

```
a = fminsearch(@ModelA,[0.1])

>>    a = 0.0555

      logl = 587.2556
```

```
a = 0.055468750000000;
syms aa
H = hessian(ModelA([aa]));
aa = a;
C = inv(eval(H));
CV = sqrt(C)/a

>>    CV = 0.0440
```

C2: Model 2, chapter 8.5.3

```
function [logl] = ModelB(a)
D = importdata('DamageDev.txt');
Q = [-a(1) a(1) 0 0 0;
     0 -a(2) a(2) 0 0;
     0 0 -a(3) a(3) 0;
     0 0 0 -a(4) a(4);
     0 0 0 0 0];
logl = 0;
for i = 1:length(D)
    P = expm(Q*(D(i,2)-D(i,1)));
    logl = logl - log(P(D(i,3)+1,D(i,4)+1));
end
end
```

```
a = fminsearch(@ModelB,[0.1 0.1 0.1 0.1])

>>    a = 0.1811   0.0356   0.0268   0.0636

      logl = 529.5559
```

```
a = [0.181144669026712 0.035649749402522 0.026822764900698
0.063631823724357];

syms aa1 aa2 aa3 aa4
H = hessian(ModelB([aa1 aa2 aa3 aa4]));
aa1 = a(1); aa2 = a(2); aa3 = a(3); aa4 = a(4);
C = inv(eval(H));

s = zeros(1,length(C)); CV = zeros(1,length(C)); CORRC = zeros(length(C));
for i = 1:length(C)
    s(i) = sqrt(C(i,i));
    CV(i) = s(i)/a(i);
end
for i = 1:length(C)
    for j = 1:length(C)
    CORRC(i,j) = C(i,j)/s(i)/s(j);
    end
end
CORRC
CV

>>    CORRC = 1.0000   -0.4530   -0.1144   -0.0284
             -0.4530    1.0000   -0.0161   -0.0013
             -0.1144   -0.0161    1.0000   -0.0263
             -0.0284   -0.0013   -0.0263    1.0000

      CV = 0.1995    0.0880    0.1295    0.2291
```